INL/EXT-06-11725

HyPEP FY06 Report: Models and Methods

C.H. Oh
C.B. Davis
J. Han
R. Barner
S.R. Sherman
R. Vilim
Y. J. Lee
W.J. Lee

September 2006

The INL is a U.S. Department of Energy National Laboratory
operated by Battelle Energy Alliance

INL/EXT-06-11725

HyPEP FY06 Report: Models and Methods

C.H. Oh, INL
C.B. Davis, INL
J. Han, INL
R. Barner, INL
S.R. Sherman, INL
R. Vilim, ANL
Y.J. Lee, KAERI
W.J. Lee, KAERI

September 2006

Idaho National Laboratory
Idaho Falls, Idaho 83415

Prepared for the
U.S. Department of Energy
Under DOE Idaho Operations Office
Contract DE-AC07-05ID14517

ABSTRACT

The Department of Energy envisions the next generation very high-temperature gas-cooled reactor (VHTR) as a single-purpose or dual-purpose facility that produces hydrogen and electricity. The Ministry of Science and Technology (MOST) of the Republic of Korea also selected VHTR for the Nuclear Hydrogen Development and Demonstration (NHDD) Project.

This research project aims at developing a user-friendly program for evaluating and optimizing cycle efficiencies of producing hydrogen and electricity in a Very-High-Temperature Reactor (VHTR). Systems for producing electricity and hydrogen are complex and the calculations associated with optimizing these systems are intensive, involving a large number of operating parameter variations and many different system configurations. This research project will produce the HyPEP computer model, which is specifically designed to be an easy-to-use and fast running tool for evaluating nuclear hydrogen and electricity production facilities. The model accommodates flexible system layouts and its cost models will enable HyPEP to be well-suited for system optimization.

Specific activities of this research are designed to develop the HyPEP model into a working tool, including (a) identifying major systems and components for modeling, (b) establishing system operating parameters and calculation scope, (c) establishing the overall calculation scheme, (d) developing component models, (e) developing cost and optimization models, and (f) verifying and validating the program. Once the HyPEP model is fully developed and validated, it will be used to execute calculations on candidate system configurations.

FY-06 report includes a description of reference designs, methods used in this study, models and computational strategies developed for the first year effort. Results from computer codes such as HYSYS and GASS/PASS-H used by Idaho National Laboratory and Argonne National Laboratory, respectively will be benchmarked with HyPEP results in the following years.

INTERNATIONAL NUCLEAR ENERGY RESEARCH INITIATIVE

Project Title: HyPEP FY06 Report: Models and Methods

Principal Investigator (U.S)
C. H. Oh, Idaho National Laboratory (INL)
R. Vilim, Argonne National laboratory (ANL)

Principal Investigator (International):
Y. J. Kim, Korea Atomic Energy Research Institute (KAERI)
W. J. Lee, KAERI

Collaborators:
C.B. Davis, INL, J. Han, INL,
R. Barner, INL, S. Sherman, INL

Project Number: 2005-002-K

Project Start Date: October 1, 2005

Project End Date: September 30, 2006

EXECUTIVE SUMMARY

The collaborators for this research project are KAERI, INL and ANL. The first project year has been used to evaluate and select the program languages to use in developing the HyPEP computer code, to setup the overall model/calculation requirements, to establish the hierarchical system/component modeling system, to setup the Graphic User Interface, to setup the thermodynamic property calculation routines, and to produce a HyPEP alpha version.

TASK 1/ALL: Identify major systems, components, and operating parameters, and establish the calculation scope for HyPEP. The objective of this task is to define the scope of system modeling of HyPEP by identifying and hierarchically categorizing the major systems, components and the operating parameters of the NHDD and NGNP. The component hierarchy has been defined and the overview is shown in Figure 1-1. The results form the basis of the plant modeling interface of HyPEP and help define the thermal-hydraulic processes and phenomena to consider in HyPEP development. Three components (node, link, and block) form the basic component from which all other components and systems are derived. Each component or system is treated as an object in the program. Some properties and the methods for the node and the link classes have been defined and implemented in the alpha version of HyPEP.

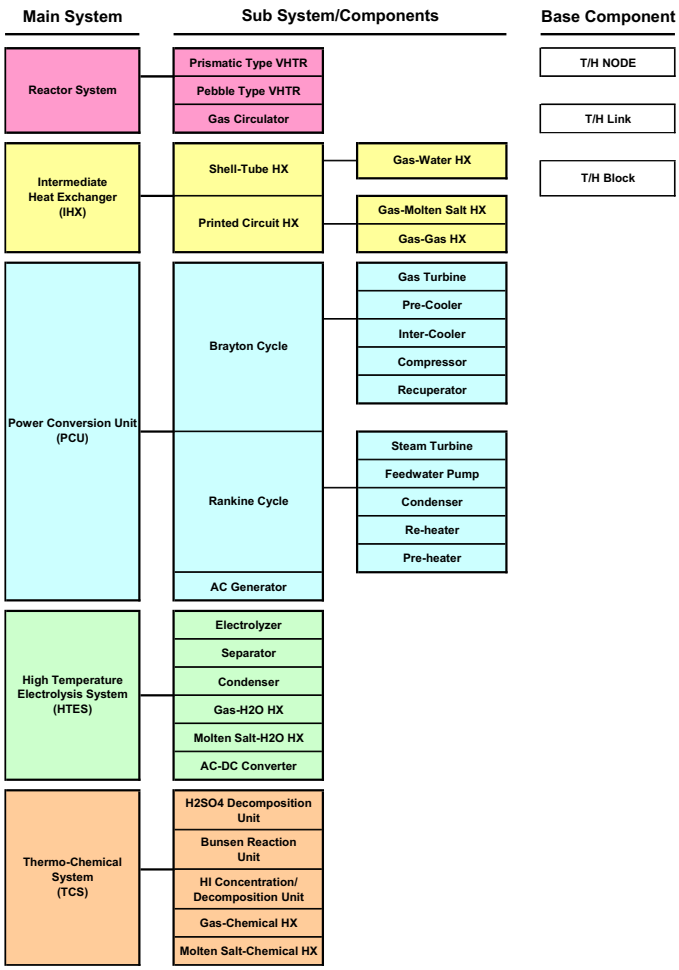

Figure 1-1. Hierarchical System/Component of HyPEP

TASK 2/KAERI : Devise the overall calculation scheme. The numerical solution scheme of HyPEP has been formulated in this task. The outlines of the scheme is as follows:

1) The concept of the node-link-block is basic to the fluid/heat flow network scheme chosen for development.
2) The node represents the thermal-hydraulic volume with scalar properties such as volume, mass, molar or mass fraction of fluid specie, energy, pressure, temperature, and pressure drops.
3) The node component handles the chemical reactions via specialized components for the High Temperature Electrolysis System and Thermo-Chemical System.
4) The link component models the flow between nodes and has such properties as mass flow rate, pressure drop, and the scalar properties of the donor-node.
5) The block component represents the solid structures that conduct or generate heat.
6) The block component also provides models for the solid-to-fluid boundaries where convection occurs.

The basic equations consider the transient mass and energy transport of multi-species fluid mixtures. The equations are setup to conserve mass and energy for the nodes, and a flow relationship using the pressure differences have been setup for the links. These equations have been discretized to evolve a general numerical scheme for gas (or gas mixture) flow network. In the scheme the heat additions and heat transfer through heat exchangers are handled by the blocks that represent the heat structures. General thermo-dynamic routines based on correlations for gas and steam/water have been written for use in the numerical scheme and these routines have been tested. In another effort, further thermodynamic property

routines are developed based on table search with options for user added property tables. The coding of the numerical scheme is in progress.

TASK 3/KAERI: Select modern high-level program language(s) for windows programming environment. Four languages, Visual Basic, C#, Delphi and Fortran, have been evaluated and Delphi program language has been selected as the main development language for the HyPEP development. The language comparison is summarized in Table 1. In part, the selection was influenced by the possibility (or need) to develop the HyPEP for the .NET environment. Whilst studying the program languages, it has surfaced that the current Windows OS is to be superceded by the .NET Operating System, and this was additionally considered in the language selection. Delphi is an object oriented version of the PASCAL language and it has versions for the .NET as well as the win32 environment. As the HyPEP will have strong hierarchical structure, the object oriented program language was deemed to best suit the programming style. The multi-language development environment was also considered where the main drive program will be written using the Delphi language, and sub-programs written in other languages (Mainly Fortran) in order to take advantage of the large scientific libraries available in other languages. Trial programs have been written to test the linking of the main-program and sub-program. More specifically, the use of DLL (Dynamic Link Library) and the sub-program execution by the main-program using the Windows API (Application Program Interface) with data exchange through input/output file exchange.

Table 1-1. Comparison of Major Programming Languages

Features/Comments	DELPHI	C#	Visual Basic	Fortran
Base Language	Pascal	C	Basic	Fortran
Win32 Version	Delphi2005	C++	MS Visual Basic	Compaq, Lahey etc.
NET Version Common Language Runtime	Delphi2005	MS C# Borland C# etc.	MS Visual Basic	Intel Fortran
OOPS Capability	Very Good	Very Good	Good	No
Structured Programming	Good	Good	Good	Poor
Body of ready-made scientific software	Small	Small	Small	Large
Code Reusability	Good	Good	Fair	Poor
Web Programming Capability	Good (ASPX, ActiveX))	Good	Good (ActiveX)	Poor
Integrated Development Environment	Good	Good	Good	Good
Rapid Application Development (RAD)	Good	Fair	Fair	Poor

TASK 4/ALL: Develop component models. The development Graphical User Interface (GUI) for the alpha version of HyPEP has been completed. A screen capture of the GUI for the HyPEP alpha version is shown in Figure 2-1. The HyPEP alpha version is being programmed using the win32 version of the Delphi language.

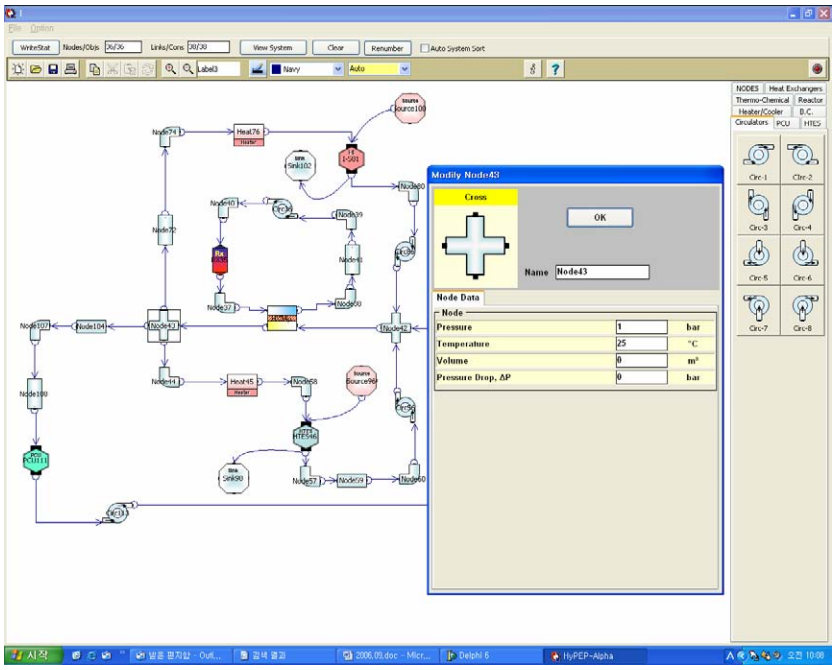

Figure 1-2. Screen Capture of the HyPEP alpha

Various routines have been developed for the GUI and these routines include routines for component generation and deletion, the drag-drop of components, on-screen manipulation of the components, the automatic line generation for the link component, connection maintenance, and thermal hydraulic system build up. The definitions for the object classes TNode and TLink (for Node and Link components) which form the base components for the HyPEP alpha have been setup and are also being tested in the prototype windows form.
The TNode and TLink Objects have been derived from the graphic objects of the main canvas using the inheritance of the Object Oriented Program paradigm. In this way, the correspondence between the object in the graphic canvas and the thermal-hydraulic component can be ensured. Preliminary component templates have been created with a total of 32 components categorized into 9 component categories.

TASK 5/KAERI: Develop cost and Optimization Model This task is to be carried out in the year 2008.

TASK 6/ALL: Identify the program qualification methodology This task is to be carried out in the year 2007~2008.

TASK 7/INL, ANL: System Integration: As part of system integration, INL and ANL developed high-temperature electrolysis model and the power requirement for the HTE was calculated and implemented into the codes being used. INL also calculated the sizing of all the heat exchangers in the coupled VHTR and HTE. Results are presented in Appendix D in this report.

All tasks were performed on schedule and there are no concerns/issues.

Planned Activities

At the end of year 2006, it is expected that a working preliminary version (alpha version) of the HyPEP program will be produced.

Major R&D activities for the year 2006~2008 are as follow:

1) **Basic Equation Setup and Numerical Solution Development**: Robust numerical solution scheme will be developed for the flexible network topology. Ancillary routines to obtain T/H properties, heat transfer correlations, pressure drop correlations, etc. will further be developed and coded. The numerical scheme will be coded to and produce a working code. The program coding will be based on the object-oriented programming techniques. The verification and refinement of the numerical scheme are planned for the third Fiscal Year.

2) **GUI Development**: GUI will be improved with trial user feedback and the bug-fixing will be carried out. Main activity will be the further object class definitions to increase the number of components and the component palettes. The HyPEP alpha version, planned to be completed by October 2006, will be used to test the general behavior of the GUI and to acquire the user feedback.

3) **Component Model Development**: Component specific models will be developed for specialized components. The models to be developed include 1) VHTR and IHX model, 2) PCU T/H Model (Brayton Cycle), 3) HTES T/H Model, and 4) Thermo-Chemical Model (I-S Cycle). The Node, Link and Block component will be further improved. The template for the palette, on-screen input/output template for the component will be defined and developed.

4) **NHDD System Model & Preliminary Calculation**: With the alpha and beta versions of the HyPEP, a simple NHDD System layout will be modeled and preliminary calculations will be carried out to confirm integrity of the numerical scheme and the ancillary routines.

5) **Component Sizing Model Development**: Simple models will be developed to evaluate the component sizing. As the model will basically rely on a database, main task will be the collection and categorization of reliable database.

6) **Cost Model Development**: This model will be a very rough model. Simple model (based on database) to calculate the overnight construction cost will be developed and an algorithm to develop simple interest assessment will be developed and implemented.

7) **HyPEP Verification & Validation**: The HyPEP beta version, planned to be completed by October 2007, the assessments against established codes such as HYSYS , ASPEN, and GAS-PASS/H will be carried out for the program verification and validation.

8) **Development of System OptimizationMethod**: A calculation method/procedure will be developed for the optimization of a Nuclear Hydrogen Production Facility. The HyPEP beta version will be used as the main tool in the method.

Results and Products

The major products of the first year of project are:

1) Document on HyPEP Introduction (due in October 2006)
2) Technical paper presentations at a number of conferences including:

a. C. H. Oh**,** R. Barner, C. Davis, and S. Sherman, "Evaluation of Working Fluids in an Indirect Combined Cycle in a Very High Temperature Gas-Cooled Reactor," Accepted (October 2006) for publication in *Nuclear Technology* in 2006.

b. C. H. Oh, C. Davis, Robert Barner, and Steven Sherman, "Design Configurations for Very High Temperature Gas-Cooled Reactor Designed to Generate Electricity and Hydrogen," ICONE14-89868, the 14th International Conference on Nuclear Engineering, July 17-22, Miami, Fl., 2006.

c. C. H. Oh, R. Barner, C. Davis, and S. Sherman, "Thermal Hydraulic Analyses for Coupling High Temperature Gas-Cooled Reactor to Hydrogen Plant," the 13th International Heat Transfer Conference in Sydney, Australia, August 13-18, 2006.

d. C.H. Oh, C. Davis, S. Sherman, and Robert Barner, "Thermal Hydraulic Analysis of HTGR Coupled with Hydrogen Plant," ANS Annual Meeting, Reno, June 4-8, 2006, pp. 621-622.

e. J. W. Park et al, "Development of Flow Net Solver for HyPEP: A Hydrogen Production Plant Efficiency Calculation", Proceedings of ICAPP'06, June 2006.

3) Alpha version of HyPEP code (due in October 2006).

CONTENTS

1. INTRODUCTION

1.1. Project Description

The Department of Energy envisions the next generation very high-temperature gas-cooled reactor (VHTR) as a single-purpose or dual-purpose facility that produces hydrogen and electricity. The Ministry of Science and Technology (MOST) of the Republic of Korea (ROK) also selected VHTR for the Nuclear Hydrogen Development and Demonstration (NHDD) Project.

The objective of the FY-06 study is (1) to select a reference design that links the reactor, a power conversion system and hydrogen process through an intermediate heat transfer loop (2) to identify key requirements and assumptions, (3) to define methods to be used, (4) to provide ROK collaborators with detailed models of system components such as heat exchanger and others with appropriate heat transfer correlations for their HyPEP development.

HyPEP computer program will have the capability to model and to calculate the electrical generation efficiencies of a Brayton or Rankine cycle, and the hydrogen production efficiencies of the high temperature electrolysis and the S-I thermo-chemical cycles. The primary application of HyPEP will be for the VHTR (Very High Temperature Reactor) coupled to hydrogen production plants such as NHDD. The principal applications for HyPEP are in the scoping analyses on plant configurations, and the optimizations on various design and operating parameters. HyPEP will be developed to run under the PC-Windows environment and will use the Graphic User Interface (GUI) extensively to enhance user friendliness. HyPEP will be available to support analyses for both the United States and Korean governments.

1.2. Background

The abundant cheap fossil energy resources such as oil and coal fuelled the great technological advances of the 19^{th} and 20^{th} that have dramatically improved the quality of human life. However, the massive use of fossil fuels has brought serious problems in pollution and global warming. In particular, if the current rate of oil usage is continued, the oil is forecasted to be depleted in the 21^{st} century. The supply of high quality energy at a reasonable price is essential to maintain and improve the quality of life, and there is an urgent need to develop energy resources to replace oil.

Hydrogen is being promoted as the future energy-carrier under the proposed “hydrogen economy” scheme. Hydrogen is proposed to replace oil primarily in the transportation sector. Hydrogen may be burned in an Internal Combustion Engine (ICE) or oxidized in fuel cells to provide the motive power. Hydrogen is environmentally clean as the byproduct of hydrogen burn or oxidation is pure water. Although hydrogen is the most abundant element in the universe, hydrogen in molecular form (H_2) does not exist in appreciable quantities on earth. Thus, it is necessary to produce molecular hydrogen from base materials such as water or methane using energy from such primary sources as coal, solar, wind or nuclear energy.

The Nuclear Hydrogen Initiative (NHI) calls for the demonstration of hydrogen production technologies utilizing nuclear energy. The goal is to demonstrate hydrogen production compatible with nuclear energy systems by way of scaled demonstrations, and then to couple a commercial-sized demonstration plant with a Generation IV demonstration facility by approximately 2015. The process of producing the hydrogen from water is highly energy intensive and the efficiency of the process depends on different factors for different processes. The high temperature electrolysis and the thermo-chemical cycles can produce hydrogen from water and these processes are being developed.

For the demonstration of hydrogen generation using nuclear power, the INL (Idaho National Laboratory) in the US, and KAERI (Korea Atomic Energy Research Institute) in the Republic of Korea have proposed the developments of the VHTR (Very High Temperature Reactor) and the NHDD (Nuclear Hydrogen Development and Demonstration), respectively. The potential layouts of the VHTR and NHDD are shown in Figure 1-1 and Figure 1-2.

Both plants use the VHTR (Very High Temperature Reactor) to supply the power, while they are designed to use two different hydrogen production processes; the high temperature electrolysis and the I-S thermo-chemical process. The VHTR is used because the high temperature is essential in maximizing the hydrogen production efficiencies for both electrolysis and the thermo-chemical process.

In order to optimize the designs of such plant systems as VHTR and NHDD, it is necessary to be able to evaluate the operating parameters and production efficiencies of various design layouts. The presently proposed project aims to develop a computer program HyPEP to easily and quickly evaluate the efficiencies and operating parameters.

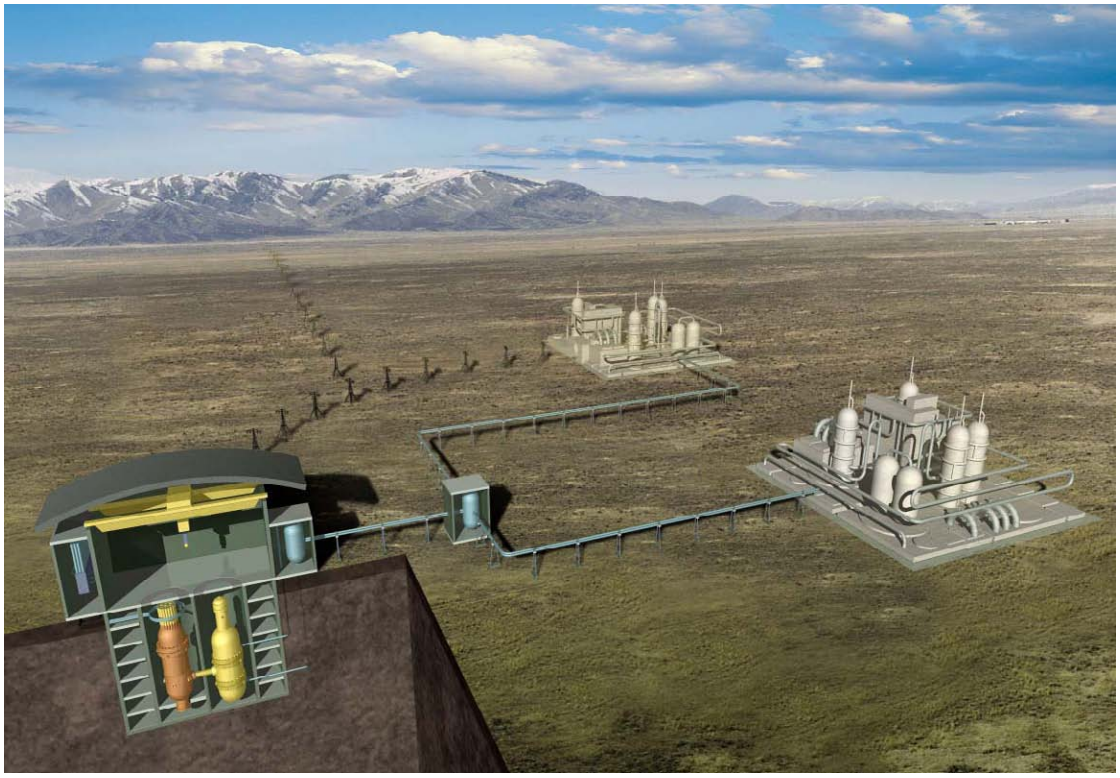

Figure 1-1. Potential Layout of VHTR for Hydrogen Production.

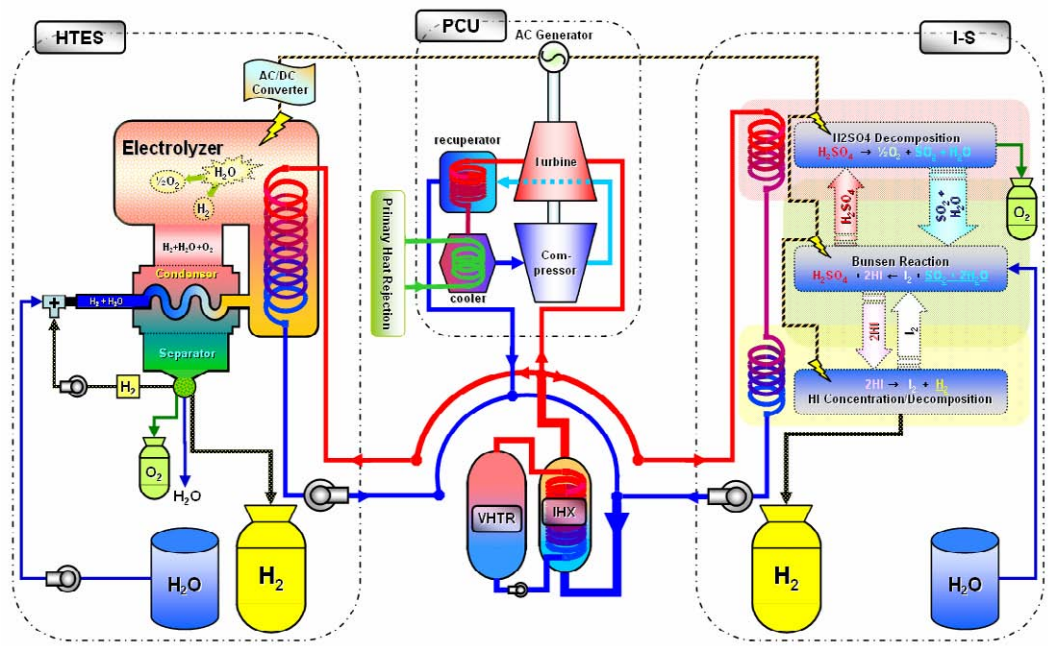

Figure 1-2. Potential Layout of Proposed NHDD Plant.

2. REFERENCE DESIGN

A reference design of a coupled nuclear reactor and hydrogen production plant has been established to aid in the development of HyPEP. The reference design incorporates many of the systems and components that HyPEP must eventually be able to model. The reference design is expected to be representative of the eventual design and will be used to focus the development of HyPEP. The reference design has not been optimized and many changes are expected between the concept described here and any design ultimately selected for hydrogen production.

The reference design contains a high-temperature gas-cooled reactor that is used simultaneously for the production of electricity and hydrogen. Less than 10% of the nuclear reactor's thermal energy is dedicated to hydrogen production, consistent with that expected in early demonstration plants, such as the Next Generation Nuclear Plant (NGNP) (MacDonald et al. 2003). The power conversion unit (PCU) utilizes an indirect electrical cycle based on the recommendations of the Independent Technology Review Group (2004) for the NGNP. An intermediate heat transport loop is used to transfer heat from the nuclear reactor to the hydrogen production plant and to provide separation between the nuclear and hydrogen plants. Helium is used as a working fluid in both the secondary coolant system and the intermediate heat transport loop. The hydrogen production process is based on the thermochemical sulfur-iodine cycle described by Brown et al. (2003). A schematic of the reference design is illustrated in Figure 2-1. Various systems are described in more detail below.

An alternative design is the high temperature electrolysis process (HTE). GA report (2002) indicates that due to lack of thermodynamic models, GA was not able to regress the simple H_2SO4/H_2O and GA did not even attempt to regress more complicated systems of $HI/I_2/H_2O$ along with $H_2SO_4/HI/I_2/H_2O$ in the S-I thermo chemical process.

Therefore, until the thermodynamic model is developed, the full-detailed ASPEN PLUS model on the S-I process is not accurate when the ASPEN's ELECNRTL thermodynamic model is used. Without the thermodynamic model, HYSYS cannot be used for the S-I process model either. We expect to obtain thermo-equilibrium data of the S-I process from CEA/Grenoble in France next year. Therefore, for FY-06 study, our research focus was in HTE process. A typical simplified model is shown in Figure 2-2.

The HTE process is simpler than that of S-I process. The detailed coupling of VHTR and HTE was not included in the original proposal. In order to evaluate the potential hydrogen production performance of large-scale HTE operations, INL has developed a detailed process flowsheet that includes all of the components that would be present in an actual plant such as pumps, compressors, heat exchangers, turbines, and the electrolyzer. Since the electrolyzer is not a standard HYSYS component, a custom one-dimensional electrolyzer model was developed and optimized for incorporation into the overall HYSYS process flowsheet. This electrolyzer model allows for the determination of the operating voltage, gas outlet temperatures, and electrolyzer efficiency for any specified inlet gas flow rates, current density, cell active area, and external heat loss or gain. Then the model will be incorporated into the reference design and the entire detailed major component sizing calculations can be performed. HYSYS calculations were performed and some preliminary results are presented in this report.

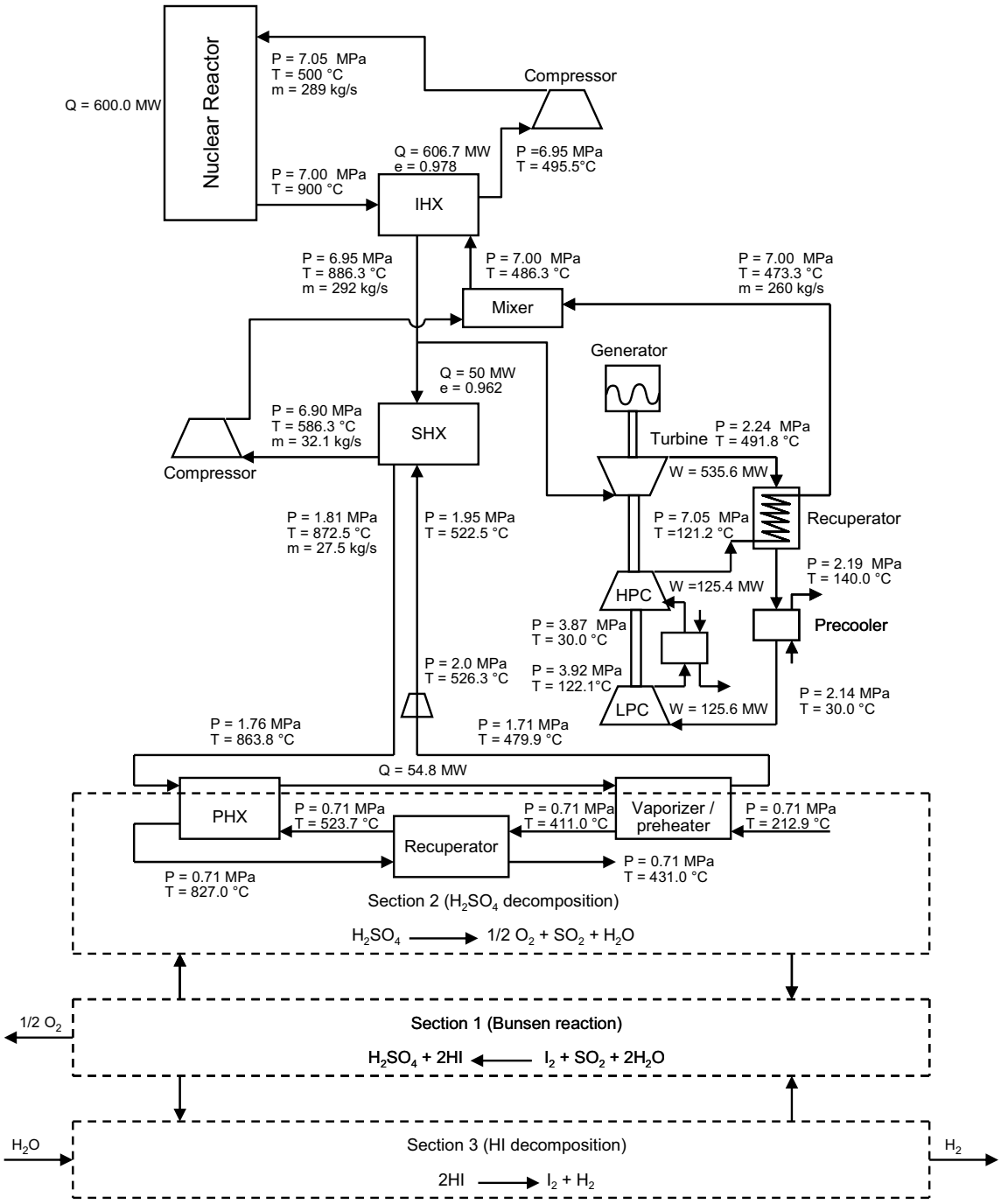

Figure 2-1. Schematic of the reference design of the integrated nuclear and hydrogen production plants.

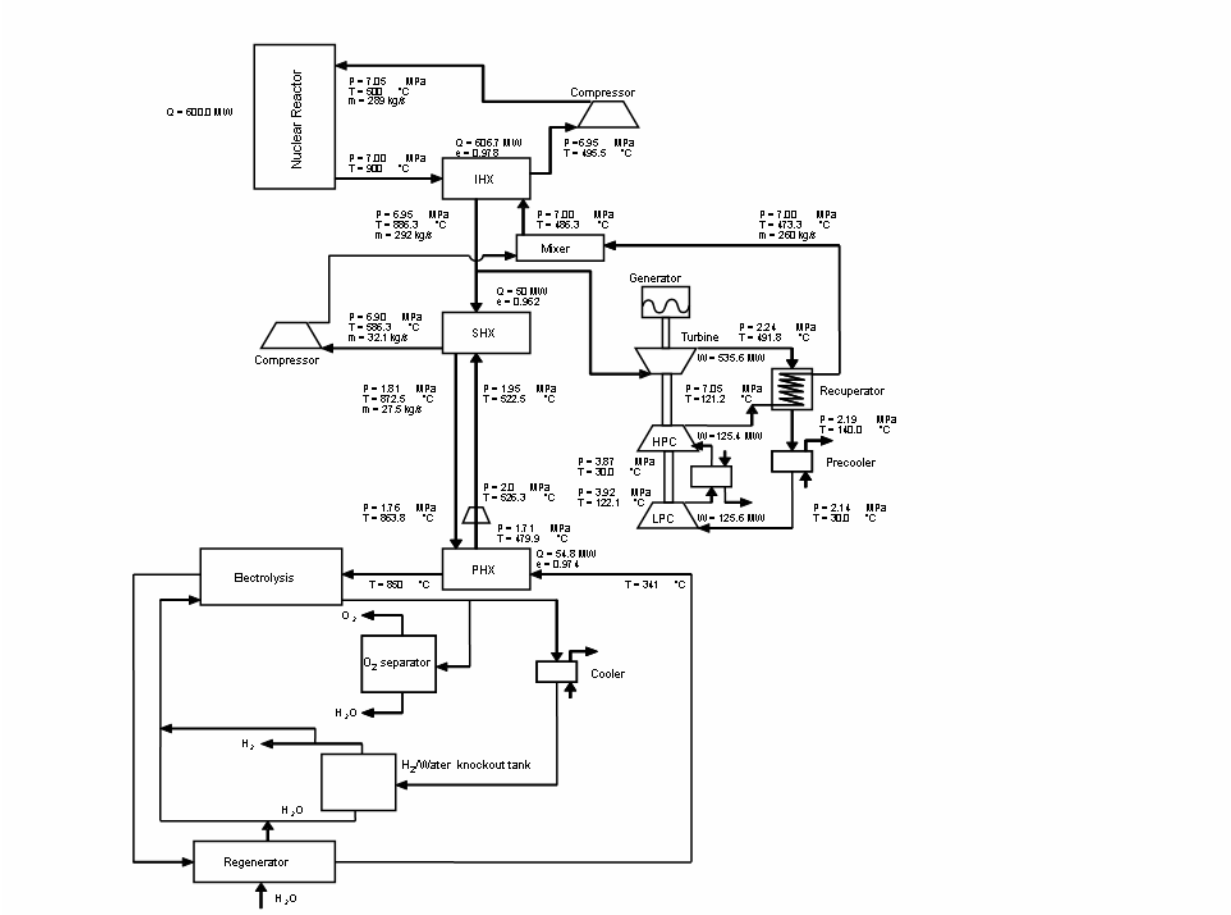

Figure 2-2. Schematic of the alternative reference design of the integrated nuclear and hydrogen production plants.

The working fluid selection affects the cycle operating condition, the efficiency, and the size of the unit-operation components, which will be a major factor for the system cost. Some fluids such as CO_2 are not recommended for use in the direct cycle due to chemical reactions with the graphite matrix in the VHTR core at temperatures greater than 550^0C, due to heat transfer, neutronics impacts, or activation concerns. For the indirect cycles, there exists a freedom to examine a number of working fluids. These coolants will be examined to see if they provide improved efficiency, cost reduction or reduced development risk when compared to a baseline cycle.

For this study, the following working fluids will be investigated:

Helium in the primary, the secondary, and the tertiary loop.

Molten salts in the primary and the tertiary loop

CO_2 in the secondary and tertiary loop.

A number of the power conversion unit (PCU) will be studied to determine if the best overall configuration can be found. The PCU configurations to be examined are a recuperated gas Brayton cycle and recuperated combined cycle.

2.1 Primary Coolant System

The primary coolant system is assumed to consist of a nuclear reactor, an intermediate heat exchanger, and a circulator. The nuclear reactor is assumed to be a high-temperature helium-cooled reactor. The reactor core is assumed to contain prismatic fuel blocks similar to those in the Gas Turbine-Modular Helium Reactor (GT-MHR) (General Atomics 1996). Because of the expected simplicity of the HyPEP reactor model, a pebble bed reactor could be simulated by changing the pressure drop across the core.

The assumed thermal-hydraulic parameters for the primary coolant system are described by Davis et al. (2005) and are summarized in Table 2-1.

Table 2-1. Thermal-hydraulic parameters assumed for the primary coolant system.

Parameter	Value
Coolant	Helium
Pressure, MPa	7.0
Power, MW	600
Outlet temperature, °C	900
Temperature rise, °C	400
Differential pressure, MPa:	
Core	0.05
IHX	0.05

2.2 Secondary Coolant System

The secondary coolant system of the reference design consists of a PCU that is arranged in parallel with a secondary heat exchanger (SHX) that directs less than 10% of the reactor power towards the hydrogen production plant. This arrangement corresponds to Configuration 6 recommended by Davis et al. (2005) for an indirect electrical cycle.

The PCU contains a turbine, two compressors, and an electrical generator that are located on a single shaft. The PCU also contains a recuperator, precooler, and another cooler located between the low pressure compressor (LPC) and the high pressure compressor (HPC). Two compressors and coolers are used to improve the efficiency of the electrical cycle. The thermodynamic states at various locations in the PCU were determined by Davis et al. (2005) and are summarized in Figure 2-1. The PCU heat exchangers were not sized. Although Davis et al. made assumptions concerning their performance, the actual geometries of the heat exchangers were not determined.

The IHX and SHX are assumed to be printed circuit heat exchangers (PCHEs) with straight semi-circular flow channels. The flow channels are contained within plates. Half of the plates are assumed to contain hot fluid, while the others contain cold fluid. The flow path is characterized by the diameter of the semi-circular channels, the pitch between adjacent channels in a plate, and the thickness of the plate. Davis et al. (2005) assumed a channel diameter of 1.5 mm and estimated the pitch-to-diameter and thickness-to-diameter ratios based on a simplified stress analysis. Although more rigorous stress calculations would probably result in larger ratios, these estimates are considered to be sufficiently representative to be used in the reference design. These inputs can be easily changed in HyPEP once

better data become available. Davis et al. adjusted the width of the front face of the heat exchangers, which were assumed to be square, and the channel length to obtain the desired pressure drop in the hot fluid and thermal performance. The resulting geometries of the IHX and SHX are summarized in Table 2-2. Thermodynamic states were shown previously in Figure 2-1.

Table 2-2. IHX and SHX parameters.

Parameter	IHX	SHX
Nominal power, MW	600	50
Differential pressure (hot / cold), MPa	0.050 / 0.050	0.050 / 0.14
Heat exchanger width, m	4.77	1.51
Flow channels:		
Diameter, mm	1.5	1.5
Pitch-to-diameter ratio	1.20	1.5
Thickness-to-diameter ratio	0.57	0.78
Length	2.26	1.11

HyPEP should be flexible enough to accommodate alternate PCHE designs. Specifically, the options to account for zigzag, rather than straight, flow channels and different numbers of hot and cold plates should be allowed. For example, Ishizuka et al. (2005) measured pressure drop and heat transfer data for a PCHE in which the flow channels had zigzags. The PCHE also had half as many cold plates as hot plates. These modifications result in a more compact, and presumably cheaper, heat exchanger than would be obtained otherwise. It is likely that the eventual design will incorporate similar modifications to enhance the heat transfer and reduce the size of the heat exchangers.

2.3 Intermediate Heat Transport Loop

The intermediate heat transport loop transfers heat from the nuclear reactor to the hydrogen production plant and provides physical separation between plants, which should make the nuclear plant easier to license. Estimates for the required separation distance between the nuclear and hydrogen plants depend on the design and safety criteria applied and vary considerably. For example, Verfondern and Nishihara (2004) calculated 300 m for the High-Temperature Engineering Test Reactor in Japan whereas Sochet et al. (2004) recommended 500 m for the High-Temperature Reactor. Smith et al. (2005) recommended a separation distance of from 60 to 120 m for the NGNP and the hydrogen production plant. A separation distance of 90 m is used for the reference design based on the value selected by Davis et al. (2005). The separation distance primarily affects the diameters and insulation requirements of the hot and cold legs in the heat transport loop.

Based on the analysis of Davis et al. (2005), the hot and cold legs of the intermediate loop are assumed to be separate pipes in the reference design. To limit stresses, the working fluid is assumed to be low-pressure helium as shown in Figure 2-1.

Table 2-3 provides parameters for the piping of the intermediate heat transport loop. These parameters are based on the analysis of Davis et al. (2005). Thermodynamic states are presented in Figure 2-1.

Table 2-3. Intermediate heat transport loop piping parameters.

Parameter	Hot leg	Cold leg
Differential pressure, MPa	0.050	0.050
Heat loss, MW	1.25	0.54
Length, m	90	90
Inner diameter, m	0.443	0.412
Pipe thickness-to-diameter ratio	0.11	0.01

Liquid salts are more efficient for transporting heat over long distances than helium and thus may ultimately be selected as the working fluid. Therefore, HyPEP should have the capability to simulate liquid salts as potential working fluids.

The intermediate heat transport loop is assumed to be coupled to the hydrogen production plant through two heat exchangers as shown in Figure 2-1. The first heat exchanger preheats and partially vaporizes the H_2SO_4/H_2O mixture. The mixture is fully vaporized by a recuperator that is located entirely within the hydrogen production plant. The mixture is then heated up to its maximal temperature by a process heat exchanger (PHX) that takes heat from the intermediate heat transport loop. The thermodynamic conditions given in Figure 2-1 on the hot side of the preheater/vaporizer and the PHX were taken from the values given by Davis et al. (2005). The thermodynamic conditions on the cold side of these heat exchangers were based on the values given by Brown et al. (2003).

Davis et al. (2005) assumed that the PHX was a tube-in-shell heat exchanger, with the process fluid on the tube side. Brown et al. (2003) assumed that the PHX was a PCHE. Lillo et al. (2005) did a simple analysis comparing the relative surface area required for the catalyst versus that required for heat transfer. For the tube-in-shell heat exchanger, the catalytic size requirements were somewhat more limiting that the thermal requirements. For the PCHE, the size was definitely controlled by the catalytic requirements. In fact, for reasonable channel diameters, the PCHE was actually larger than the tube-in-shell heat exchanger. Thus, a tube-in-shell heat exchanger was selected for the PHX in the reference design. HyPEP needs to have the capability to model tube-in-shell heat exchangers anyway because this type of exchanger is common in PCUs and chemical plants.

PHX parameters are summarized in Table 2-4. These parameters are based the values given by Davis et al. (2005). Note that the specification of PHX parameters is incomplete because the PHX has not yet been sized to meet the thermal and catalytic requirements for coupling the intermediate heat transport loop to the hydrogen production plant.

Table 2-4. PHX parameters.

Parameter	Value
Tube inner diameter, cm	1.0
Tube thickness-to-inner diameter ratio	0.15
Tube pitch-to-outer diameter ratio	1.3
Tube pitch	Triangular

Parameters for the preheater/vaporizer are not yet available. For the purposes of the reference design, any configuration that results in thermodynamic states at the inlet of the PHX and the outlet of the preheater/vaporizer on the hot side and the inlet of the preheater/vaporizer and the outlet of the PHX on the process side would be acceptable.

2.4 Hydrogen Production Plant

The hydrogen production process in the reference design is based on the thermochemical sulfur-iodine cycle described by Brown et al. (2003). As illustrated in Figure 2-1, the cycle is represented by three sections. The first section represents the Bunsen reaction, which generates sulfuric and hydroic acids and produces oxygen. The second section receives heat from the intermediate heat transport loop to concentrate and decompose the sulfuric acid. The third section, which receives distilled water as a feedstock, decomposes the hydrogen iodide and produces hydrogen.

General Atomics has been working on improving the thermochemical cycle. A report describing the improved cycle is expected in April of 2006. It is expected that the thermochemical portion of the reference design will be revised once the new results from General Atomics are available. As indicated in Section 2, S-I process was not simulated in FY-06 due to lack of thermo-chemical equilibrium data.

The hydrogen production process in the reference design is based on the HTE. A research program is under way at INL to simultaneously address the research and scale-up issues associated with the implementation of planar solid-oxide electrolysis cell technology for hydrogen production from steam. A typical electrolyte stack is shown in Figure 2-3. A 90 % (mole fraction) of steam and 10% hydrogen is fed into the electrolyte at 850 C. Steam is converted to hydrogen at the cathode and oxygen is produced at the anode that is swept out by air or other sweeping gas.

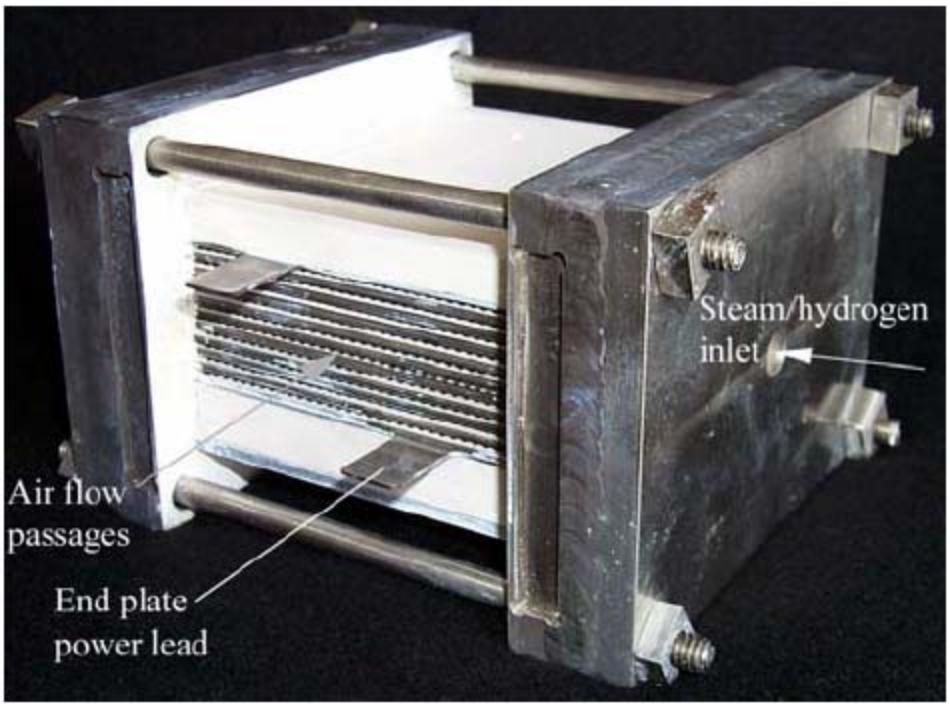

Figure 2-3. Solid-oxide electrolysis cell (Hawkes et al., 2005).

2.5 Requirements

The selection of the reference and alternative designs imposes requirements that HyPEP must satisfy if it is to be capable of representing the combined nuclear, PCU, and hydrogen plants. These requirements are related to the working fluids, components, and phenomena that must be modeled. The

working fluids, components, phenomena associated with the reference design should have the highest priority for HyPEP development. The fluids, components, and phenomena associated with the alternate designs can be added as needed or as time becomes available.

HyPEP must be able to simulate many different fluids to represent the combined plant. For the reference design, these fluids include helium, sulfuric acid, water, hydrogen iodine, iodine, and hydrogen. HyPEP must be able to simulate mixtures in which the concentrations of the various components vary as a function of position to represent the thermochemical cycle. HyPEP needs to simulate additional fluids to represent the alternative designs. These fluids for the IHTC include supercritical carbon dioxide, nitrogen, and liquid salts.

The reference design contains the following components: a nuclear reactor, heat exchangers, compressors, pumps, turbines, generators, separators, scrubbers, and other specialized equipment used in chemical plants. The reference design includes PCHE and tube-in-shell heat exchangers. Alternate heat exchangers, such as an offset strip fin type, probably need to be considered.

HyPEP should model various phenomena associated with the components described above. Descriptions of important phenomena that HyPEP must simulate are provided below.

Nuclear reactor: The nuclear reactor will be modeled simply as a heat source with a specified flow and pressure drop. The effects of these parameters on the overall efficiency of the plant need to be accounted for, but internal details, such as fuel temperature, do not need to be simulated.

Turbomachinery: The most important phenomenon associated with these components is efficiency. In order to perform optimization studies, HyPEP should be able to determine efficiency and head as a function of flow and temperature.

Heat exchangers: Two important parameters associated with these components are heat transfer and pressure drop. To simulate the heat transfer, HyPEP must be able to simulate the thermal resistances associated with convection and heat conduction. The model should be able to account for the effects of wavy channels in the PCHE on heat transfer and pressure drop. Either laminar or turbulent flow conditions may occur. Multi-node models are probably required to represent heat exchangers in which phase change occurs, such as steam generators, to account for the different heat transfer regimes including forced convection to liquid, nucleate boiling and forced convection to vapor.

3 HyPEP Development

3.1 Introduction

The viability of hydrogen as an economical energy carrier will depend much on how economically the hydrogen can be produced. This in turn is linked directly to the efficiency of the hydrogen production plant. It is therefore important to accurately evaluate the efficiency of the hydrogen production facility and the overall cost of the hydrogen production. The overall efficiency of the hydrogen production depends not only on the efficiencies of individual components but also how the plant system is configured.

The HyPEP (Hydrogen Production Efficiency Calculation Program) is conceived to calculate the hydrogen production efficiencies for different hydrogen production facility layouts. Y. J. Lee et al. aim to design HyPEP to rapidly evaluate the overall hydrogen efficiencies for plant configurations that are built on-screen by the user.

The HyPEP will have models and components that will be sufficiently sophisticated to allow build-up of complex plant layouts with multiple hydrogen producing systems configured in parallel or in series. In addition, simple basic cost-analysis and the component sizing models will be incorporated to allow rudimentary estimation of the hydrogen production cost.

The HyPEP is being developed in three stages following the normal software development stages. There will be two major developmental versions of HyPEP before the final version is developed. The alpha version is basically the test bed for the program developers and will be very limited in capability. Main purpose of the alpha version is to 1) examine whether the overall program structure is indeed workable, 2) improve and bug-fix the GUI and the T/H system build up logic of the HyPEP code, and 3) provide the platform on which to test the numerical scheme and 4) provide the platform on which the model developers can test their numerical models. The first alpha version of HyPEP will be developed by the October 2006.

The full implementation of system numerical scheme will conclude the alpha version development and the next major developmental version, the HyPEP beta version, will be released to the test users. The beta version is expected to be released by October 2007. The main purpose of the beta version is to 1) test numerical performance through Validation &Verification, 2) provide platform on which to incorporate the component sizing mode and the cost analysis model.

3.2 Features and Program Layout

The final version of HyPEP will be capable of :

1) The evaluation of
   - hydrogen production efficiency of the thermo-chemical processes
   - hydrogen production efficiency of the electrolysis processes
   - electricity generation efficiency
2) The assessment of the component sizing for major components of the plant.
3) The estimation of the plant construction cost.

The primary application area of HyPEP will be the scoping analysis for plant layout optimizations. However, the HyPEP is not conceived to be used for applications in plant transient analyses.

The HyPEP is being designed in such a way to allow flexible modeling of the hydrogen production plant layouts. For the Input/Output interface, major emphases are placed on the use of the GUI (Graphic User Interface) features to make the HyPEP a very user-friendly application program. The user will be able to construct most of the desired simulated plant system 'on-screen' using the plant system canvas of the HyPEP. For this, the GUI will provide various component/system palettes consisting of multiple pages of basic and pre-made components or sub-systems. The conceptual schematic layout of the canvas and the component/sub-system layout is shown in Figure 3-1.

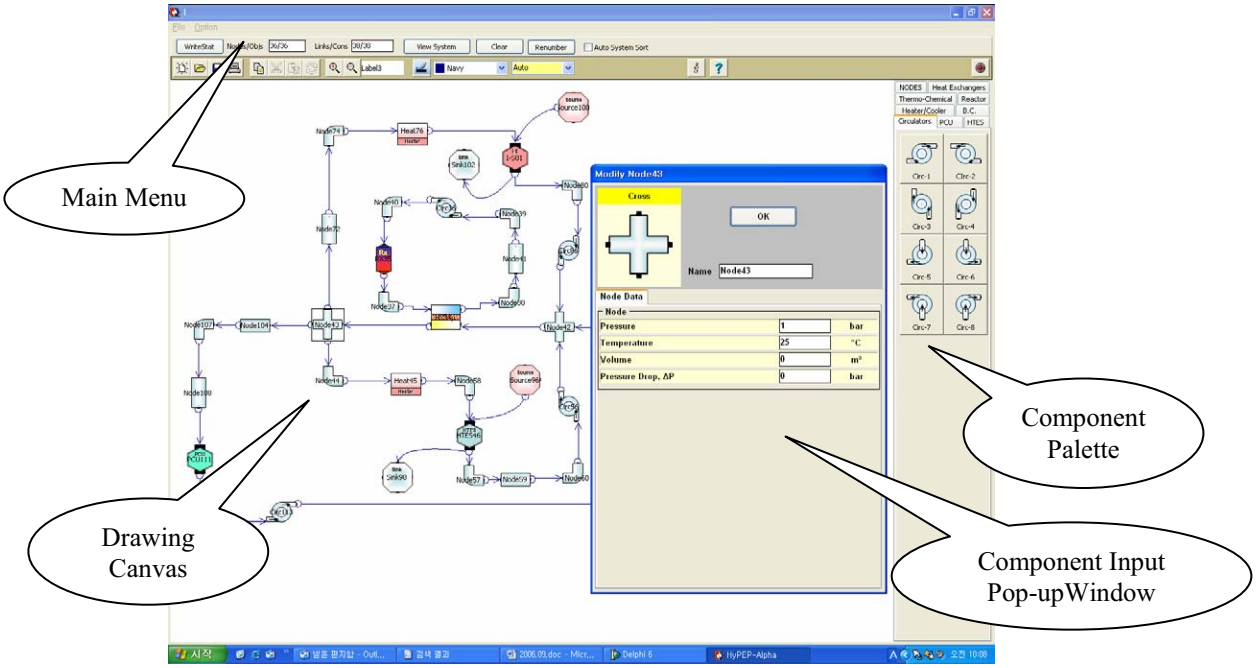

Figure 3-1. Basic Layout of the HyPEP Program.

With HyPEP, users are able to build the simulated plant system by dragging and dropping the necessary components or (ready-made) sub-systems from the component palettes onto the drawing canvas. The user then uses the link-class components to connect the components or sub-systems on the canvas. The user can activate the on-screen pop-up menus (e.g. by right-clicking the components) to enter the necessary inputs. All these functionalities are accomplished by extensively using the GUI.

In later developmental versions, the palettes of the often used components and the ready-made systems are to be provided to simplify the input process. The thermal hydraulic calculations will be carried out as the inputs are completed and the major thermo-hydraulic parameters will be displayed on-screen as they are calculated. Other T/H parameters will be displayed in output windows as well as in the component information windows.

The resulting thermodynamic states and the consumption and the generation of the hydrogen, electricity and the heat of each component can be accessed via right clicking the components which will bring up the sub-windows (or menus) with relevant inputs and calculated outputs.

The HyPEP carries out the bookkeeping on the total electricity, heat and the hydrogen used and generated in the system to estimate the overall hydrogen production efficiencies.

3.3 Program Structure

The HyPEP is being developed with hierarchical program and the data structures. To design the overall structures, it was necessary to first identify and hierarchically categorize the major systems, components and the operating parameters of the foreseeable nuclear hydrogen production plant designs. The results have been used to establish the hierarchical system/component data structure which defines the thermal-hydraulic processes and phenomena that need to be considered in HyPEP. Thusly, the basis of the plant modeling of HyPEP has been established and the established modeling basis has been used to design the component/system palette.

For the nuclear hydrogen production facility, the major system components that form the top-tier hierarchical group include Reactor System for the generation of nuclear power, Power Conversion Unit (PCU) for the electricity generation, and the High Temperature Electrolysis System (HTES) and Thermo-Chemical System (TCS) for the hydrogen generation.

The top-tier components contain sub-systems and/or components. The Reactor system will include as its sub-systems and components, the pebble type VHTR, prismatic type VHTR, Intermediate Heat Exchanger (IHX), and gas circulator. The PCU system will include the Brayton cycle, Rankine cycle, and electricity generator. The Brayton cycle will include gas compressors, gas turbines, a recuperator and coolers. The Rankine cycle will include steam generator, steam turbine, condenser, pump, reheating and superheating circuits. The HTES will include heat exchangers, electrolyser, AC-DC converter, condenser, separator, gas circulator, and water pump. For the current project, the TCS will only consider the I-S thermo-chemical process. The I-S thermo-chemical process will include the H2SO4 decomposition unit, Bunsen reaction unit, HI concentration/decomposition unit, gas circulator, water pump and heat exchangers.

The hierarchical form of program/data structure is well suited to take advantages of the Object Oriented Programming (OOP) techniques described by Bertrand Meyer, and the HyPEP will be programmed using the OOP techniques. The OOP has the advantages in the 1) Code robustness and fault tolerance, 2) code reusability, 3) program security, and 4) Code extensibility. In HyPEP, the components and the sub-systems of the simulated plant system will be represented by the ‘objects’ in the program.

An object is defined via its class, which defines and determines the properties and the methods about an object, and the objects are the individual instances of a class. For example, an object named ‘helicalHX’ can be created (or “instantiated”) from the class “THeatX.” The “THeatX” class defines what a heat exchanger object is, that is, its data structure and all the methods (or actions, functions) that it can perform. For HyPEP, a library of object classes matching the hierarchical data/component/system structure will be built (or programmed) using the inheritance and the polymorphism features of the OOP. The inheritance and the polymorphism features of the OOP will facilitate easy derivation of other object-classes from the parent class.

The inheritance feature allows easy creation of sub-classes (or children class) of an object-class. The polymorphism feature allows easy creation of variations of an object class.

For example, the “TPrintedCircuitHX” class can be created from the “THeatX” class using the inheritance feature of the OOP by adding properties (data) and methods (routines) specific to printed circuit heat exchanger to the generic a heat exchanger class “THeatX”. Whereas, the “TPrintedCircuitHXwithSquareCrossSection” object class can be created by changing the heat transfer coefficient calculation routine (Object’s method) of the “TPrintedCircuitHX” class to that specific to square cross section.

In order to effectively write and to maintain the HyPEP program, use of a modern programming language with Object Oriented Programming (OOP) features will be pursued. The inheritance, polymorphism, and encapsulation provided in OOP languages are well suited in modeling the hierarchical structure of the system and component models of HyPEP.

For the Microsoft Windows® operating system, a number of excellent development environments with modern OOP languages exists. Examples are the Microsoft Visual Studio development environment for Visual C++ and Visual Basic, and Delphi® for the rapid application development environment.

The factors to consider in the language selection are;

1) Windows programming capability.
2) Ease-of-use in application of windows API (Application Program Interface) functions and procedures.
3) Rapid program development environment.
4) Code reusability.
5) Code robustness and fault tolerance.
6) Code extensibility.
7) Amenability to interface with other program languages.

At present, it is also open to option to program the HyPEP for the .NET environment. The major advantage of the .NET environment is that the language dependence can be largely eliminated.

3.4 HyPEP Overall Numerical Scheme

The thermal hydraulic formulation of the HyPEP is based on the conservation of mass and energy equations and models for the flow network of multi-species fluid systems. The flow network is made up of systems and components. For the hydrogen production systems, the HyPEP needs to consider mass and energy conservation of multi-species fluid that undergo chemical reactions. In HyPEP, simplified form of the mass and energy transport equations are applied for different chemical species.

The node-link-block comprise the basic Flow/Heat Network for HyPEP. The node is used to represent the thermal-hydraulic volume with scalar properties such as volume, mass, molar or mass fraction of fluid specie, energy, pressure, temperature, and pressure drops. However, the node component is not designed to handle the chemical reactions. The chemical reactions are handled by specialized components in HTES and TCS. The link represents the flow between nodes and has such properties as mass flow rate, pressure drop, and scalar properties of the donor-node. Block component is used to represent the solid structures that conduct or generate heat. Block component also provides the solid-to-fluid boundaries where convection occurs.

The basic equations consider the steady-state mass and energy transport of reactive multi-species fluid mixtures. The equations have been setup to conserve mass and energy. Thermo-dynamic tables for the fluid mixtures have been setup and the procedures for calculating the properties from the correlations have been devised. However, fast and efficient routines will be devised based on the property table search to improve the execution time. The thermal hydraulic property calculation routines (based on correlations) for the following fluids have been coded and tested:

1) Hydrogen
2) Water
3) Steam
4) Oxygen

5) Carbon dioxide
6) Air
7) Nitrogen.

In addition, to allow user to add fluids, options will be provided for the user to add property tables via external input files.

The node-link-block network scheme and the basic equation setup will be integrated to devise the overall numerical solver. The numerical scheme will be devised to ensure conservation of the mass and energy of the systems and components. The numeric solver will be developed principally for the steady-state operation but with the provisions for further extension to include mild transient calculations.

The flow net of HyPEP will contain all major components associated with the hydrogen generation facility. The user will build the electronic representation of the flow net using the Flow Net Builder which is a part of the HyPEP GUI, which will process the user-specified component data and the boundary conditions.

The Solution Matrix Generator, then, utilizes the electronic flow net and produces the solution matrix which is determined by the discretized form of the flow governing equation. The temporal part of the discretized governing equation will be able to characterize the transient behavior of the flow net. However, for the steady-state condition, the flow net can be solved by using solely the spatial part. The Solution Matrix Generator is able to generate both the temporal and the spatial parts from the information of the electronic flow net. The Flow Net Solver employs solving techniques which can be categorized by: 1. the iteration of the solution matrix 2. the direct inversion of the solution matrix 3. the iteration with minor flow modifiers. In general, the flow net can be conveniently solved by using the iterative method when the diagonal dominance is guaranteed.

The diagonal dominance of the solution matrix, therefore, should be checked before choosing the solution strategy. Most of flow net with simple topology will exhibit diagonal dominance. For the flow net of complex topology, the iterative method may not be used. When the solution matrix does not show diagonal dominance, the Solution Strategy Chooser will pick the direct inversion or the iterative method with minor flow modifier.

After all the thermodynamic conditions are calculated, the production and the consumption in each component for hydrogen, electricity and the heat will be evaluated to assess the plant hydrogen production efficiency.

The discretized form of the flow-net solution scheme developed with the view to implement in HyPEP is presented as follows:

For the FlowNet solver, following method can be adopted as the numerical scheme. For a simple fluid connection layout basic continuity equations are set up :

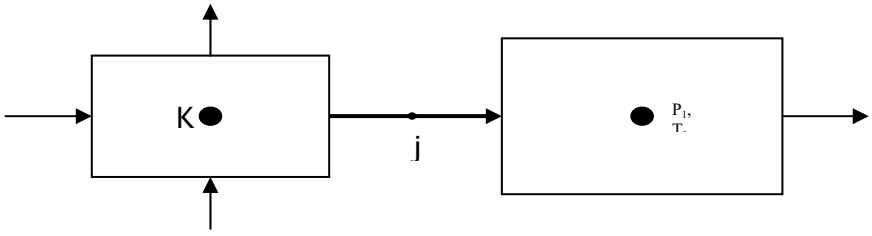

Mass Continuity (for node)

$$V\frac{\partial \rho}{\partial t} = \sum_{j=1}^{N_j} \tilde{\rho}_j A_j \, u_j + S_m V \tag{3-1}$$

Energy Continuity (for node)

$$V\frac{\partial (\rho h)}{\partial t} = \sum_{j=1}^{N_j} \tilde{\rho}_j \tilde{h}_j A_j \, u_j + S_h V$$

$$or, \quad V\left(\rho\frac{\partial h}{\partial t} + h\frac{\partial \rho}{\partial t}\right) = \sum_{j=1}^{N_j} \tilde{\rho}_j \tilde{h}_j A_j \, u_j + S_h V \tag{3-2}$$

For the consideration of the velocity the simple flow relationship is used rather than the momentum conservation equation. This will simplify the solution method greatly as the detailed considerations of the momentum correlations are not needed.

Flow Relationship (for link j)

$$f_T \frac{\rho u^2}{2} = (P_K - P_L) + \Delta P_{K,source} + \Delta P_{extra} \tag{3-3}$$

where

V = *volume of node* (m^3)

u = *fluid velocity* (m/s)

ρ = *density* (kg/m^3)

$\tilde{\rho}$ = *density of donor node* (kg/m^3)

h = *enthalpy* $(Joule/kg)$

$\tilde{h}$ = *enthalpy of donor node* $(Joule/kg)$

A_j = *flow area of link* (m^2)

N_j = *Total number of links connected to a given node* $(N_j > 0)$

S_m = *volumetric mass generation rate* $(kg/m^3/s)$

S_h = *volumetric enthapy generation rate* $(kg/m^3/s)$

f_T = *total flow resistance* $(form + friction + drag + ...)$

$\Delta P_{K,source}$ = *pressure source such as from pumps or circulators*

ΔP_{extra} = *other pressure gain* $(or\ loss)$ *e.g. gravity*

Discretize equation (3-1) and rewrite as :

$$\frac{V_i}{\Delta t}\left(\rho_i^{n+1} - \rho_i^n\right) = \sum_{j=1}^{N_j} \tilde{\rho}_j^n A_j \, u_j^{n+1} + S_{m,i}^n V_i \tag{3-4}$$

Discretize equation (3-2) and rewrite as :

$$\frac{V_i}{\Delta t}\rho_i^n\left(h_i^{n+1}-h_i^n\right)+\frac{V_i}{\Delta t}h_i^n\left(\rho_i^{n+1}-\rho_i^n\right)=\sum_{j=1}^{N_j}\tilde{\rho}_j^n\tilde{h}_j^n A_j\ u_j^{n+1}+S_{h,i}^n V_i \tag{3-5}$$

Taylor expand ρ terms of P and h, and approximate to first order terms :

$$\rho_i^{n+1}=\rho_i^n+\left(\frac{\partial\rho}{\partial h}\right)_i^n\left(h_i^{n+1}-h_i^n\right)+\left(\frac{\partial\rho}{\partial P}\right)_i^n\left(P_i^{n+1}-P_i^n\right) \tag{3-6}$$

Substitute Equation (3-6) in Equation (3-4) :

$$\frac{V_i}{\Delta t}\left[\left(\frac{\partial\rho}{\partial h}\right)_i^n\left(h_i^{n+1}-h_i^n\right)+\left(\frac{\partial\rho}{\partial P}\right)_i^n\left(P_i^{n+1}-P_i^n\right)\right]=\sum_{j=1}^{N_j}\tilde{\rho}_j^n A_j\ u_j^{n+1}+S_{m,i}^n V_i$$

$$or,\ \frac{V_i}{\Delta t}\left(\frac{\partial\rho}{\partial h}\right)_i^n\delta h_i^{n+1}+\frac{V_i}{\Delta t}\left(\frac{\partial\rho}{\partial P}\right)_i^n\delta P_i^{n+1}=S_{m,i}^n V_i+\sum_{j=1}^{N_j}\tilde{\rho}_j^n A_j\ u_j^{n+1} \tag{3-7}$$

where

$$\delta h_i^{n+1}=h_i^{n+1}-h_i^n$$

$$\delta P_i^{n+1}=P_i^{n+1}-P_i^n$$

Substitute Equation (3-6) in Equation (3-5) :

$$\frac{V_i}{\Delta t}\rho_i^n\delta h_i^{n+1}+\frac{V_i}{\Delta t}h_i^n\left(\left(\frac{\partial\rho}{\partial h}\right)_i^n\delta h_i^{n+1}+\left(\frac{\partial\rho}{\partial P}\right)_i^n\delta P_i^{n+1}\right)=S_{h,i}^n V_i+\sum_{j=1}^{N_j}\tilde{\rho}_j^n\tilde{h}_j^n A_j\ u_j^{n+1}$$

$$or,\ \frac{V_i}{\Delta t}\left[\rho_i^n+h_i^n\left(\frac{\partial\rho}{\partial h}\right)_i^n\right]\delta h_i^{n+1}+\frac{V_i}{\Delta t}h_i^n\left(\frac{\partial\rho}{\partial P}\right)_i^n\delta P_i^{n+1}=S_{h,i}^n V_i+\sum_{j=1}^{N_j}\tilde{\rho}_j^n\tilde{h}_j^n A_j\ u_j^{n+1}. \tag{3-8}$$

Put Equation (3-7) and (3-8) in Matrix form :

$$\begin{bmatrix}a_{11} & a_{12}\\ a_{21} & a_{22}\end{bmatrix}\bullet\begin{bmatrix}\delta h_i^{n+1}\\ \delta P_i^{n+1}\end{bmatrix}=\begin{bmatrix}S_1\\ S_2\end{bmatrix}+\sum_{j=1}^{N_j}\left\{\begin{bmatrix}C_{1j}\\ C_{2j}\end{bmatrix}u_j^{n+1}\right\} \tag{3-9}$$

where

$$a_{11} = \frac{V_i}{\Delta t}\left(\frac{\partial \rho}{\partial h}\right)_i^n, \qquad a_{12} = \frac{V_i}{\Delta t}\left(\frac{\partial \rho}{\partial P}\right)_i^n$$

$$a_{21} = \frac{V_i}{\Delta t}\left[\rho_i^n + h_i^n\left(\frac{\partial \rho}{\partial h}\right)_i^n\right], \quad a_{22} = \frac{V_i}{\Delta t}h_i^n\left(\frac{\partial \rho}{\partial h}\right)_i^n$$

$$S_1 = S_{m,i}^n V_i, \qquad S_2 = S_{h,i}^n V_i$$

$$C_{1j} = \widetilde{\rho}_j^n A_j, \qquad C_{2j} = \widetilde{\rho}_j^n \widetilde{h}_j^n A_j$$

Equation (3-9) can be re-written as

$$[A] \bullet \begin{bmatrix} \delta h_i^{n+1} \\ \delta P_i^{n+1} \end{bmatrix} = \begin{bmatrix} S_1 \\ S_2 \end{bmatrix} + \sum_{j=1}^{N_j} \left\{ \begin{bmatrix} C_{1j} \\ C_{2j} \end{bmatrix} u_j^{n+1} \right\} \tag{3-10}$$

Find inverse of [A] and multiplying both sides :

$$\begin{bmatrix} \delta h_i^{n+1} \\ \delta P_i^{n+1} \end{bmatrix} = [A]^{-1} \bullet \begin{bmatrix} S_1 \\ S_2 \end{bmatrix} + \sum_{j=1}^{N_j} \left\{ [A]^{-1} \bullet \begin{bmatrix} C_{1j} \\ C_{2j} \end{bmatrix} u_j^{n+1} \right\}$$

$$or, \quad \begin{bmatrix} \delta h_i^{n+1} \\ \delta P_i^{n+1} \end{bmatrix} = \begin{bmatrix} \sigma_1 \\ \sigma_2 \end{bmatrix} + \sum_{j=1}^{N_j} \left\{ \begin{bmatrix} \phi_{1j} \\ \phi_{2j} \end{bmatrix} u_j^{n+1} \right\} \tag{3-11}$$

where

$$[A]^{-1} = \begin{bmatrix} \alpha_{11} & \alpha_{12} \\ \alpha_{21} & \alpha_{22} \end{bmatrix}, \qquad \begin{bmatrix} \sigma_1 \\ \sigma_2 \end{bmatrix} = [A]^{-1} \bullet \begin{bmatrix} S_1 \\ S_2 \end{bmatrix}, \qquad \begin{bmatrix} \phi_{1j} \\ \phi_{2j} \end{bmatrix} = [A]^{-1} \bullet \begin{bmatrix} C_{1j} \\ C_{2j} \end{bmatrix}$$

Collecting pressure terms only,

$$\delta P_i^{n+1} = \sigma_2 + \sum_{j=1}^{N_j} \left\{ \phi_{2j}\, u_j^{n+1} \right\} \tag{3-12}$$

Now Equation (3-3) can be discretized and re-written as

$$\begin{aligned} u_j^{n+1} &= \frac{2}{f_{T,j}\widetilde{\rho}_j^n u_j^n}\left[(P_{from,j}^{n+1} - P_{to,j}^{n+1}) + \Delta P_{from,source,j} + \Delta P_{extra,j}\right] \\ &= \frac{2}{f_{T,j}\widetilde{\rho}_j^n u_j^n}\left[(P_{from,j}^{n+1} - P_{from,j}^{n}) - (P_{to,j}^{n+1} - P_{to,j}^{n}) + (P_{from,j}^{n} - P_{to,j}^{n}) + \Delta P_{from,source,j} + \Delta P_{extra,j}\right] \\ &= \eta_j(\delta P_{from,j}^{n+1} - \delta P_{to,j}^{n+1}) + \theta_j \end{aligned} \tag{3-13}$$

where

$$\eta_j = \frac{2}{f_{T,j}\tilde{\rho}_j^n u_j^n}$$

$$\theta_j = \eta_j \cdot \left[(P_{from,j}^n - P_{to,j}^n) + \Delta P_{from,source,j} + \Delta P_{extra,j} \right]$$

Substitute Equation (3-12) into Equation (3-11) gives Pressure Equations for a node :

$$\delta P_i^{n+1} = \sigma_{2i} + \sum_{j=1}^{N_j} \left\{ \phi_{2j} \left(\eta_j (\delta P_{from,j}^{n+1} - \delta P_{to,j}^{n+1}) + \theta_j \right) \right\}$$

$$or, \quad \delta P_i^{n+1} - \sum_{j=1}^{N_j} \left\{ \phi_{2j} \eta_j (\delta P_{from,j}^{n+1} - \delta P_{to,j}^{n+1}) \right\} = \sigma_{2i} + \sum_{j=1}^{N_j} \phi_{2j} \theta_j \qquad (3\text{-}14)$$

Using Equation (3-14), setup (n x n) Pressure Matrix and solve for pressure.
then, use Equation (3-12) to calculate velocity as :

$$\text{new} \quad u_j^{n+1} = \eta_j (\delta P_{from,j}^{n+1} - \delta P_{to,j}^{n+1}) + \theta_j \qquad (3\text{-}15)$$

With new velocity and Equation (3-11), calculate new enthalpy :

$$\delta h_i^{n+1} = \sigma_1 + \sum_{j=1}^{N_j} \left\{ \phi_{1j} \, u_j^{n+1} \right\} \qquad (3\text{-}16)$$

Now, all unknown variables have been calculated for the new time step.
Using new variables, thermal hydraulic states at the new time step can be calculated.

The time step calculations are repeated until satisfactory convergence in velocity, pressure and enthalpy are achieved. The single fluid equations will be extended to multi-specie fluid equation by considering the molar fractions and the partial pressures.

4 MODELS

An appropriate level of detail is an important consideration in the development of models for HyPEP. The code will be used to predict combined plant efficiency under two scenarios. The first is early in the project when *scoping* studies among design options may be performed; the second is later in the project when *optimization* of a particular design choice is performed. The quality of the prediction is determined by three factors: the phenomena to be modeled, the quality of the models, and the degree of spatial resolution. Engineering judgment will be used to determine the quality of prediction needed and to estimate the model uncertainty. Methods exist to more rigorously asses the level of model detail needed but they were developed for final safety analysis (Boyack 1990) and can require man-years of effort

4.1 Component and System Models

For HyPEP, high quality system and component models are essential. As previously stated, these systems and components will form the basis of the hierarchical system/component palettes.

One of the major functional requirements for the HyPEP is the flexible system build up. The HyPEP will have the capability to easily and flexibly model the plant system layout. To facilitate user friendly and flexible plant configuration modeling, component palettes are used. The user can select components or sub-systems from the palettes to build up the plant configuration using the drag/drop/connect feature. The components are designed to have a hierarchical structure, for example, the top-tier palette may contain VHTR, IHX, PCU, HTES and I-S components. These top-tier components will each be able to contain sub-components such as circulators, heat exchangers, electrolyzer, etc. General purpose components such as heat exchangers, nodes, links, and blocks will also be provided. The program will employ a graphic user interface extensively to enhance the user friendliness in modeling the system, preparing the input and to view the results. The system will be built by drag-dropping a component from the palette to the drawing canvas and then connecting them using the link component. Each primitive component (TNode and TLink) will have, associated with it, an on-screen input window to configure the component in detail.

The main work is to develop detailed thermal-hydraulic models for the components and to incorporate these into the model palette for the drag-drop-connect scheme to work. In order to realize such scheme, the OOP language issued. It is anticipated that the inheritance and the polymorphism features of the OOP language will greatly facilitate the creation of hierarchical component system.

A database will also be setup for the design parameters of various components and systems. For the reactor system the publicized design or operational data of the PBMR of South Africa, HTR-10 of China, HTTR-30 of Japan, and THTR and AVR of Germany will be good references. For the IHX, various designs are to be considered and the design data will be referenced from manufacturer's data sheet. For the PCU, the design data of PBMR, HTTR-30 can be referenced. For the I-S thermo-chemical process, the efforts of JAERI (Japan Atomic Energy Research Institute) are expected to provide relevant data. For the high temperature electrolysis, findings of various on-going researches are expected to provide necessary base data.

Base Components

The base components are the simplest of all components. They will include the node, link and the heat block components. These base components will be the top-most ancestor to other 'derived' components.

Node component (TNode)

A node component represents a volume of fluid having properties such as the pressure, temperature, density, molar composition, etc. The physical dimensions of a node are defined by the volume, height, inclination angle, the inlet ports, and the outlet ports. The node component is modeled using the TNode class in the OOP language.

Link component (TLink)

A link component represents the flow paths. The T/H properties of the link component include the fluid flow rates, and the pressure drop. The link component connects to the inlet or the outlet ports of the node-type components. The physical modeling of a link component is defined by the from-node, to-node, and the flow area. The fluid composition of the from-node and the to-node should be identical (i.e., no chemical reaction or heat exchanges in the link component). The link component will be modeled using the TLink class in the OOP language.

Heat block component (THeatBlock)

A heat block component represents the solid structure that thermally interacts with the fluids. The heat exchanger tubes, reactor vessel walls, heaters, heat losses will be represented by the heat block component. The heat block component will be modeled using the TBlock class in the OOP language.

TH System component (TSystem)

A TH System component represents the connected nodes and links that form a complete system. The system component contains all necessary details to carry out the TH numerical calculations. There may be more than one system in the overall plant, and any two systems may be thermally connected via the heat block component. As an example, the primary system of a reactor system can form the first TH system whereas the secondary system can form the second system. The two systems are connected via the Heat Exchanger (Steam Generators in PWRs, IHX in Gas Cooled Reactors). In numerical sense, each system forms a pressure solution matrix of size N×N where N is the total number of the node component in any given system.

Chemical node component (TChemNode)

A chemical node component models the components where chemical reaction occurs and this component is derived from the TNode component using the inheritance feature of the OOP. In this component, chemical reactions are modeled. Thus, the mass and energy fractions of the fluid species are allowed to change. This component will be used to model such component/system as the electrolyzer of the high temperature electolysis unit, and the Bunsen reaction, H2SO4 decomposition, and the HI decomposition units of the I-S thermo-chemical unit. In addition to the inputs required for the node component, the chemical reactions that occur in this component need to be defined and supplied by the user. The chemical node will be modeled using the TChemNode class created by inheritance from the TNode class.

Reactor System Components

The reactor system components will include the specialized components for the pebble bed reactors and the prismatic reactors.

Reactor component (TReactor)

The reactor component models the nuclear reactor. The component includes the specialized components for the pebble bed reactors and the prismatic reactors. For the hydrogen production efficiencies, the main differences of the reactor systems to consider are the core and vessel pressure drops. The pebble bed reactor component and the prismatic reactor component will have empirically derived correlations suitable to each design for estimating the core and vessel-wide pressure drops. The base reactor component will consist of a node component to represent reactor volume, and a heat block

component to provide the nuclear power.

Gas circulator component (TGasCirculator)

The gas circulator component is a specialized model component and will have the empirical formulae to calculate the power requirements and the developed pumping head. User inputs will include the efficiency of the circulator, the mass flow rates and others inputs needed for the estimation of the sizing and the cost.

Heat Exchanger Components

Heat Exchanger (THeatX)

A wide variety of heat exchanger types can be installed in a nuclear hydrogen production system. The THeatX component will be the base heat exchanger component and will contain the data and the methods of a generic heat exchanger. This component will consist of two node components representing primary and the secondary side volumes, and a heat block components. The primary and the secondary fluids may be different. Thus, Helium-Helium, Helium-CO2, CO2-Helium, etc. heat exchangers can be modeled.

Shell-Tube Type Heat Exchanger (TShellTubeHeatX)

This component will have thermo-dynamic empirical correlations, and the sizing and cost analysis models suitable for the shell-tube type heat exchangers.

Plate Type Heat Exchanger (TPlateHeatX)

This component will have thermo-dynamic empirical correlations, and the sizing and cost analysis models suitable for the plate type heat exchangers.

Printed Circuit Heat Exchanger (TPrintedCircuitHeatX)

This component will have thermo-dynamic empirical correlations, and the sizing and cost analysis models suitable for printed circuit type heat exchangers.

Helical Heat Exchanger (THelicalHeatX)

This component will have thermo-dynamic empirical correlations, and the sizing and cost analysis models suitable for helical tube type heat exchangers.

PCU Components

PCU components will include Brayton cycle component and the Rankine cycle component. Reheats and the superheating circuits may be modeled using the base components of HyPEP. However, user can design combined cycles and then save the layouts as a user-defined component. The PCU components will calculate the electricity generation efficiencies.

Brayton Cycle (TBrayton)

This component will model the Brayton Cycle and will contain the following components :

- Gas turbine component (TBraytonGasTurbine)
- Compressor component(TBraytonCompressor)
- Pre-cooler component(TBraytonPreCooler)
- Inter-cooler component(TBraytonInterCooler)
- Recuperator component(TBraytonRecuperator)

Rankine Cycle (TRankine)

This component models the Rankine Cycle and will contain the following components :

- Steam generator component(TRankineSteamGenerator)
- Steam turbine component (TRankineSteamTurbine)

- Condenser component(TRankineCondenser)
- Pump component(TRankinePump)

Generator (TRankineGenerator)

This component models the electricity generator.

HTES Components

HTES components will be provided to model the High Temperature Electrolysis System. The HTES will be formed by the Electrolyzer, Separator, Condenser, AC-DC Converter, Heat Exchanger, etc. components.

Electrolyzer (THTESElectrolyzer)

This component models the electrolyzer. The chemical reaction of the electrolysis will be modeled in this component.

Separator (THTESSeparator)

This component models the separator. A model will be developed to separate the various chemicals (hydrogen, oxygen and steam).

Condenser (THTESCondenser)

This component models the separator. A model will be developed to separate the various chemicals (hydrogen, oxygen and steam).

AC-DC Converter (TAC_DC)

This component models the conversion of AC current into DC needed by the HTES.

Thermo-Chemical Components

Thermochemical components will include the I-S models. I-S models will consist of the H2SO4 Decomposition component, Bunsen Reaction component, HI concentration/Decomposition component, Heat exchanger component, etc.

H2SO4 Decomposition (TH2SO4Decomposition)

This component models the conversion of AC current into DC needed by the HTES.

Bunsen (T Bunsen Decomposition)

This component models the conversion of AC current into DC needed by the HTES.

H2SO4 Decomposition (TH2SO4Decomposition)

This component models the conversion of AC current into DC needed by the HTES.

The details of the steam generator model for the combined cycle is summarized in Appendix A.The details of the electrolyzer model, HTE process model that includes pressure step-up unit, pressure work-recovery unit, boiler with non-condensable gas streams, condenser with non-condensable gas stream, single phase heat exchanger, fluid properties, component inter-connections, and a GAS-PASS/H simulation are listed in Appendix B.

4.2 Component Sizing Models

Component sizing models will be developed for the important major components. For the components with the sizing models, the components will be defined in such a way as collection and categorization of cost models for various major components and systems. With the component cost models incorporated, the cost model for HyPEP will be further developed to estimate the overnight cost of the system.

The major components with component sizing models will include:
- Heat Exchanger components
- Gas circulator components
- Electrolyzer components

The method for sizing heat exchangers is given by Davis et al. (2005). Basically, the method requires the basic geometry to be input. For a PCHE, the basic geometry includes the diameter of the semicircular flow channel, the pitch-to-diameter of the channels, and the plate thickness. Iterations are then performed on the size of the heat exchanger until it provides the desired amount of heat transfer and pressure drop on one side of the heat exchanger.

Pipe components can be sized to produce the desired amount of pressure drop for the given length, flow rate, and thermodynamic conditions in the pipe.

Turbomachinery size can be estimated from the power produced or consumed by the component. The cost of new turbomachinery can be scaled from the cost of existing machines if the changes in power and operating pressure and temperature are known. Dostal et al. (2004) used this method to estimate the cost for turbomachinery in a Brayton cycle that utilized supercritical carbon dioxide. Thus, the power and operating conditions should also provide an indication of component size.

Sizing calculations and results are shown in Appendix D.

4.3 Cost Analysis Model

In this task, models for overnight capital cost and component cost are to be developed. As the determination of the “true cost” of a nuclear plant requires consideration of a large number of empirical and difficult-to-establish factors, the models to be developed will be very simple models. The developed models will essentially provide rough guidance on the economics of various plant layouts.

The cost analysis model will involve collection and categorization of cost models for various major components and systems. With the component cost models incorporated, the cost model for HyPEP will be further developed to estimate the overnight cost of the system.

An optimization model will also be developed. A scheme will be provided by which the optimization can be performed by a large number of calculations by varying the parameters of interest. A batch style calculation scheme is deemed to be best-suited for the optimization calculations, and an automatic way to carry out the calculation will be pursued in this task.

4.4 Thermophysical Properties

4.4.1 Water/Steam Thermodynamic Properties

The thermodynamic property calculation routines for water/steam have been developed using the 1967 IFC Formulation for Industrial Use in conformity with the 1963 International skeleton tables. In the 1967 IFC formulation, the property regions are divided into 6 sub-regions including a sub-region for the saturation line and a sub-region near the critical point. The correlations for the specific Helmholtz function, the specific Gibbs functions, the K-function for saturation line are provided in the formulation. These correlations have been coded in pascal language for use in Delphi program environment which has been selected for the HyPEP development. The routines have been packaged as a Delphi unit in which several routines have been defined as the interface routines.

The Delphi interface routines are coded in ASME.pas and which is compiled to generate the ASME.dcu which essentially act as a library which is callable from any Delphi program by including the ASME in the unit declaration of the calling program. The list of routines available in ASME.pas are as follows :

- procedure calc_Prop (P, T, v, h, s, cp, e, c)
  This routine calculates v, h, s, cp, e, c for given pressure P, and temperature T.
- procedure T_sat_Prop (T, Psat, v_f, v_g, h_f, h_g, s_f, s_g, cp_f, cp_g, e_f, e_g, c_f, c_g)
  This routine calculates Psat, v_f, v_g, h_f, h_g, s_f, s_g, cp_f, cp_g, e_f, e_g, c_f, c_g for a given temperature T.
- procedure P_sat_Prop (P, Tsat, v_f, v_g, h_f, h_g, s_f, s_g, cp_f, cp_g, e_f, e_g, c_f, c_g)
  This routine calculates Tsat, v_f, v_g, h_f, h_g, s_f, s_g, cp_f, cp_g, e_f, e_g, c_f, c_g for a given pressure P.
- function SurTen (T) : real
  This function returns surface tension for a given pressure P.
- function satT (P) : real
  This function returns saturation temperature for a given pressure P.
- function satP (T) : real
  This function returns saturation pressure for a given pressure T.
- function th_k (P, T, ρ) : real
  This function returns thermal conductivity for given pressure P, temperature T, and density ρ.
- function visc (P, T, ρ) : real
  This function returns dynamic viscosity for given pressure P, temperature T, and density ρ.

where

P = pressure, MPa
T = temperature, K
v = specific volume in m^3/kg
ρ = density, kg/m^3
h = specific enthalpy, J/kg
s = specific entropy, J/kg/K
cp = specific heat capacity, J/kg/K
e = expansivity
c = compressibility
subscript f = liquid water
subscript g = gaseous steam
subscript sat = saturation

The sub-regions of IFC formulations are as shown in Figure 4-1. As can be seen in the diagram, there are 6 sub-regions including the saturation line and near critical point line. The IFC formulation provides correlations for the 4 sub-regions (1 ~ 4). For the saturation line, the steam and the liquid properties are calculated using the appropriate sub-regions for the given temperature or the pressure.

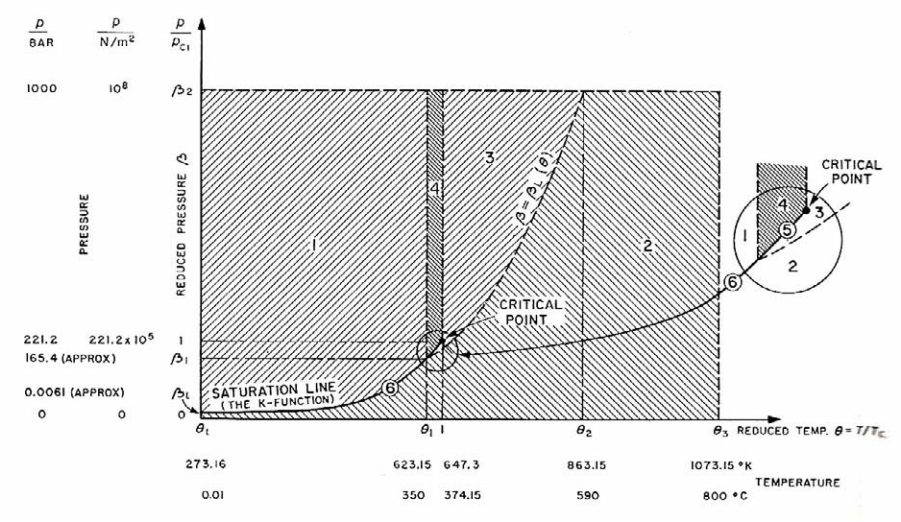

Figure 4-1. Sub-regions on the Pressure-Temperature Diagram[4]

The saturation pressure is calculated using the K-function and the 4 canonical functions are used to calculate the specific volume, the specific entropy, and the specific enthalpy for the 2 sub-regions. These properties are calculated using derived functions

K-function (Reduced Saturation Pressure)

K-function gives the saturation line which lies in the boundary between sub-regions. The equation for the K-function is as follows:

$$\beta_k(\theta) = \exp\left[\frac{1}{\theta}\frac{\sum_{v=1}^{5} k_v(1-\theta)^v}{1+k_6(1-\theta)+k_7(1-\theta)^2} - \frac{(1-\theta)}{k_8(1-\theta)^2+k_9}\right]$$

where

$\beta = reduced\ pressure,\ p / p_{c1}$

$\theta = reduced\ temperature,\ T / T_{c1}$

$k_i = correlation\ constants$

A-function (Reduced Free Enthalpy)

A-function gives the reduced free enthalpy (Gibbs function) equation for the sub-region 1. The equation for the A-function is as follows:

$$\zeta_A(\theta,\beta) = A_0\theta(1-\ln\theta) + \sum_{v=1}^{10} A_v\theta^{v-1} + A_{11}\left(\frac{17}{29}Z - \frac{17}{29}Y\right)Z^{12/17}$$
$$+ \left\{A_{12} + A_{13}\theta + A_{14}\theta^2 + A_{15}(a_6-\theta)^{10} + A_{16}(a_7-\theta^{19})^{-1}\right\}\beta$$
$$- (a_8+\theta^{11})^{-1}\left(A_{17}\beta + A_{18}\beta^2 + A_{19}\beta^3\right)$$
$$- A_{20}\theta^{18}(a_9+\theta^2)\left\{(a_{10}-\beta)^{-3} + a_{11}\beta\right\}$$
$$+ A_{21}(a_{12}-\theta)\beta^3 + A_{22}\theta^{-20}\beta^4$$

where

$$Z = Y + (a_3Y^2 - 2a_4\theta + 2a_5\beta)^{\frac{1}{2}}$$
$$Y = 1 - a_1\theta^2 - a_2\theta^{-6}$$
$$A_i = \textit{correlation constants}$$
$$a_i = \textit{correlation constants}$$

B-function (Reduced Free Enthalpy)

B-function gives the reduced free enthalpy (Gibbs function) equation for the sub-region 2. The equation for the B-function is as follows:

$$\zeta_B(\theta,\beta) = I_1\theta\ln\beta + B_0\theta(1-\ln\theta) + \sum_{v=1}^{5} B_{0v}\theta^{v-1} - \left(B_{11}X^{13} + B_{12}X^3\right)\beta$$
$$- \left(B_{21}X^{18} + B_{22}X^2 + B_{23}X\right)\beta^2 - \left(B_{31}X^{18} + B_{32}X^{10}\right)\beta^3$$
$$- \left(B_{41}X^{25} + B_{42}X^{14}\right)\beta^4 - \left(B_{51}X^{32} + B_{52}X^{28} + B_{53}X^{24}\right)\beta^5$$
$$- \frac{\left(B_{61}X^{12} + B_{62}X^{11}\right)\beta^4}{1 + b_{61}X^{14}\beta^4} - \frac{\left(B_{71}X^{24} + B_{72}X^{18}\right)\beta^5}{1 + b_{71}X^{19}\beta^5} - \frac{\left(B_{81}X^{24} + B_{82}X^{18}\right)\beta^6}{1 + \left(b_{81}X^{54} + b_{82}X^{27}\right)\beta^6}$$
$$+ \beta\left(\frac{\beta}{\beta_L}\right)^{10}\sum_{v=0}^{9} B_{9v}X^v$$

where

$$X = \exp\{b(1-\theta)\}$$
$$\beta_L = \beta_L(\theta)$$

C-function (Reduced Free Energy)

C-function gives the reduced free energy (Helmholtz function) equation for the sub-region 3. The equation for the C-function is as follows:

$$\psi_C(\theta,\chi) = C_{00} + C_{01}\chi + \sum_{v=2}^{11} C_{0v}\chi^{1-v} + C_{012}\ln\chi + \left\{C_{11}\chi + \sum_{v=2}^{6} C_{1v}\chi^{1-v} + C_{17}\ln\chi\right\}(\theta-1)$$
$$+ \left\{C_{21}\chi + \sum_{v=2}^{7} C_{2v}\chi^{1-v} + C_{28}\ln\chi\right\}(\theta-1)^2$$
$$+ \left\{C_{31}\chi + \sum_{v=2}^{7} C_{3v}\chi^{1-v} + C_{310}\ln\chi\right\}(\theta-1)^3$$
$$+ \left(C_{40} + C_{41}\chi^{-5}\right)\theta^{-23}(\theta-1) + C_{50}\theta\ln\theta$$
$$+ \chi^6\sum_{v=0}^{4} C_{6v}\theta^{-2-v} + \sum_{v=0}^{8} C_{7v}(\theta-1)^{v+1}$$

D-function (Reduced Free Energy)

D-function gives the reduced free energy (Helmholtz function) equation for the sub-region 4. The equation for the D-function is as follows:

$$\psi_D(\theta,\chi) = \sum_{\mu=3}^{4}\sum_{v=0}^{4} D_{\mu v} y^{\mu}\chi^{-v} + y^{32}\sum_{v=0}^{2} D_{5v}\chi^{v}$$

where

$$y = (1-\theta)/(1-\theta_1)$$

4.4.2 Gas Thermodynamic Properties

The thermodynamic property calculation routines for gas substances have been developed using the "Thermodynamic Properties in SI" by W.C. Reynolds Correlations where correlations for a total of 40 substances are provided. Of the 40 substances available, helium, hydrogen (para), nitrogen, oxygen, argon, carbon dioxide, butane, and propane have been coded in pascal language for use in Delphi program environment.[2] The correlations are based on the PvT relationships which are different for the different substances. The internal energy and the entropy values are derived from the PvT relations using the following relationships:

$$u = \int_{T_0}^{T} c_v^0(T)\,dT + \int_0^{\rho}\frac{1}{\rho^2}\left[P - T\left(\frac{\partial P}{\partial T}\right)_{\rho}\right]d\rho + u_0$$

$$h = u + pv$$

$$s = \int_{T_0}^{T}\frac{c_v^0(T)}{T}\,dT - R\ln\rho + \int_0^{\rho}\frac{1}{\rho^2}\left[\rho R - \left(\frac{\partial P}{\partial T}\right)_{\rho}\right]d\rho + s_0$$

More substances can be added by providing appropriate correlation constants. The gas mixture (e.g. air) properties are calculated by summing (using molar fraction) constituent substance properties.

These routines are programmed as the Delphi program unit, THProps.pas (THProps.dcu). This unit can be easily be converted to a DLL (Dynamic Link Library) if needs to be. Following interface routines are currently programmed in the THProps unit.

- call GetProps (Substance, P, T, v, h, s, u)

This routine calculates v, h, s,u for given pressure P, and temperature T for the named "Subatance".

- call AirProps (P, T, v, h, s, u)

  This routine calculates v, h, s,u for given pressure P, and temperature T for air (mixture)

- function PvT_eqn (Substance, T, rho) : real

  This routine returns pressure P for given temperature T and density ρ for the named "Substance".

- function u_eqn (Substance, T, rho) : real

  This routine returns energy u for given temperature T and density ρ for the named "Substance".

- function s_eqn (Substance, T, rho) : real

  This routine returns entropy s for given temperature T and density ρ for the named "Substance".

- function dPdT_eqn (Substance, T, rho) : real

  This routine returns dP/dT for given temperature T and density ρ for the named "Substance".

- function dPdRho_eqn (Substance, T, rho) : real

  This routine returns dP/dρ for given temperature T and density ρ for the named "Substance".

- function rho_P_T (Substance, P, T) : real;

  This routine returns density, ρ for given temperature T and density ρ for the named "Substance".

- function Rliq_Eqn (Substance,T) : real;

  This routine returns liquid density, ρ for given temperature T for the named "Substance".

- function Psat_Eqn (Substance,T) : real;

  This routine returns saturation pressure Psat for given temperature T for the named "Substance".

The substances are defined by the structured record defined as recSubstance. Figure 4-2 shows the sample substance definition (in this case Argon).

```
//+++++++++++++++++++++++++++++++++++++++++++++++++++++++++++++
  Argon : recSubstance       // Argon
     =(subsname   : 'Argon';
       PvT_Index  : 3;
       Psat_Index : 2;
       Cv0_Index  : 0;
       Rliq_Index : 2;

       // General Data
       R    :  208.128;
       M    :   39.948;
       Tc   :   150.70;
       Pc   : 4.8649e6;
       rhoc :   513.00;
       T0   :    83.8;

       PvTData :
        (alpha : 0.0; gamma : 3.5e-6;
         A :( 1.9825921e-1, -8.1733119e1,  1.7777470e3,  -8.2406544e5,   3.1666098e7,
             -4.4202671e-5,  6.216142e-2,  1.1443248,     4.7797520e-7, -1.9645227e-4,
             -2.1572754e-10, 1.6544141e-7,-2.8142112e-11, 8.2532059e1,  -9.1538377e3,
             -1.8340752e6,  -3.3858136e-3, 1.5532886,    -6.7479568e1,   0.0,
              0.0,           0.0,          0.0,           0.0,           0.0,
              0.0,           0.0,          0.0,           0.0,           0.0,
              0.0,           0.0,          0.0,           0.0,           0.0);

         a_ : 0.0; b_ : 0.0; c_ : 0.0; d_ : 0.0;
         A0 : 0.0; B0 : 0.0; C0 : 0.0; D0 : 0.0; E0 : 0.0;
         Tau_c : 0.0);
       PsatData :
        (Tp : 100.0;
         F : (-5.340410,    -2.371280e-1,  -9.490142e-1,  1.187040,     -5.889895,
               5.627790,     2.674117e1,   -6.661814e1,   0.0,           0.0);
         alpha : 0.0;  gamma : 0.0; Tt : 0.0; Pt : 0.0);
       CvData   :
        (cv  : 312.192; u0 : 1.4935540e5;
         s0 : 2.2706700e3;  T1  : 0.0;     T2 :0.0;          beta : 0.0;
         G : ( 0.0,          0.0,           0.0,          0.0,           0.0,
               0.0,          0.0,           0.0,          0.0,           0.0,
               0.0,          0.0,           0.0,          0.0,           0.0,
               0.0,          0.0));
       RliqData :
        (alpha : 0.0;
         D : ( 5.1299940e2,  8.3581370e2,   1.1958780e3, -3.1968580e3,   4.5022760e3,
              -2.0863750e3,  0.0));
        );
```

Figure 4-2 Sample Substance Definition File

4.4.3 Liquid salts

Liquid salts are being considered as the working fluid in the intermediate heat transport loop (Davis et al., 2005). The salts considered were LiF-NaF-KF (Flinak) in molar concentrations of 46.5%, 11.5%, and 42%, respectively, and $NaBF_4$-NaF in molar concentrations of 92% and 8%. $NaBF_4$-NaF is considered to be a better candidate for the intermediate heat transport loop because of its lower melting point (385 vs. 454 °C). Thermodynamic and transport properties for these salts are described by Davis (2005). The correlations given by Davis (2005) should be acceptable to use for implementing liquid salt properties in HyPEP.

4.4.4 Process fluids

The hydrogen production process utilizes three separate fluid systems: H_2SO_4-H_2O, HI-I_2-H_2O, and H_2SO_4-HI_x-H_2O (Brown et al. 2003). Thus, the primary fluids of interest are H_2SO_4, H_2O, HI, and I_2. Both liquid and vapor phases of each of the primary fluids exist at some point in the process. Thermodynamic data are generally available for the pure fluids, although not necessarily at the temperatures and pressures needed for the hydrogen production process. For example, Perry and Green (1997) present thermodynamic data for H_2SO_4 at temperatures up to 350 °C. However, the temperature of H_2SO_4 in the proposed hydrogen production process exceeds 800 °C. Furthermore, the thermodynamic properties of liquid mixtures do not depend solely on the properties of the pure components and their respective molar concentrations. Consequently, the thermodynamic properties must be determined by measurement for each separate fluid system. Because of the lack of experimental data, Brown et al. (2003) developed empirical models that fit the existing low-temperature data and applied the models to predict properties at the proposed conditions for hydrogen production. Brown et al. concluded that the model for the H_2SO_4-H_2O system would provide a reliable description for Section 2 of the Sulfur-Iodine cycle. The model for the HI-I_2-H_2O system was expected to provide reasonable predictions of Section 3, but experimental data were needed for validation. The results from the model of the H_2SO_4-HI_x-H_2O system were judged to require caution because of the small range of the underlying data.

At the current time, the existing models of Brown et al. (2003) are expected to provide the best estimates of thermodynamic properties. These flowsheet models could be obtained from General Atomics to provide thermodynamic properties for use in HyPEP. However, better properties might be obtained from General Atomic's improved thermodynamic models that should be available early in 2006. The French are also expected to report basic thermodynamic data at conditions more applicable to the hydrogen production process in 2006. Improved models could also be generated using the French data and the regression feature of Aspen Plus.

The transport properties of dynamic viscosity and thermal conductivity are also available for the pure fluids required in the hydrogen production process. For example, Daubert et al. (2000) present correlations for both liquid and vapor phases of H_2SO_4, H_2O, HI, and I_2. As was the case for the thermodynamic properties, the combination of properties of the pure fluids to determine mixture properties is more difficult. According to Govier and Aziz (1972), the viscosity of a miscible liquid mixture cannot be predicted reliably. Thus, they recommend an approximate method, such as linear weighting of the viscosities of the pure components based on the mass fraction. A similar method could be used for the thermal conductivity. For mixtures of gases, the Wilke formula described by Bird et al. (1960) should be sufficiently accurate.

When the gas must be treated as real the NIST database (NIST Reference 7.0) will be used. The evaluation of properties in NIST, however, can be numerically intensive and result in long execution

times which would not be in keeping with HyPEP objectives, i.e. to rapidly prototype different design options. In this case a tabular approach to property evaluation can be used to speed execution (Hejzlar 2005).

4.5 High Temperature Electrolysis (HTE)

In general, for an operating electrolysis stack, there will be a temperature change associated with the electrolysis process. For these cases, the energy equation for electrolysis process can be written as:

$$\dot{Q} - \dot{W} = \sum_{P} \dot{N}_i [\Delta H^o_{f_i} + H_i(T_P) - H^o_i] - \sum_{R} \dot{N}_i [\Delta H^o_{f_i} + H_i(T_R) - H^o_i] \qquad (4\text{-}1)$$

where $\dot{Q}$ is the external heat transfer rate to or from the electrolyzer, $\dot{W}$ is the rate of electrical work supplied to the electrolyzer, $\dot{N}_i$ is the molar flow rate of each reactant or product, $\Delta H^o_{f_i}$ is the standard-state enthalpy of formation of each reactant or product and $H_i(T) - H^o_i$ is the sensible enthalpy for each reactant or product. Applying the energy equation in this form, all reacting and non-reacting species included in the inlet and outlet streams can be accounted for, including inert gases, inlet hydrogen (introduced to maintain reducing conditions on the steam/hydrogen electrode), and any excess unreacted steam. Determination of the outlet temperature from Eqn. (4-1) is an iterative process. The heat transferred during the process must first be specified (e.g., zero for the adiabatic case). The temperature-dependent enthalpy values of all species must be available from curve fits or some other data base. The solution procedure begins with specification of the cathode-side inlet flow rates of steam, hydrogen, and any inert carrier gas such as nitrogen (if applicable). The inlet flow rate of the sweep gas (e.g., air or steam) on the anode side must also be specified. Specification of the gas flow rates allows for the determination of the inlet mole fractions of steam, hydrogen, and oxygen that appear in the Nernst equation. The steam mole fraction is expressed in terms of the hydrogen mole fraction as $1\text{-}y_{H2}\text{-}y_{N2}$.

The current density and active cell area are then specified, yielding the total operating current. Care must be taken to insure that the specified inlet gas flow rates and total cell current are compatible. The minimum required inlet steam molar flow rate is the same as the steam consumption rate, given by:

$$\dot{N}_{i,H2O,\min} = \Delta\dot{N}_{H2O} = \frac{I}{2F} N_{cells} = \frac{i\,A_{cell}}{2F} N_{cells} = \Delta\dot{N}_{H2} \qquad (4\text{-}2)$$

which is of course also equal to the hydrogen production rate.

Once the total and per-cell hydrogen production rates are known, the outlet flow rates of hydrogen and steam on the cathode side and oxygen on the anode side can be determined. The flow rates of any inert gases, the anode-side sweep gas, and any excess steam or hydrogen are the same at the inlet and the outlet. Once all these flow rates are known, the summations in Eqn. (4-1) can be evaluated. The product summation must be evaluated initially at a guessed value of the product temperature, T_P.

The operating voltage corresponding to the specified current density is obtained from:

$$V_{op} = \overline{V}_{Nernst} + i \times ASR(T) \qquad (4\text{-}3)$$

where the stack area-specific resistance, *ASR(T)*, must be estimated and specified as a function of temperature. The cell-mean Nernst potential can then be obtained from an integrated Nernst equation:

$$\overline{V}_{Nernst} = \frac{1}{2F(T_P - T_R)(y_{o,O_2,A} - y_{i,O_2,A})(y_{o,H_2,C} - y_{i,H_2,C})} \times$$
$$\int_{T_R}^{T_P} \int_{y_{i,O2,A}}^{y_{o,O2,A}} \int_{y_{i,H2,C}}^{y_{o,H2,C}} \Delta G_R(T) - RT \ln\left(\frac{1 - y_{H_2} - y_{N_2}}{y_{H_2} y_{O_2}^{1/2}}\right) dy_{H_2} dy_{O_2} dT \qquad (4\text{-}4)$$

where $y_{i,\,O2,\,A}$ is the anode-side inlet mole fraction of oxygen, etc. Note that the upper limit of integration on the temperature integral, T_P, is initially unknown. Once the *ASR* and the mean Nernst potential are known, the operating voltage is obtained from Eqn. (4-3) and the electrical work term in Eqn. (4-1) is obtained from $\dot{W} = -V_{op} I$. An algorithm then must be developed to iteratively solve for the product temperature, T_P, in order to satisfy Eqn. (4-1). This algorithm can then be imbedded in a loop so that a full numerical "sweep" can be performed. We have implemented this procedure in MathCad. The MathCad model provides accurate estimates of electrolyzer operating voltage (and corresponding electrolyzer efficiency) and outlet temperatures, for any specified electrolyzer heat loss or gain, gas flow rates, current density, and per-cell *ASR(T)*. This electrolyzer model was developed for incorporation into system-level electrolysis plant models being developed using HYSYS system simulation software. With a realistic electrolyzer model incorporated into the overall HYSYS plant model, good estimates of overall hydrogen-production efficiencies can be obtained over a wide range of prospective operating conditions.

The detail of mathematical derivation of Gibbs free energy of Eqn (4-4) is listed in Appendix C. Using all equations described above, the power requirement of the HTE was calculated and preliminary calculation and results are listed in Appendix D. Appendix D includes coupling the reference configuration 6 and HTE with cases of a detailed HTE model and a simplified HTE block model. It also lists heat exchanger sizing calculations and results.

5 COMPUTATIONAL STRATEGIES

The computational strategy for the HyPEP code is being developed by KAERI under an I-NERI agreement. The agreement is to develop the steady state solution scheme for the coupled nuclear and chemical plant (Oh, 2005). Separately, in the U.S. there is interest outside of the I-NERI agreement in the laying groundwork for a transient code capability. The GAS-PASS/H code (Vilim, 2004) is one potential starting point. The code parallels HyPEP in capabilities in that it is a module-based network systems code. Both codes allow reactor configurations to be assembled from existing plant component modules without having to reprogram source code. A brief description of the computational scheme in GAS-PASS/H provides perspective on how new models for the nuclear and chemical plant components are interfaced to the code. In FY06 a GAS-PASS/H model of the HTE process described earlier in this report was built from newly created component modules.

5.1 Network-Based Method

The GAS-PASS/H code is based on the assumption that the plant the user wishes to simulate consists of a set of individual equipment components. Some definitions prove useful. A component is a piece of equipment whose behavior can be represented by a set of conservation balances. A node is a collection of structure and/or coolant material within a component and whose energy content is represented by an average temperature. A component output state point is that node in a component whose state variables feed into the next component downstream.

The user first creates a network diagram of his plant system which he communicates to the code through an input deck. An example of a network diagram appears in Figure 5.1. In this figure each component consists of one or more component nodes with each node appearing as a unique color and labeled with an identifying integer. In Figure 5.1 the node identification number appears as a large font integer inside the component. If the node represents a coolant volume then there is a flow channel at the outlet of the volume. The flow channel identification number is the same as the component node number and appears in the network diagram as an integer in smaller bold font. In Figure 5.1 the turbine component node number is “2” shown in large font. The number of the flow channel associated with the turbine is “2” shown in small font.

The information in the network diagram provided through the input deck is used to assemble a sequence of calls to software modules that contain component conservation balances. When all components in the network diagram have been cast as calls to these software modules, the numerical solution procedure solves for the plant conditions.

Each component software module has an interface through which the component interacts with other components according to the network diagram. This interface provides access to input and output process variables. Input variables are the forcing functions that drive the component and are either process variables at state points in other components that link with the component or are user supplied forcing functions. Output variables are at the state point where the component response appears. For two linked components, the output variables from the upstream module are the input variables for the downstream module.

Figure 5.2 is used to illustrate how component modules are configured to model interaction between components. In Figure 5.2 a turbine interacts with a reactor and recuperator. The user network diagram specifies the interconnections between turbine, reactor, shaft, and recuperator modules to reflect

this. Figure 5.2 shows the output variables associated with each module. In the figure an arrow leaving a module represents those modules output variables while an arrow entering a module represents input variables. From the conservation equations for the turbine the input variables to the turbine module are the shaft speed, ω, and temperature, pressure, and mass flowrate, T1, P1, m1, respectively at the inlet to the turbine. The output variables from the turbine module are temperature, pressure, and mass flowrate, T2, P2, m2, respectively at the outlet of the turbine and mechanical power, Wt, delivered to the shaft.

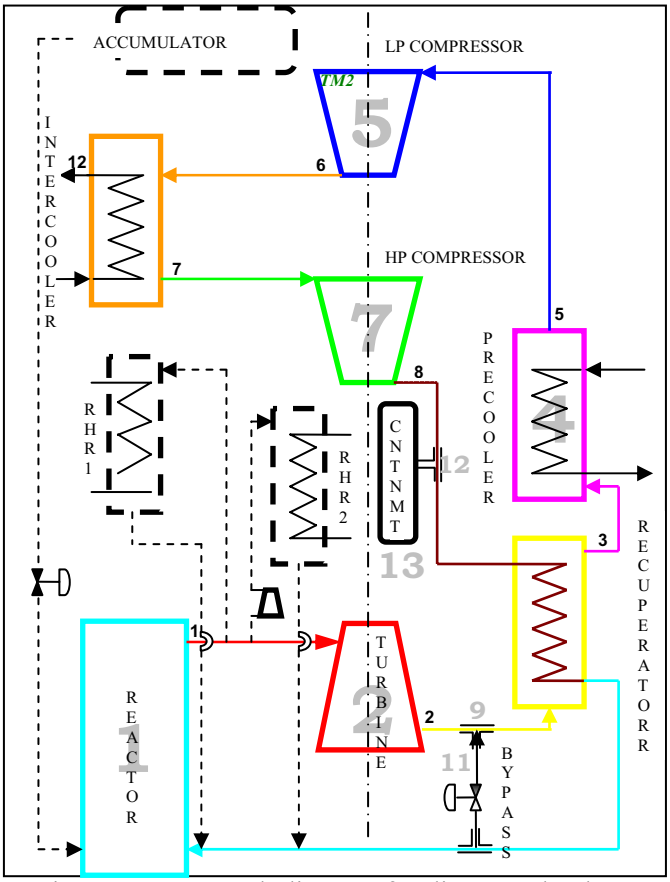

Figure 5.1 Network diagram for direct cycle plant.

5.2 Numerical Solution

The GAS-PASS/H code assumes that a plant component such as a pump or heat exchanger can be written as a set of ordinary differential equations in the dynamic case or as algebraic equations in the quasi-static case. The equations in a component module appear as first order time differenced equations of the form 0=f(xi+1,xi,ui) where xi+1 is a vector of the variables to be solved for at the new time, xi are the values at the old time, and ui is a vector of forcing functions held constant between time i and i+1. The equations are stored in a subroutine set aside for that component. The input deck the user assembled from his network diagram is used by the code to determine the inter-connections among plant components and to link modules to the numerical scheme. The user input also specifies which variables are to be treated as unknowns to be solved for and which are to be treated as forcing functions. Two conditions must be satisfied before a reliable solution can be returned. Model variables are either solved or are forcing function variables and must be marked as such in the input. Second, for the complete system the total number of unknowns solved for must equal the number of equations.

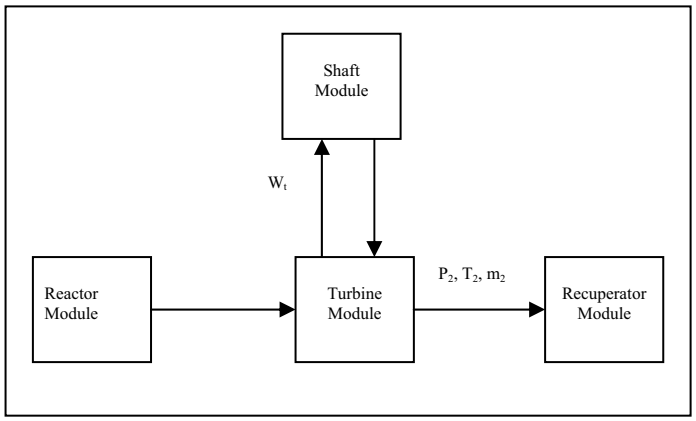

Figure 5.2 Turbine Module Links to Other Modules

The GAS-PASS/H code uses the information in the input deck to assemble arrays that specify which variables are to be forcing functions and which variables are to be solved for. These arrays are used to configure a nonlinear solver that obtains the steady-state and transient solutions. The arrays and the nonlinear solver are described below.

A variable that drives the solution and whose value or time behavior is known a priori is referred to as forcing function. A variable whose value is dependant on forcing functions is an unknown. An array *a(nvar)* of variables where *nvar* is the length is formed from the forcing functions and the unknowns where each element of a is one of these variables. The value of *nvar* is the sum of the number of forcing functions and the number of unknowns. The code input processor compiles arrays *ibcss(nvar)* and *ibctr(nvar)* from the users input. Nonzero elements of *ibcss* identify elements of *a* that remain fixed in the steady state and correspond to forcing functions. That is, if *ibcss(i)* $\neq$0, then the value of *a(i)* remains fixed while solving for the steady state. Similarly, if *ibctr(i)* $\neq$0, then the value of *a(i)* remains fixed while solving for the transient solution. The number of forcing functions in the steady state, *nbcss*, equals the number of nonzero elements of *ibcss*. Similarly, the number of forcing functions in the transient, *nbctr*, equals the number of nonzero elements of *ibctr*. Through the user input one can arrange for the value of an unknown solved for at steady state to be used as a forcing function in the transient.

The steady-state and transient solutions are the roots of nonlinear functions of the unknowns. The solver that finds these roots is provided with the indices of those elements of *a* that correspond to unknowns. For the steady state, these indices are stored in array *inds(nus)* of length *nus* (= *nvar-nbcss*). Similarly, for the transient, these indices are stored in array *indt(nut)* of length *nut* (= *nvar-nbctr*). *Inds* and *indt* are compiled from *ibcss* and *ibctr*, respectively.

The values of the forcing functions that drive a component are passed to the equations in the component module as a list of arguments. Rather than passing elements of the *a* array in the call to the module, the appropriate elements of *a* are first copied into arrays whose names are descriptive of the process variable being passed. Pressure is passed in array *P*, temperature in array *T*, channel flow in array *flowin*, and turbomachine enthalpy change in array *dh*, for example. Each of these arrays has its own indexing scheme that depends on where the variable is defined in the network diagram. Elements of array *P* and *T* are component node quantities and thus are indexed according to the component node labeling in the network diagram. Elements of array *flowin* are indexed according to the flow channel labeling in the network diagram. Elements of the array *dh* are indexed according to the turbomachine labeling in the network diagram. The first element of each of arrays *P*, *T*, *flowin*, and *dh* corresponds to element i*tbeg*, *ipbeg*, *iturbeg,* and *iflowbeg*, respectively, minus one of array *a*.

The module calls that implement the network diagram form a set of *nvar* equations in *nvar* unknowns. For variables that appear in a derivative, the value at time n+1 is treated as an unknown while the value at time n is taken from the previous time step. A nonlinear solver is used to find the roots of this equation set. One must ensure that the number of forcing functions provided results in the number of unknowns equal to the number of equations.

The steady state solution is obtained as a special case of the transient solution. The Kroneker delta premultiplies each time derivative in a component module. If the steady-state solution is sought, then the value of the Kroneker delta is zero. In the transient its value is unity.

6 CONCLUSIONS

A reference design of a coupled nuclear reactor and hydrogen production plant has been established to aid in the development of HyPEP. The reference design incorporates many of the systems and components that HyPEP must eventually be able to model. The reference design contains a high-temperature gas-cooled reactor that is used simultaneously for the production of electricity and hydrogen. Less than 10% of the nuclear reactor's thermal energy is dedicated to hydrogen production, consistent with that expected in the NGNP. The PCU utilizes an indirect electrical cycle. An intermediate heat transport loop is used to transfer heat from the nuclear reactor to the hydrogen production plant and to provide separation between the nuclear and hydrogen plants. Helium is used as a working fluid in both the secondary coolant system and the intermediate heat transport loop. Initial HyPEP model development concentrated on a HTE hydrogen production process.

HyPEP is being developed with hierarchical program and the data structures and will utilize object oriented programming techniques. The thermal hydraulic formulation of HyPEP is based on the conservation of mass and energy equations and models for the flow network of multi-species fluid systems. The flow network is made up of systems and components. Preliminary computational methods have also been identified.

Required component models have been identified. Preliminary models have been identified for steam generators and the various components needed for modeling HTE. Methods to obtain required fluid properties for a variety of fluids, including water, various gases, and liquid salts have been identified.

7 REFERENCES

Aspen Technology, *HYSYS Process Version 2.2.2*, www.aspentech.com, 2005.

Bird, R. B., W. E. Stewart, and E. N. Lightfoot, *Transport Phenomena*, John Wiley & Sons, Inc., New York, 1960.

Brown, L. C., G. E. Besenbruch, R. D. Lentsch, K. R. Schultz, J. F. Funk, P. S. Pickard, A. C. Marshall, and S. K. Showalter, *High Efficiency Generation of Hydrogen Fuels Using Nuclear Power, Final Technical Report for the Period August 1, 1999 through September, 30, 2002*, GA-A24285, June 2003.

Boyack, B. E., et al., "An Overview of Code Scaling, Applicability, and Uncertainty Methodology," Nuclear Engineering and Design 119 (1990), pp. 1-15.

Collier, J. G., and J. R. Thome, *Convective Boiling and Condensation*, Third Edition, Oxford University Press, Oxford, 1994.

Daubert, T. E. et al., *Physical and Thermodynamic Properties of Pure Chemicals Evaluated Process Design Data,* American Institute of Chemical Engineers and Design Institute for Physical Property Data, 2000.

Davis, C. B., *Implementation of Molten Salt Properties into RELAP5-3D/ATHENA,* INEEL/EXT-05-02658, January, 2005.

Davis, C. B., C. H. Oh, R. B. Barner, S. R. Sherman, and D. F. Wilson, *Thermal-Hydraulic Analyses of Heat Transfer Fluid Requirements and Characteristics for Coupling a Hydrogen Production to a High-Temperature Nuclear Reactor*, INL/EXT-05-00453, June 2005.

Dodge,B. F., "Condensation of Vapors from Mixtures of Vapors and Noncondensable Gas," *The Journal of Industrial and Engineering Chemistry*," Vol. 14, No. 11.

Dostal, V., M. J. Driscoll, and P. Hejzlar, *A Supercritical Carbon Dioxide Cycle for Next Generation Nuclear Reactors*, MIT-ANP-TR-100, March 10, 2004.

General Atomics, 1996, *Gas Turbine-Modular Helium Reactor (GT-MHR) Conceptual Design Description Report,* GA Project No. 7658, 910720 Revision 1, July 1996.

Govier, G. W. and K. Aziz, *The Flow of Complex Mixtures in Pipes*, Van Nostrand Reinhold Company, New York, 1972.

Hawkes, G.L., J.E. O'Brien, C.M. Stoots, and J.S. Herring, "CFD Model of a Planar Solid Oxide Electrolysis Cell for Hydrogen Production from nuclear energy", the 11th NURETH, Avignon, France, October 2-6, 2005.

Hejzlar, Pavel, personal communication, Massachusetts Institute of Technology, 2005.

Independent Technology Review Group, *Design Features and Technology Uncertainties for the Next Generation Nuclear Plant*, INEEL/EXT-04-01816, June 30, 2004.

INEEL, *RELAP5-3D Code Manual Volume 4: Models and Correlations*, INEEL-98-00834, Revision 2.2, April 2005.

Ishizuka, T., Y. Kato, Y. Muto, K. Nikitin, N. L. Tri, and H. Hashimoto, "Thermal-Hydraulic Characteristics of a Printed Circuit Heat Exchanger in a Supercritical CO_2 Loop," *The 11th International Topical Meeting on Nuclear Reactor Thermal-Hydraulics (NURETH-11), Avignon, France, October 2-6, 2005*.

Kayes, W. M., and M.E. Crawford, *Convective Heat and Mass Transfer, Second Edition*, McGraw-Hill Book Company, New York, 1980.

Lee, Y. J., et al., "HyPEP Introduction: Features and Development Path", Project Internal Report, February 2006.

Lillo, T. M., R. L. Williamson, T. R. Reed, C. B. Davis, and D. M. Ginosar, Engineering Analysis of Intermediate Loop and Process Heat Exchanger Requirements to Include Configuration Analysis and Materials Needs, INL-EXT-05-00690, September, 2005.

MacDonald, P. E. and J. Buongiorno, *Design of an Actinide Burning, Lead or Lead-Bismuth Cooled*

Reactor That Produces Low Cost Electricity, INEEL/EXT-02-01249, October 2002.

MacDonald, P. E., J. W. Sterbentz, R. L. Sant, P. D. Bayless, R. R. Schultz, H. D. Gougar, R. L. Moore, A. M. Ougouag, and W. K. Terry, 2003, *NGNP Preliminary Point Design – Results of the Initial Neutronics and Thermal-Hydraulic Assessments*, INEEL/EXT-03-00870, July 2003.

Meyer, B., "Object Oriented Software Construction", Prentice Hall, 1997.

Meyer, C.A. et al., "Thermodynamic and Transport Properties of Steam, Fifth Edition", The American Society of Mechanical Engineers, 1992.

NIST Reference Fluid Thermodynamic and Transport Properties Database (REFPROP):Version 7.0

Perry, R. H. and D. W. Green, *Perry's Chemical Engineers' Handbook, Seventh Edition*, McGraw-Hill, 1997.

Oh, C. H., C. B. Davis, S. R. Sherman, and R. Vilim, "Development of HyPEP, A Hydrogen Production Plant Efficiency Calculation Program," U.S./Republic of Korea I-NERI agreement, 2005.

Oh, C. H., R. B. Barner, C. B. Davis, B. D. Hawkes, *Energy Conversion Advanced Heat Transport Loop and Power Cycle*, INL/EXT-06-11681, August 2006.

Reynolds,W.C., "Thermodynamic Properties in SI: Graphs, Tables, and Computational Equations for 40 Substances", Department of Mechanical Engineering, Stanford University, Stanford CA, 1979.

The SAS4A/SASSYS-1 LMR Analysis Code System, Argonne National Laboratory, ANL-FRA-1996-3 August, 1996.

Sochet, I., J. L. Rouyer, and P. Hemmerich, 2004, "Safe Hydrogen Generation by Nuclear HTR," Paper 4261, *Proceedings of ICAPP '04, Pittsburgh, PA, USA, June 13-17*.

Smith, C., S. Beck, and B. Galyean, 2005, *An Engineering Analysis for Separation Requirements of a Hydrogen Production Plant and High-Temperature Nuclear Reactor*, INL/EXT-05-00137 Rev 0, March 2005.

Stoots, C. M., "Engineering Process Model for High-Temperature Electrolysis System Performance Evaluation," AICHE conference, Cincinnati OH, October 2005.

Todreas, N. E. and M. S. Kazimi, *Nuclear Systems I. Thermal Hydraulic Fundamentals*, Hemisphere Publishing Corporation, 1990.

Vernondern, K. and T. Nishihara, 2004, *Valuation of the Safety Concept of the Combined Nuclear/Chemical Complex for Hydrogen Production with HTTR*, JUEL-4135.

Vilim, R.B., U. Mertyurek, and J. Cahalan, "Passive Safety Analysis of the Gas Fast Reactor Using the GAS-PASS/H Systems Code," ICAPP 2004, Pittsburgh, PA, June 2004.

Xehe,M. J., S. Gordon, and B. J. McBride, "CAP: A Computer Code for Generating Tabular Thermodynamic Functions from NASA Lewis Coefficients," NASA, NASA/TP-2001-210959/REV1, 2002.

Appendix A

Steam Generator Component Model

A steam generator component model (Oh et al. 2006) was developed for the HYSYS (Aspen Technology 2005) process code. The following appendix describes the development and validation of the HYSYS steam generator component model. The same model could easily be adapted for use with HyPEP.

A combined cycle could be envisioned for the power conversion unit to be coupled to the very high-temperature gas-cooled reactor (VHTR). In Figure A-1 the combined cycle configuration consists of a Brayton top cycle coupled to a Rankine bottoming cycle by means of a steam generator. A detailed sizing and pressure drop model of a steam generator is not available in the HYSYS processes code. Therefore a four region model was developed for implementation into HYSYS.

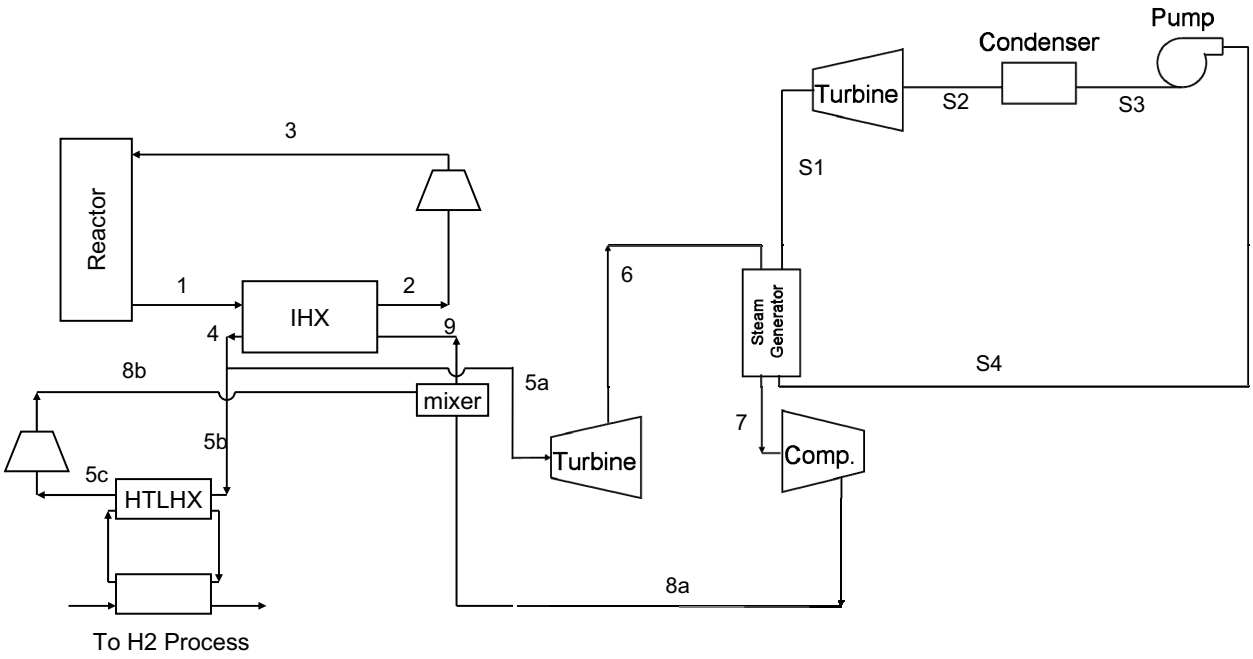

Figure A-1. Simplified schematic of the combined cycle configuration.

The steam generator was assumed to be a counter flow shell and tube heat exchanger with the Brayton cycle working fluid (helium) on the shell side and the Rankine cycle working fluid (water) on the tube side. Since the Brayton cycle working pressure, approximately 7 MPa, is lower than that for the Rankine cycle, 15 MPa, the pressure boundary requirements on the shell will be reduced. Because the diameter of the tubes is small, normal tube thicknesses can endure the high pressure. A shell diameter of 4.5 m, an inner and outer diameter of 6 mm and 7.3 mm for the tubes, a pitch to outer diameter ratio of 1.3 and a triangular array were assumed for the steam generator. These values are typical of existing steam generator designs. Alloy 617 was used for the construction material of the steam generator. This material was chosen based on the stress analysis given in Davis et al. (2005).

To account for the phase change in the cold side, the steam generator was divided into four heat transfer regions: subcooled, nucleate boiling, post critical heat flux and superheated. The subcooled region begins at the inlet to the steam generator and ends when the water reaches saturation conditions. Here we have neglected subcooled boiling. Since this region is single phase flow, the heat transfer coefficients were calculated using the Dittus-Boelter correlation with a leading coefficient of 0.023 for turbulent flow (INEEL 2005),

$$Nu = 0.023\,\mathrm{Re}^{0.8}\,\mathrm{Pr}^{0.4} \tag{A1}$$

where

$$Nu = h\frac{D_{hy}}{k}. \tag{A2}$$

For laminar flow, the heat transfer coefficients were calculated from the exact solution for fully developed flow with constant heat rate (Kayes and Crawford 1980),

$$Nu = 4.364\,. \tag{A3}$$

The pressure drop in the subcooled region was assumed to come from friction losses and was calculated using the following equation:

$$\Delta p = f\,\frac{L}{D_{hy}}\frac{G^2}{2\rho}, \tag{A4}$$

where f is the friction factor, L is the length, D_{hy} is the hydraulic diameter of the channels, ρ is the density, and v is the velocity. The friction factor was determined using a correlation for turbulent and laminar flow. For turbulent flow f was calculated using

$$f = \frac{0.3164}{\mathrm{Re}^{.25}}, \tag{A5}$$

and for laminar flow

$$f = \frac{64}{\mathrm{Re}}. \tag{A6}$$

The nucleate boiling region begins at the saturation point and ends when the fluid reaches critical quality. The Chen correlation was used in this region to determine the convection heat transfer coefficient. Chen assumes that the total convection coefficient in this region can be thought of as the superposition of the convection and nucleate boiling heat transfer coefficient (Colllier and Thome 1994),

$$h_{2\phi} = h_c + h_{NB}\,. \tag{A7}$$

Chen assumed that the convective component, h_c, could be represented by a Dittus-Bolter type equation.

$$h_c = .023\left(\frac{G(1-x)D_{hy}}{\mu_f}\right)^{0.8}\left(\frac{\mu c_p}{k}\right)_f^{0.4}\left(\frac{k_f}{D_{hy}}\right)F\,, \tag{A8}$$

where F is an additional correction factor defined as,

$$F = \left(\frac{\mathrm{Re}_{2\phi}}{\mathrm{Re}_f}\right)^{0.8}. \tag{A9}$$

Chen originally determined F empirically; however he later derived F using a Reynolds analogy as follows,

$$F = \left(\phi_f^2\right)^{0.444}. \tag{A10}$$

where ϕ_f^2 is the two phase friction multiplier based on the pressure gradient from fluid alone. Using the Martinelli parameter ϕ_f^2 is defined as,

$$\phi_f^2 = 1 + \frac{C}{X} + \frac{1}{X^2}\,, \tag{A11}$$

where C = 20 for turbulent-turbulent flow. The Martinelli parameter is based on the fluid properties at the saturation point and is defined as,

$$X = \left(\frac{1-x}{x}\right)^{0.9}\left(\frac{\rho_g}{\rho_f}\right)^{0.5}\left(\frac{\mu_f}{\mu_g}\right)^{0.1}. \tag{A12}$$

The nucleate boiling component of the Chen correlation also uses fluid properties at the saturation point and is defined as,

$$h_{NB} = 0.00122\left[\frac{\left(k^{0.79}c_p^{0.45}\rho^{0.49}\right)_f}{\sigma^{0.5}\mu_f^{0.29}h_{fg}^{0.24}\rho_g^{0.24}}\right]\Delta T_{sat}^{0.24}\Delta p_{sat}^{0.75}S\,, \tag{A13}$$

where S is the suppression factor that takes into account the difference between the wall superheat and the mean superheat in the boundary layer. S can be calculated using (MacDonald and Buongiorno 2002),

$$S = \frac{1}{1 + 2.53\times10^{-6}\left(\mathrm{Re}_f F^{1.25}\right)^{1.17}}. \tag{A14}$$

The Chen correlation determines the heat transfer coefficient at a point where the local quality is *x*. In this analysis a value of half the critical quality was chosen to give an average heat transfer coefficient over the entire region.

To determine the length and volume of the nucleate boiling region of the heat exchanger, the critical quality must be known. In order to determine the critical quality an iterative process must be implemented. First an initial guess of the critical quality must be made; in this case 0.75 was used. Using this initial guess the tube side heat transfer coefficient is determined along with the universal heat transfer coefficient. Using the ε-NTU method, the heat transfer area is determined. The effectiveness, ε, of the heat exchanger in this region was calculated using

$$\varepsilon = \frac{q}{q_{\max}} \tag{A15}$$

where

$$q_{\max} = C_{\min}(T_{h,i} - T_{c,i}) \tag{A16}$$

and C_{min} refers to the smaller of C_{hot} or C_{cold}, where

$$C_{hot} = c_{p,hot}\dot{m}_{hot} \tag{A17}$$

$$C_{cold} = c_{p,cold}\dot{m}_{cold} \tag{A18}$$

The NTU value was calculated using,

$$NTU = \frac{1}{C_r - 1}\ln\left(\frac{\varepsilon - 1}{\varepsilon C_r - 1}\right) \qquad C_r < 1 \tag{A19}$$

$$NTU = \frac{\varepsilon}{1 - \varepsilon} \qquad C_r = 1 \tag{A20}$$

where $C_r = C_{min/} C_{max}$.

Next the heat transfer area and the length were calculated,

$$A = \frac{NTU}{U}C_{\min} \tag{A21}$$

$$l = \frac{A}{\pi d_{in} N_t} \tag{A22}$$

where d_{in} is the inside diameter of the tubes and N_t is the number of tubes in the heat exchanger. The number of tubes is given by the follow formula,

$$N_t = \frac{d_{in,shell}^2 \pi}{4p^2 \sin\left(\pi/3\right)}. \tag{A23}$$

where $d_{in,shell}$ is the inner diameter of the shell and p is the pitch. The length is then inserted into the CISE-4 correlation and a new critical quality is calculated and reiterated until it converges. The CISE-4 correlation is given by Todreas and Kazimi (1990),

$$x_{crit} = \frac{a_{CISE4} l_{crit}}{l_{crit} + b_{CISE4}} \tag{A24}$$

$$a_{CISE4} = \frac{1}{1 + 1.481 \times 10^{-4} \left(1 - \frac{p}{p_c}\right)^{-3} G} \qquad G < G^* \tag{A25}$$

$$a_{CISE4} = \frac{1 - \frac{p}{p_c}}{\left(\frac{G}{1000}\right)^{1/3}} \qquad G < G^* \tag{A26}$$

$$b_{CISE4} = 0.199 \left(\frac{p_c}{p} - 1\right)^{0.4} G * d_{in,tube}^{0.4} \tag{A27}$$

$$G^* = 3375 \left(1 - \frac{p_c}{p}\right)^3 \tag{A28}$$

where p_c is the critical pressure of water.

The pressure drop calculation was obtained by multiplying the pressure drop calculated assuming the total fluid was liquid, Δp_{fo} by a two phase friction multiplier, ϕ_{fo}^2.

$$\Delta p = \Delta p_{fo} \phi_{fo}^2 \tag{A29}$$

$$\Delta p = f_{fo} \frac{L}{D_{hy}} \frac{G^2}{2\rho_f} \tag{A30}$$

Collier and Thome (1994) recommend the Friedel correlation for the two phase friction multiplier for flows where

$\mu_f / \mu_g < 1000$.

The Friedel correlation is given in Collier and Thome (1994) as,

$$\phi_{fo}^2 = A_1 + \frac{3.24 A_2 A_3}{Fr^{0.045} We^{0.035}} \tag{A31}$$

where

$$A_1 = \left(1-x\right)^2 + x^2\left(\frac{\rho_f f_{go}}{\rho_g f_{fo}}\right) \tag{A32}$$

$$A_2 = x^{0.78}\left(1-x\right)^{0.224} \tag{A33}$$

$$A_3 = \left(\frac{\rho_f}{\rho_g}\right)^{0.91}\left(\frac{\mu_g}{\mu_f}\right)^{0.19}\left(1-\frac{\mu_g}{\mu_f}\right)^{.7} \tag{A34}$$

$$Fr = \frac{G^2}{gD\overline{\rho}^2} \tag{A35}$$

$$We = \frac{G^2 D}{\overline{\rho}\sigma} \tag{A36}$$

In the post critical heat flux region, which ranges from dry-out to saturation, the Groeneveld correlation was used. This is a common method used in calculating the heat transfer in the region (MacDonald and Buongiorno 2002) and is given by the following equation,

$$Nu = 0.00109\left\{\mathrm{Re}_g\left[x+\frac{\rho_g}{\rho_f}\left(1-x\right)\right]\right\}^{0.989}\mathrm{Pr}_g^{1.41}\,Y \tag{A37}$$

$$Y = \left[1-0.1\left(\frac{\rho_f-\rho_g}{\rho_g}\right)^{0.4}\left(1-x\right)^{0.4}\right]^{-1.15}. \tag{A38}$$

Again an average quality is used to give an average heat transfer coefficient over the region.

The pressure drop calculation in the post critical heat flux region was obtained using the same Friedel correlation that was used in the nucleate boiling region.

For the superheat region the heat transfer becomes single phase and methodology from the single phase region was used to calculate the heat transfer coefficient and the pressure drop. Average properties were used to calculate the heat transfer coefficient and the pressure drop.

On the hot side there is no phase change and Equations A1- A3 were used to calculate the heat transfer coefficient and Equations A4-A6 were used for the pressure drop.

The overall heat transfer coefficient in each region was calculated as (Bird et al. 1960)

$$U = \left({}^{1}\!/_{h_{cold}} + {}^{d_{out}}\!/_{2k_{metal}} \ln\left({}^{d_{out}}\!/_{d_{in}} \right) + {}^{d_{out}}\!/_{d_{in}h_{hot}} \right)^{-1}, \qquad \text{(A39)}$$

where h_{hot} is the heat transfer coefficient for the hot channels, h_{cold} is the heat transfer coefficient for the cold channels, k_{metal} is the thermal conductivity of the metal and d_{in} and d_{out} are the inner and outer diameters of the tubes.

Using the assumed shell diameter, tube inner and outer diameter, pitch, triangular array and pressure drops the overall heat transfer coefficient and heat transfer area were found for each heat transfer region. The length of each region was then obtained from the heat transfer area and the shell diameter. The hot and cold side pressure drops were then calculated. The pressure drop was then iterated until the input and output values converged. Once all the regions were solved the total volume and pressure drop in the steam generator was calculated by summing the volume and pressure drops from each region.

A baseline combined cycle using helium as the Brayton cycle working fluid was modeled in HYSYS. The four regions of the steam generator are modeled as four heat exchangers in HYSYS as seen in Figure A2. The HYSYS model predicted a steam generator volume of 133.9 m^3, length of 11.6 m and an overall heat transfer of 457.3 MW.

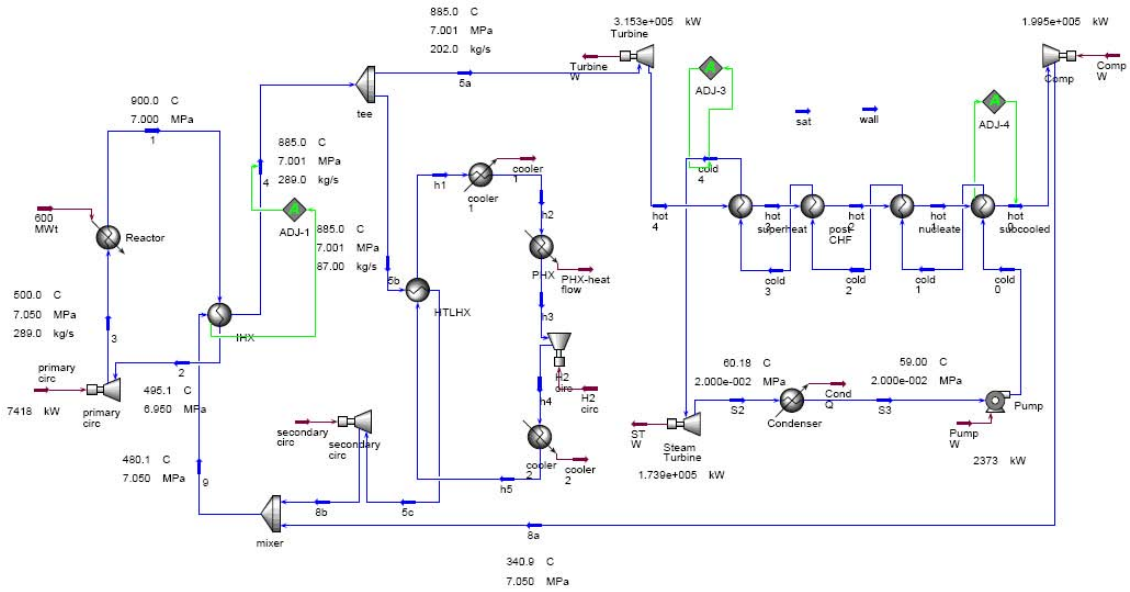

Figure A2. HYSYS model of the combined cycle with a four-region steam generator model.

To validate the HYSYS model, a RELAP5 (INEEL 2005) model of the steam generator was created and is depicted in Figure A3. The steam generator was modeled as a once through shell-in-tube vertical heat exchanger. The water served as the cold-side coolant in the tubes and the helium served as the hot-side fluid in the shell.

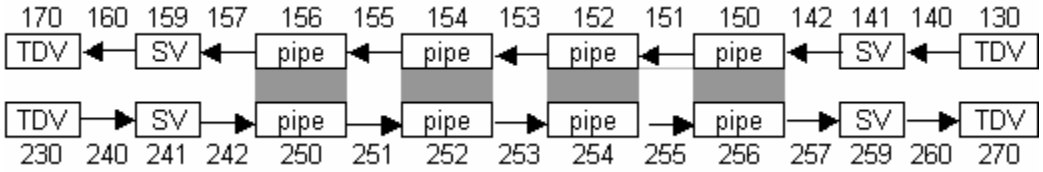

Figure A3. RELAP5 model of the steam generator.

The input parameters of the RELAP5 model were taken from the HYSYS model and are shown in Table A1. A small error, marked by an asterisk, can be seen on the shell side. The error was due to a pressure change that occurred as the flow moved from the time-dependent volume 230 to the single volume 241. The input conditions were originally set for 860.65 K and 3.12 MPa, but were altered because of physical reasons by RELAP5 to 862.46 K and 3.1395 MPa. For our purposes and also because of the small change in temperature and pressure, this error was ignored.

Table A1. Input parameters for the RELAP5 steam generator model.

Input Parameter	Tubes	Shell
	Cold-side – H20	Hot-side - He
RELAP Volume Number Range	130-170	230-270
Inlet Temperature (K)	332.94	**862.46***
Inlet Pressure (Pa)	1.50E+07	**3.1395E+06***
Mass Flow (kg/s)	140.7	202
Rod Pitch to Diameter Ratio	1	1.3
Heated Diameter (m)	6.00E-03	6.735E-03
Hydraulic Diameter (m)	6.00E-03	6.711E-03
RELAP Geometry Type	101	110
Cross Sectional Area (m^2)	3.697	5.394

The heat exchanger total length was taken from the HYSYS calculation and divided into four pipes as shown in Figure A3 and Table A2. The reason the heat exchanger was divided into four separate pipes was to adjust the pipes for refinement in nodalization of a particular region of flow in the event it would be needed and also to avoid the 99 node limitation per pipe of RELAP5.

Table A2. RELAP5 pipe and node sizes.

PIPE	No. of Nodes	Pipe Length (m)	Node Size (m/node)
150/256	20	3	0.15
152/254	20	3	0.15
154/256	30	3	0.1
146/250	30	2.6021	0.08674

Table A3 summarizes the results of the heat transfer and lengths for the HYSYS and RELAP5 models. The results are summarized graphically Figures A4 through A6. From Figure A4, it can be seen that the overall heat transfer is in good agreement, with a difference of about 2.1 % between models. The outlet temperatures and temperature drops across the steam generator also show reasonable agreement of less than 5.1% difference as illustrated in Tables A4 and A5.

Table A3. Regime length and heat transfer comparison.

Regions	Length HYSYS (m)	Length RELAP5 (m)	Q HYSYS (MW)	Q RELAP5 (MW)
Single-phase Liquid, Sub Nucleate Boiling	7.955	8.8	210.9	204.84
Saturated Nucleate Boiling	2.505	0.547	117.8	78.38
Post Critical Heat Flux	0.153	1.301	23.2	114.46
Superheated Vapor	0.989	0.954	105.4	50.20
Total	11.602	11.602	457.3	447.87

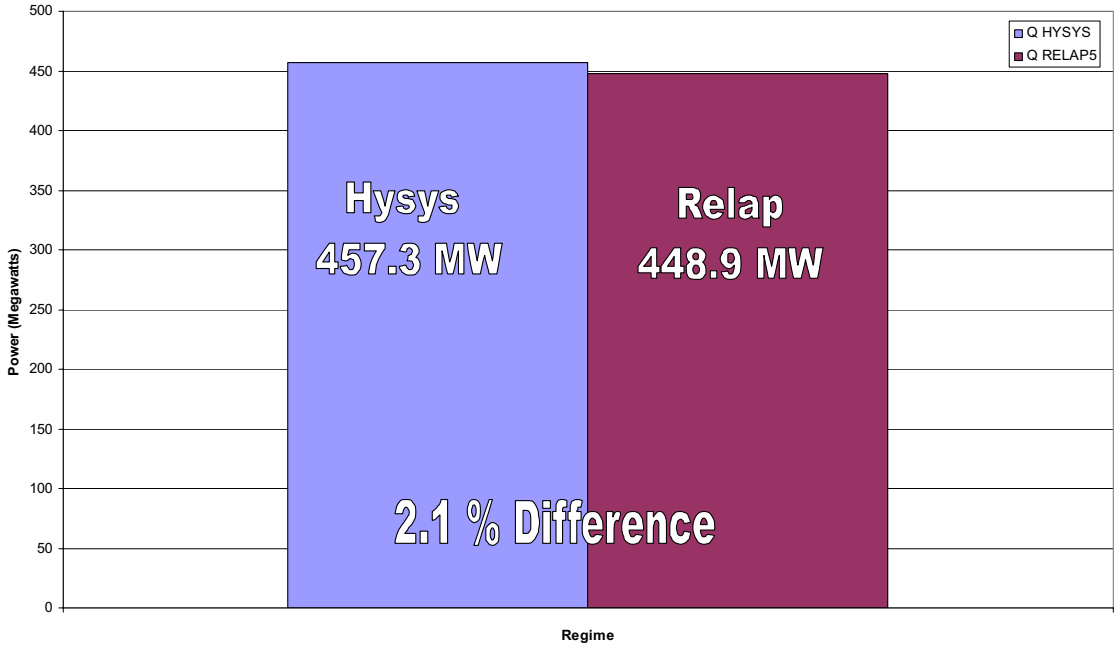

Figure A4. Overall heat transfer comparison.

Table A4. Comparison of outlet temperatures.

	Temperature Hot-side (K)	Temperature Cold-side (K)
HYSYS	424.65	848.15
RELAP5	441.75	822.87
Difference (°)	17.1	25.28
% Difference	4.0%	3.1%

Table A5. Comparison of temperature drops.

Temperature Drops	Hot-side	Cold-side
HYSYS	436	515
RELAP5	420.7	489.92
% Difference	3.6%	5.1%

Larger differences can be seen when examining the individual components of heat transfer and length as shown in Figures A5 and A6. In Figure A5, the heat transfer in the single phase forced convection and sub-cooled nucleate boiling regions show results within fair agreement, less than 3 %

difference. The other regions show greater variance. The length comparison in Figure A6 shows a fair agreement in the single-phase forced convection/sub-cooled nucleate boiling and the superheated vapor regions.

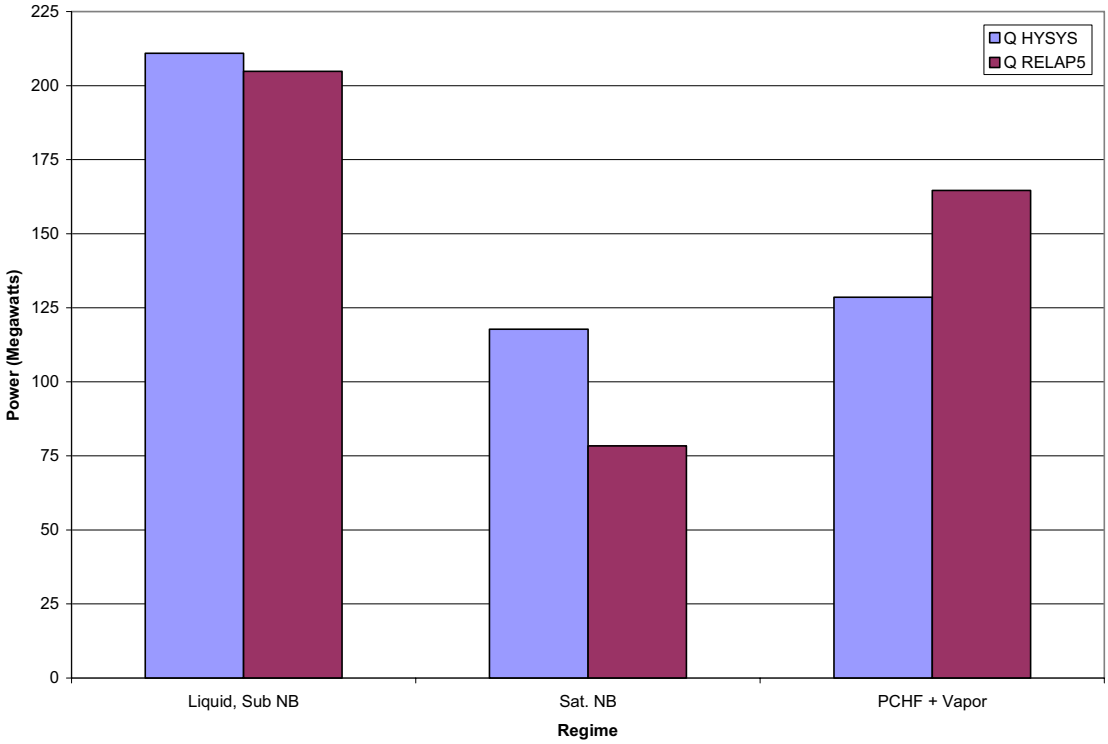

Figure A5. Regime heat transfer comparison.

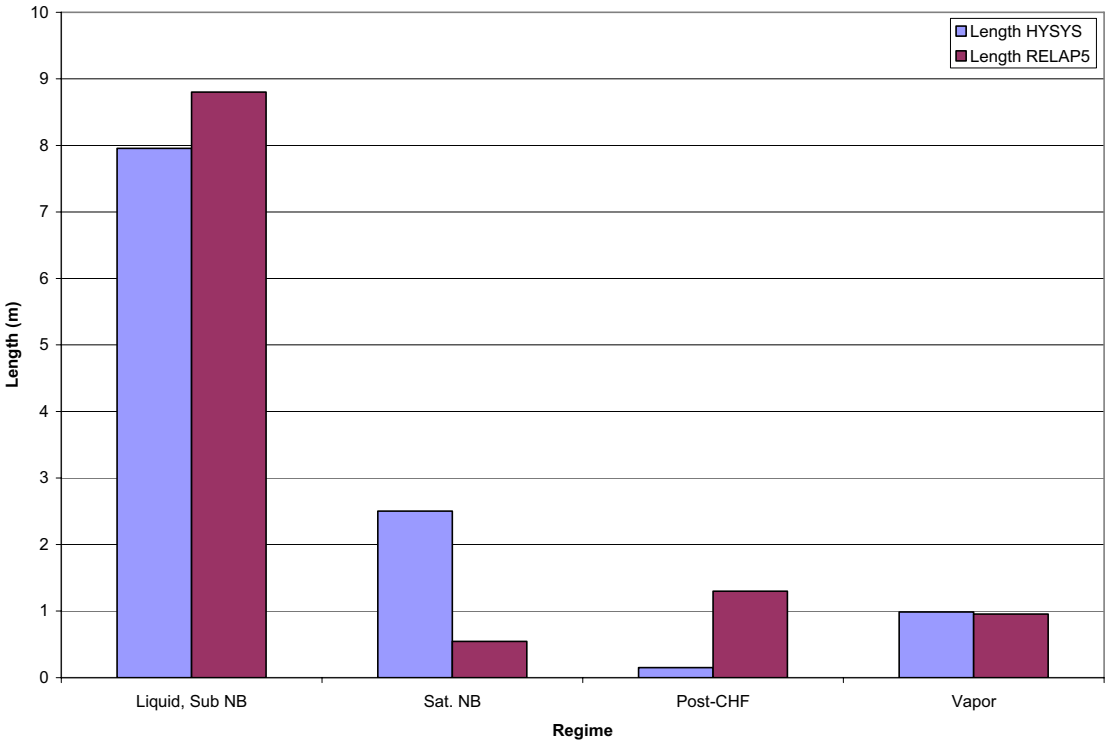

Figure A6. Regime length comparison.

Looking further into the differences of the two models, we can see that the different nodalizations and methods used in the two models affect the temperature distributions as shown in Figure A7. The influence of the multiple nodes in RELAP5 versus the single node in HYSYS is shown over the subcooled region (for lengths less than about 8 m). The thermodynamic properties associated with the more detailed RELAP5 model more accurately represent the actual profile than the single, average value used in HYSYS model. Figure A7 also illustrates a difference between methods in the film boiling regime (colored in purple for the RELAP5 model). The temperature in RELAP5 rises as opposed to the temperature in HYSYS, which remains constant until the quality is one. The cause of this discrepancy is from the two different approaches of HYSYS and RELAP5. In RELAP5, heat transfer during film boiling is contributed directly to the vapor. The vapor heats up and then transfers heat to the liquid which causes vaporization. HYSYS, on the other hand, directs its heat transfer solely to the liquid and therefore, its temperature does not change until all of the liquid is converted to vapor.

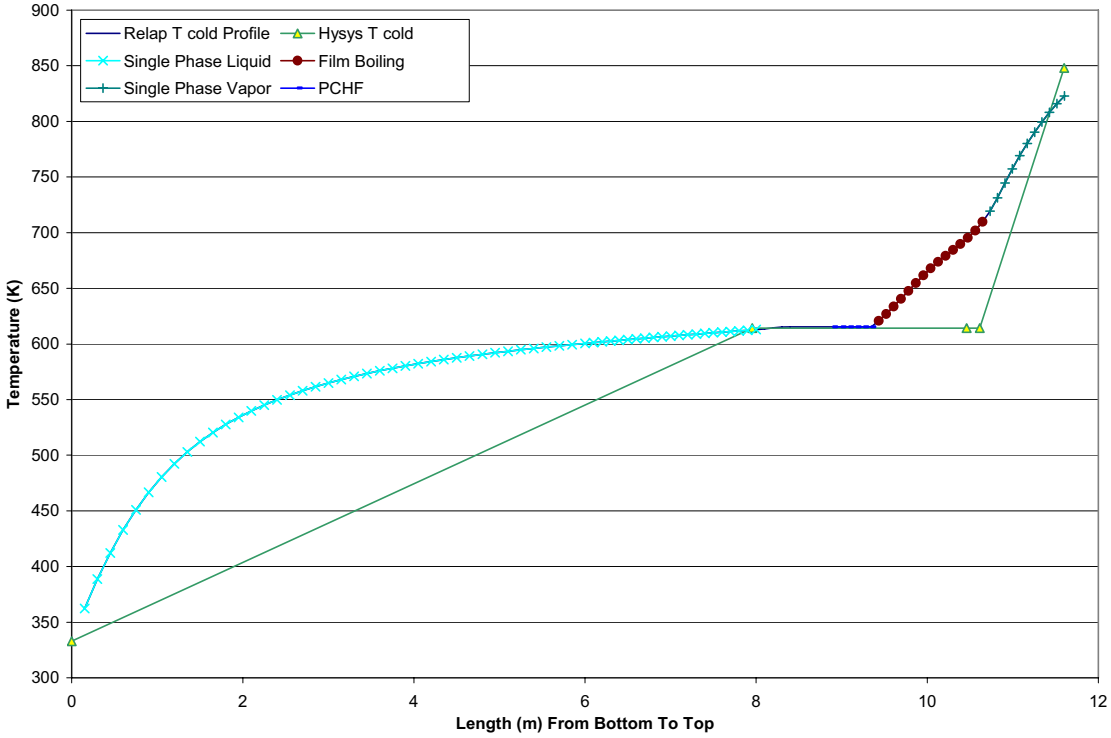

Figure A7. Comparison of cold fluid temperatures.

The detailed comparisons showed many differences in the parameters and methods used in RELAP and HYSYS. The different methods explained many of the disagreeing results seen in the regime wide comparisons. In the post critical heat flux region, the different correlations, Bromley and Groeneveld, lead to different heat transfer coefficients. Similarly, the heat transfer coefficients in the saturated nucleate boiling region were different because of the Chen correlation coefficients were determined from different equations. The critical quality and critical heat flux were also determined from different correlations, CISE-4 in HYSYS and the AECL lookup table in RELAP5. Nodalization also contributed to the differences in the regime specific comparisons because it affected the calculation of fluid properties. HYSYS computed averaged values of fluid properties such as specific heat, viscosity, and thermal conductivity from the input and output conditions between each flow regime. Because fluid properties were not always linear as shown in the RELAP5 results, using the average of the in and out conditions of each regime produced large differences in the areas of large temperature changes such as in the subcooled – single phase region and the superheated vapor region because it affected the values of fluid properties.

Despite these differences, the overall results showed good agreement. The overall heat transfer had only about 2.1 % difference. The outlet temperatures and temperature drops across the steam generator also show reasonable agreement with less than 5.1% difference. To eliminate the possibility that RELAP and HYSYS coincidentally had agreement only in the tested conditions of heat transfer of approximately 450 MW, another case was tested with a total heat transfer of 370 MW. The heat transfer was changed by increasing the inlet temperature of the cold-side from 60° C to 200°C. The overall heat transferred between RELAP and HYSYS models differed by less than 2% for this case. These calculations indicate that the four-region steam general model developed for HYSYS produces reasonable overall agreement with a much more detailed RELAP5 model. Similar agreement would be expected with HyPEP.

Appendix B

Electrolyzer Model, HTE Process Heat Model, Interconnections, and GAS-PASS/H Simulations

HTE Model - Introduction

The choice of an appropriate level of detail is an important consideration in the development of models. In the HYPEP code phenomena important to efficiency need to be included since the code is to be used to study how efficiency in the combined plant trends with design variations. A list of important phenomena includes heat recuperation, mechanical pumping power, and heat exchanger temperature drop from hot to cold side. But capital costs also compete with efficiency in the larger task of plant economic optimization. For example, heat exchanger surface area can be increased to improve heat recuperation but at increased capital cost. While an economic analysis is beyond the project goal of model development it was possible to incorporate elements of economic optimization as described below.

Many years of design experience in the chemical industry have led to simple rules for component performance for balancing increased efficiency against increased cost. These rules are expressed in terms of simple figures of merit that correlate with the results of more detailed economic and engineering analyses. Examples include citing heat exchanger performance in terms of effectiveness rather than heat transfer area. The latter requires specifying geometry and dimensions of heat transfer surfaces while the former is based on representative values for effectiveness given in the literature. Another example is pump and compressor performance cited in terms of characteristic curves rather than hydraulics. The latter requires specifying geometry and dimensions of vanes and passages while the former adopts prototypic curves from the literature. Similarly, targeting a literature-based range of desirable fluid velocities rather than designing with respect to pressure drop is preferred since ultimately the latter approach requires an economic optimization. The desirable fluid velocities on the other hand reflect findings of economic analyses that went before. Adopting such rules in the early stages of this project reduces the need for more complex component modeling, postponing it to a later stage when detailed economic optimization and, hence, individual component design becomes more important.

The main equipment components in the high temperature steam electrolysis process are shown in Figure B1. Liquid water enters from the left-hand side, is vaporized, and is superheated through a series of heat exchangers. The water vapor then enters the electrolyzer. The heat is supplied by heat exchangers coupled to a nuclear reactor and by recuperation of heat from the reaction products exiting the electrolyzer. In practice the electrolyzer operates above atmospheric pressure. To preserve electrode life hydrogen is also combined with the inlet vapor steam while nitrogen may be used to sweep the oxygen produced at the anode. Figure B2 shows these gases and typical operating conditions.

Electrolyzer Model

In the electrolyzer model the oxygen stream produced at the anode is assumed to mix with a sweep gas stream that is introduced at the anode. Presently, the sweep gas is assumed to be an arbitrary mix of oxygen and nitrogen. The combined stream then exits the electrolyzer. The hydrogen stream produced at the cathode is assumed to mix with a feed stream that is introduced at the cathode. The feed stream is composed of water vapor to be electrolyzed, hydrogen gas for maintaining reducing environment, and possibly an inert gas, presently assumed to be nitrogen. The flow of materials is shown in Figure B3.

A. Energy Equation

An energy balance on the electrolyzer gives

$$\sum_i \dot{n}_{P-i} H_{P-i}(T_P, P) = \sum_i \dot{n}_{R-i} H_{R-i}(T_R, P) + Q + W \tag{B1}$$

where

$\dot{n}$	=	species mole flow rate,
H	=	enthalpy per mole,
Q	=	rate of heat transfer to the electrolyzer,
W	=	rate of electrical work supplied to the electrolyzer,
T	=	temperature,
P	=	pressure,

and where we have used subscripts *R* for reactants and *P* for products. Expressed in terms of the individual species shown in Figure B1 and their mass flowrates we have

$$\begin{aligned} & m_{H_2O-o-cath}\, h_{H_2O}\,(T_o, P) + m_{H_2-o-cath}\, h_{H_2}(T_o, P) + m_{N_2-o-cath}\, h_{N_2}(T_o, P) \\ & \quad m_{O_2-o-anode}\, h_{O_2}(T_o, P) + m_{N_2-o-anode}\, h_{N_2}(T_o, P) = \\ & m_{H_2O-i-cath}\, h_{H_2O}\,(T_i, P) + m_{H_2-i-cath}\, h_{H_2}(T_i, P) + m_{N_2-i-cath}\, h_{N_2}(T_i, P) \\ & \quad m_{O_2-i-anode}\, h_{O_2}(T_i, P) + m_{N_2-i-anode}\, h_{N_2}(T_i, P) + Q + W \end{aligned} \tag{B2}$$

where

m	=	species mass flow rate (kg/s),
h	=	specific enthalpy (joules/kg),

and where subscripts *i* and *o* represent inlet and outlet, respectively.

B. Species Mole and Mass Flowrates

The species mole flowrates entering and leaving the electrolyzer are related to the current density through the relationships

$$\dot{n}_{H_2O-o-cath} = \dot{n}_{H_2O-i-cath} - \frac{iA}{2F}$$

$$\dot{n}_{H_2-o-cath} = \dot{n}_{H_2-i-cath} + \frac{iA}{2F}$$

$$\dot{n}_{O_2-o-anode} = \dot{n}_{O_2-i-anode} + \frac{iA}{4F} \qquad \text{(B3)}$$

$$\dot{n}_{N_2-o-anode} = \dot{n}_{N_2-i-anode}$$

$$\dot{n}_{N_2-o-cath} = \dot{n}_{N_2-i-cath}$$

where

i	=	current density (amps/m^2),
A	=	electrode surface area, (m^2) and
F	=	Faradays constant.

The species mass flowrates and mole flowrates are related as follows: For an individual species

$$\dot{m}_{k-o} = A_k \ \dot{n}_{k-o} \text{ and } \dot{m}_{k-i} = A_k \ \dot{n}_{k-i} \ , \quad k = H_2O, H_2 , O_2, \text{ and } N_2 \qquad \text{(B4)}$$

where A_k is the atomic weight of species k in kg per mole and subscript o is the outlet and i is the inlet.

C. Cell Voltage and Electrical Work

The voltage drop across the electrolyzer is the sum of the electrode Nernst potential and the resistance of the cell. In estimating the resistance, the activation and the concentration overpotentials are lumped in with the cell internal resistance. The cell voltage is then assumed given by

$$V_{cell} = V_N + i \cdot r \qquad \text{(B5)}$$

where

V_N	=	is the Nernst potential, and
r	=	is the area-specific cell resistance (ohms-m^2).

The electrical work done in the cell is

$$W = V_{cell} \cdot i \cdot A \ . \qquad \text{(B6)}$$

The active species giving rise to the Nernst potential satisfy the chemical balance equation

$$H_2O\,(g) \rightarrow H_2\,(g) + \frac{1}{2} O_2\,(g) . \qquad \text{(B7)}$$

The change in Gibbs free energy for this reaction carried out at temperature T and pressure P is from the Appendix C.

$$\Delta G(T,P) = \Delta G_f(T,P) + RT \ln\left[\frac{f_{H_2}\, f_{O_2}{}^{\frac{1}{2}}}{f_{H_2O}}\right] \tag{C.13}$$

where f is the molar fraction of a species and where

$$\Delta G_f(T,P) = G_{f-H_2}(T,P) + 1/2\, G_{f-O_2}(T,P) - G_{f-H_2O}(T,P)\,. \tag{C.14}$$

where the $G_{f\text{-}i}(T,P)$ are on a per mole basis.

The mole fractions at any point in the electrolyzer are related to the molar mass flowrates at that point through

$$f_{H_2O-cath} = \frac{\dot{n}_{H_2O}}{\dot{n}_{H_2O} + \dot{n}_{H_2} + \dot{n}_{N_2}} \qquad f_{H_2-cath} = \frac{\dot{n}_{H_2}}{\dot{n}_{H_2O} + \dot{n}_{H_2} + \dot{n}_{N_2}}$$

$$f_{O_2-anode} = \frac{\dot{n}_{O_2}}{\dot{n}_{N_2} + \dot{n}_{O_2}} \qquad f_{N_2-anode} = \frac{\dot{n}_{N_2}}{\dot{n}_{N_2} + \dot{n}_{O_2}}. \tag{B8}$$

The Appendix derives the following expression for the electrical voltage developed

$$V_N = \frac{-1}{2F}\left[\Delta G_f{}^0(T) + RT \ln\left[\left(\frac{f_{H_2}\, f_{O_2}{}^{\frac{1}{2}}}{f_{H_2O}}\right)\left(\frac{P}{P_{STD}}\right)^{\frac{1}{2}}\right]\right] \tag{C.19}$$

where P_{STD} = 0.101 MPa and P is the cell pressure.

In the electrolyzer there is a species concentration and temperature gradient from input to output. In this model, however, perfect mixing of all streams at each electrode is assumed with the Nernst potential calculated for the conditions at the exit of the cell.

HTE Process Heat Model

A key task was to identify the level of model detail consistent with project objectives. One guideline is that the main phenomena must be captured in a way that avoids including extraneous detail. One way to gauge the cutoff point with regard to specific detail is to determine if the predicted behavior would be sensitive to neglecting to model the associated phenomena. If not, then individual breakout of the phenomenon should be considered extraneous. The main application of this principle in this work involved identifying the appropriate level of reactant and process stream representation.

A representation of the thermal processing equipment based on the HYSYS process equipment diagrams presented by Stoots (2005) is shown in Figure B2. Operation occurs at two different pressures, the low-side pressure of 0.1 MPa and the high-side pressure of 5.0 MPa. The process raises reactant

streams at the same temperature and pressure (0.1 MPa, 25^{o} C) to a new temperature and pressure (5.0 MPa, 850^{o} C) for inlet to the electrolyzer. The process is reversed for the products that exit the electrolyzer. The process equipment provides for pressurizing of reactants, heating of reactants by reactor process heat, cooling of products by recuperation between reactant and product streams, and product de-pressurization. Phase change in the reactant stream takes place in a single boiler. Similarly, phase change in the product stream takes place in a single condenser.

In an assessment of the appropriate level of model detail for representing the important phenomena in Figure B2 the following were considered. The main phenomena are mechanical work and heat recuperation involving condensable and non-condensable gases. Significant model simplification derives from noting that parallel streams (classified separately by reactants and by products) undergo the same overall transition in pressure-temperature condition. Essentially, predicted behavior should be insensitive to lumping of such streams with respect to heat transfer and mechanical work processes. The lumping process is achieved by requiring parallel streams to have the same temperature and pressure at the point where they enter a component and the point where they leave the component. As a consequence heat transfer or mechanical work is performed for multiple streams by a single component model as shown in Figure B5 rather than parallel components (one for each stream) as shown in Figure B4. This merging of streams is an abstraction that allows for simpler models and the exclusion of what for now is considered extraneous detail until such time as detailed design of components is performed with the goal of economic optimization.

A. Pressure Step-Up Unit

The reactant streams consist of liquid water and non-condensable gases. All streams are raised to the same pressure adiabatically.

A.1 Simplified Pump Model

A pump is used to raise the pressure of the liquid water. Since liquid water is very nearly incompressible, shaft power applied reversibly to a control volume is given by

$$W_{rev} = \frac{\left(P_o - P_i\right)\dot{m}}{\rho} \tag{B9}$$

where

$\dot{m}$	=	liquid water mass flowrate,
ρ	=	density, and
P	=	pressure

and subscripts *i* and *o* represent inlet and outlet, respectively.

The actual shaft power, W_{act}, is related to the pump efficiency, η, through $W_{act} = \eta\ W_{rev}$. In practice to get from pressure P_i to P_o shaft power delivered irreversibly results in an enthalpy change in the control volume given by

$$W_{act} = \dot{m}\left[h(T_o, P_o) - h(T_i, P_i)\right] \tag{B10}$$

where *h* is enthalpy and *T* is temperature. Eliminating the power terms in the above three equations gives

$$P_o - P_i = \rho \eta \left[h(T_o, P_o) - h(T_i, P_i) \right] \tag{B11}$$

A.2 Detailed Pump Model

A more detailed representation of the pump would include pump characteristic curves. These curves express any two of efficiency, pressure ratio, and enthalpy change in terms of mass flowrate and shaft speed. For efficiency and pressure ratio

$$\frac{P_o}{P_i} = f_{\mathrm{Pr}}(\overline{\dot{m}}, \overline{\omega}) \tag{B12}$$

$$\eta = f_{\eta}(\overline{\dot{m}}, \overline{\omega}) \tag{B13}$$

where $\overline{\omega}$ is normalized shaft speed and $\overline{\dot{m}}$ is normalized mass flowrate.

The shaft work is given by Eq. (10). Additionally, from the definition of efficiency

$$\eta = \frac{h(T_{ideal-o}, P_o) - h(T_i, P_i)}{h(T_o, P_o) - h(T_i, P_i)} \tag{B14}$$

where $T_{ideal\text{-}o}$ is the temperature reached upon arriving at pressure P_o when the shaft work is performed reversibly. From this definition of $T_{ideal\text{-}o}$ it follows that

$$S(T_{ideal-o}, P_o) - S(T_i, P_i) = 0 \tag{B15}$$

where S is entropy.

A.3 Compressor Model

The compressor model for a single non-condensable gas uses the same conservation equations as the detailed pump model. But in the case of the compressor the fluid is compressible rather than incompressible. This is captured in the fluid properties and the characteristic curves.

A.4 Compressor Model for Multiple Gas Streams

In the representation of Figure B2 there are two separate non-condensable gas streams that enter the Pressure Step-up Unit. The cathode stream is a mixture of hydrogen and nitrogen and the anode stream is a mixture of oxygen and nitrogen. It is assumed both streams enter and leave the Pressure Step-Up Unit at the same temperatures and pressures.

The case of a single stream composed of a mixture of gases is treated first. Non-dimensionless flow and shaft speed are functions are defined

$$\overline{\dot{m}} = \dot{m}\,\frac{\sqrt{\frac{T_i R}{\gamma}}}{(2r)^2 P_i} \quad \text{and} \quad \overline{\omega} = \frac{\omega 2r}{\sqrt{\gamma R T_i}} \tag{B16}$$

where

ω	=	actual shaft speed,
r	=	tip radius,
γ	=	ratio of specific heats, and
R	=	gas constant

where the last two parameters are for the gas mixture. The characteristic curves relate pressure ratio and efficiency to non-dimensional flow and speed through

$$\frac{P_o}{P_i} = f_{\mathrm{Pr}}(\overline{\dot{m}}, \overline{\omega}) \tag{B17}$$

$$\eta = f_{\eta}(\overline{\dot{m}}, \overline{\omega}) \ . \tag{B18}$$

The compressor equations are

$$W_{act} = \dot{m}\left[h(T_o, P_o) - h(T_i, P_i)\right] \tag{B19}$$

$$\eta = \frac{h(T_{ideal-o}, P_o) - h(T_i, P_i)}{h(T_o, P_o) - h(T_i, P_i)} \tag{B20}$$

$$S(T_{ideal-o}, P_o) - S(T_i, P_i) = 0 \quad . \tag{B21}$$

The compressor equations are examined for the existence and uniqueness of a solution. If the variables $\dot{m}$, ω, P_i, and T_i are taken as boundary conditions, then there remain five variables that must be solved for: P_o, T_o, $T_{ideal-o}$, W_{act}, and η. There are five equations so a unique solution exists for these boundary conditions. This solution can be obtained as follows. Eq. (B17) and P_i give P_o. Eq. (B21) is then solved for $T_{ideal-o}$. Eq. (B19) and (B20) are then solved for W_{act} which is then substituted in Eq. (B19) to obtain T_o.

The above can be extended to multiple separate streams. It is assumed that each of the streams entering the compressor is at the same temperature and pressure and that this is true for the streams exiting (as is the case of the cathode and anode streams above). In particular the inlet streams are each at low-side system pressure P_L and the outlet streams are at high-side pressure P_H.

From a model standpoint, simplification results when a single averaged stream is used to represent the two streams. The treatment below of the anode and cathode streams as a single stream is rigorous for the case where the mass flowrates of the two streams vary in direct proportion to each other. That is, their ratio is constant. Early studies will focus on quasi-static and dynamic transients where the HTE power varies in response to change in load. The water and oxygen flowrates will vary in direct proportion to electrolyzer power for which case the ratio of the cathode and anode streams will be constant. One sees in

the expression for dimensionless flow that given a design for the compressor in one stream there exists a tip diameter for the compressor in the other stream such that the two compressors have the same dimensionless flowrate. Similarly, for dimensionless speed there exists a shaft speed for the second compressor such that both compressors have the same dimensionless speed. We arrange for these two conditions to be true at the full power condition. Then for load changes where the ratio of mass flowrates is preserved, the two compressors share the same performance curves.

The combined stream equations are as follows. Define for stream *j* consisting of species indexed by *k*

$$\begin{aligned} \overline{\dot{m}_j} &= \sum_k \dot{m}_{k-j} \\ \overline{h_j \dot{m}_j} &= \sum_k h_k \dot{m}_{k-j} \\ \overline{s_j \dot{m}_j} &= \sum_k s_j \dot{m}_{k-j} \end{aligned} \tag{B22}$$

where the index *j* has values *cath* and *anod*.

The equations for each stream then combine to give

$$W_{act} = \sum_j \overline{h_j(P_o, T_o)\dot{m}_j} - \overline{h_j(P_i, T_i)\dot{m}_j} \tag{B23}$$

$$\eta W_{act} = \sum_j \overline{h_j(P_o, T_{ideal})\dot{m}_j} - \overline{h_j(P_i, T_i)\dot{m}_j} \tag{B24}$$

$$\sum_j \overline{s_j(T_{ideal-o}, P_o)\dot{m}_j} - \overline{(s_j(T_i, P_i)\dot{m}_j} = 0\,. \tag{B25}$$

where

W_{act} = combined work of the compressors

and where the second equation follows when the compressors have the same dimensionless set of characteristic curves, as when the stream flowrates are in direct proportion to each other. This set of equations is the analog of the set for a single compressor. As in the single compressor case variables $\dot{m}$, ω, P_i, and T_i can be taken as boundary conditions leaving five variables that must be solved for: P_o, T_o, T_{ideal}, W_{act}, and η and where there are five equations including the two characteristic curves.

B. Pressure-Work Recovery Unit

B.1 Turbine Model for Multiple Compressible Gas Streams

The discussion for the compressor applies equally to the turbine. The turbine equations are the same as those for the compressor with three exceptions. The pressure ratio is given as inlet pressure divided by outlet pressure, the efficiency is given as actual work divided by ideal work, and the terms present in an enthalpy difference are the negative of what they are for the condenser.

C. Boiler with Non-Condensable Gas Streams

The streams output from the Pressure Step-Up Unit in Figure B2 enter the cold side of the boiler. The concept of mixing streams allows model simplification and is warranted given the current state of design as described below.

C.1 Cold Side

There are three streams that enter the cold side of boiler. The first cathode stream is composed of liquid water and the second of oxygen and nitrogen. The anode stream is composed of oxygen and nitrogen. All streams are assumed to be at the same temperature at the entrance. The three streams are assumed to be in thermal equilibrium when they exit the boiler. All streams are assumed to be at the same high-side system pressure, P_H, at the inlet and outlet of the boiler.

The two cathode streams described above create a liquid phase and gas phase in the boiler. It is assumed the two phases are in thermal equilibrium and that each phase is perfectly mixed. The liquid phase is saturated water and the gas phase is saturated water vapor and non-condensable gases. The water vapor partial pressure is the saturation pressure corresponding to the temperature of the saturated liquid. This follows from the assumption of thermal equilibrium. [Dodge] The liquid water entering the boiler may be subcooled.

The mass flowrate of cathode stream saturated vapor leaving the boiler is

$$\dot{m}_{H_2O(g)-cath-o} = A_{H_2O} \frac{P_{H_2O(g)-cath-o}}{P_L} \sum_k \frac{\dot{m}_{k-cath-o}}{A_k} \tag{B26}$$

where the subscripts *k*, *cath*, and *o* represent, respectively, an index over the cathode species, cathode stream, and boiler outlet. It is assumed that the partial pressure of the water vapor equals the saturation vapor pressure and, hence, is given by

$$P_{H_2O(g)-cath-o} = f(T_{sat}) \tag{B27}$$

where *f* is a function that gives vapor pressure as a function of saturation temperature, T_{sat}. Similarly, the mass flowrates of the other cathode species *j* leaving the boiler are

$$\dot{m}_{j-cath-o} = A_j \frac{P_{j-cath-o}}{P_L} \sum_k \frac{\dot{m}_{k-cath-o}}{A_k} \tag{B28}$$

The partial pressures of the cathode species leaving the boiler satisfy

$$P_L = P_{H_2O(g)-cath-o} + \sum_j P_{j-cath-o} \, . \tag{B29}$$

The anode and cathode streams are assumed to be in thermal equilibrium entering and exiting the boiler so an energy balance on the cold side gives

$$0 = \dot{m}_{H_2O(l)-cath}\left[h_{H_2O(l)}(P_L, T_{c-i}) - h_{H_2O(g)}(T_{sat})\right] + Q_{tp} + \sum_j \dot{m}_{j-cath}\left[h_j(P_{j-cath-i}, T_{c-i}) - h_j(P_{j-cath-o}, T_{sat})\right] + \sum_j \dot{m}_{j-anod}\left[h_j(P_{j-anod-i}, T_{c-i}) - h_j(P_{j-anod-o}, T_{sat})\right] \quad \text{(B30)}$$

where

$T_{c\text{-}I}$ = temperature of the hot side streams entering the boiler, and
Q_{tp} = rate of heat transfer from hot to cold side.

For the anode stream

$$P_{j-anod-o} = P_{j-anod-i} \quad \text{(B31)}$$

The cold side equations are examined for the existence and uniqueness of a solution. If the variables $\dot{m}_{k-i}$, $P_{k\text{-}I}$, $T_{c\text{-}I}$, and Q_{tp} are taken as boundary conditions, then there remain eight variables that must be solved for $P_{H_2O(g)-cath-o}$, $P_{H_2-cath-o}$, $P_{N_2-cath-o}$, $P_{O_2-anod-o}$, $P_{H_2-anod-o}$, P_L, T_{sat}, and $\dot{m}_{H_2O(g)-cath-o}$. There are eight equations for the cold side so a solution exists for these boundary conditions. Not written are mass balances for individual species where it is assumed that the outlet mass flowrate equals the inlet.

C.2 Hot Side

There is one stream, helium that enters the hot side of boiler.

The anode and cathode streams are assumed to be in thermal equilibrium entering and exiting the boiler so an energy balance on the cold side gives

$$0 = \dot{m}_{He}\left(h_{He}(T_{h-i}) - h_{He}(T_{h-o})\right) - Q_{tp} \quad \text{(B32)}$$

where

$T_{h\text{-}I}$ = temperature of the hot side streams entering the boiler, and
$T_{h\text{-}o}$ = temperature of the hot side streams exiting the boiler.

C.3 Interface

The temperatures and the heat transferred are related by

$$Q_{tp} = (UA)_{cond}\,\frac{(T_{h-o} - T_{sat}) - (T_{h-i} - T_{sat})}{\ln\left((T_{h-o} - T_{sat})/(T_{h-i} - T_{sat})\right)} \quad \text{(B33)}$$

where *UA* is the product of the overall heat transfer coefficient and the heat transfer area. The superheat and two-phase regions have been lumped as a single region so the value for *UA* must reflect this.

In the early stages of design it is more appropriate to work with heat exchanger effectiveness, ε, rather than overall heat transfer coefficient, UA. A value for UA is typically meaningful only when generated in an economic analysis performed late in a design study. Heat exchanger effectiveness on the other hand is dimensionless and values that reflect chemical industry practices which takes in economics

are given in the literature. Heat exchanger effectiveness is the actual heat transferred to the thermodynamically maximum for infinite heat transfer area. The heat exchanger effectiveness then is

$$\varepsilon = \frac{T_{h-i} - T_{h-o}}{T_{h-i} - T_{sat}} . \tag{B34}$$

When a solution is sought with heat exchanger effectiveness used in place of UA, then Eq. (B34) replaces Eq. (B33).

D. Condenser with Non-Condensable Gas Streams

The streams output from the Pressure Work-Recovery Unit in Figure B2 enter the condenser. The concept of mixing streams again allows model simplification and is warranted for reasons that parallel those for the boiler. It is assumed that the water entering the condenser is superheated, and that there is perfect mixing of the water in the condenser.

D.1 Hot Side

There are two streams that enter the hot side of the condenser. The cathode stream is composed of water vapor, oxygen, and nitrogen and the anode stream is composed of oxygen and nitrogen. Both streams are assumed to be at the same temperature and pressure. The streams are assumed to be in thermal equilibrium when they exit the condenser. It is assumed that the temperature of the streams is reduced sufficiently that there is condensation of water vapor. Both streams are assumed to be at the same low-side system pressure, P_L, at the inlet and outlet of the condenser.

The mass flowrate of cathode stream saturated vapor leaving the condenser is

$$\dot{m}_{H_2O(g)-cath-o} = A_{H_2O} \frac{P_{H_2O(g)-cath-o}}{P_L} \sum_k \frac{\dot{m}_{k-cath-o}}{A_k} \tag{B35}$$

where the subscripts *k*, *cath*, and *o* represent, respectively, an index over the cathode species, cathode stream, and condenser outlet. It is assumed that the partial pressure of the water vapor equals the saturation vapor pressure and, hence, is given by

$$P_{H_2O(g)-cath-o} = f(T_{sat}) \tag{B36}$$

where *f* is a function that gives vapor pressure as a function of saturation temperature, T_{sat}. Similarly, the mass flowrates of the other cathode species leaving the condenser are

$$\dot{m}_{j-cath-o} = A_j \frac{P_{j-cath-o}}{P_L} \sum_k \frac{\dot{m}_{k-cath-o}}{A_k} \tag{B37}$$

The mass flowrate of the saturated liquid leaving the condenser satisfies the mass balance

$$\dot{m}_{H_2O(g)-cath-i} = \dot{m}_{H_2O(l)-cath-o} + \dot{m}_{H_2O(g)-cath-o} \quad . \tag{B38}$$

The partial pressures of the cathode species entering the condenser satisfy

$$P_L = P_{H_2O(g)-cath-i} + \sum_j P_{j-cath-i} \,. \tag{B39}$$

The anode and cathode streams are assumed to be in thermal equilibrium entering and exiting the condenser so an energy balance on the hot side gives

$$\begin{aligned} 0 = \dot{m}_{H_2O(g)-cath-i}\, h_{H_2O(g)}(P_{H_2O(g)-cath-i}, T_{h-i}) - Q_{tp} - \\ [\dot{m}_{H_2O(l)-cath-o}\, h_{H_2O(l)}(T_{sat}) + \dot{m}_{H_2O(g)-cath-o}\, h_{H_2O(g)}(T_{sat})] + \\ \sum_j \dot{m}_{j-cath}\,[h_j(P_{j-cath-i}, T_{h-i}) - h_j(P_{j-cath-o}, T_{sat})] + \\ \sum_j \dot{m}_{j-anod}\,[h_j(P_{j-anod-i}, T_{h-i}) - h_j(P_{j-anod-o}, T_{sat})] \end{aligned} \tag{B40}$$

where

$T_{h\text{-}I}$ = temperature of the hot side streams entering the condenser, and
Q_{tp} = rate of heat transfer from hot to cold side.

For the anode stream

$$P_{j-anod-o} = P_{j-anod-i} \tag{B41}$$

The hot side equations are examined for the existence and uniqueness of a solution. If the variables $\dot{m}_{k-i}$, $P_{k\text{-}I}$, $T_{h\text{-}I}$, and Q_{tp} are taken as boundary conditions, then there remain nine variables that must be solved for $P_{H_2O(g)-cath-o}$, $P_{H_2-cath-o}$, $P_{N_2-cath-o}$, $P_{O_2-anod-o}$, $P_{H_2-anod-o}$, P_L, T_{sat}, $\dot{m}_{H_2O(l)-cath-o}$, and $\dot{m}_{H_2O(g)-cath-o}$. There are nine equations for the hot side so a solution exists for these boundary conditions. Not written are mass balances for species other than water. For these the outlet mass flowrate equals the inlet.

D.2 Cold Side

There are three streams that enter the cold side of condenser. The first cathode stream is composed of liquid water and the second of oxygen and nitrogen. The anode stream is composed of oxygen and nitrogen. Both streams are assumed to be at the same temperature and pressure. The streams are assumed to be in thermal equilibrium when they exit the condenser. Both streams are assumed to be at the same low-side system pressure, P_L, at the inlet and outlet of the condenser.

The partial pressures of the gas species *j* entering and exiting the condenser satisfy

$$P_L = \sum_j P_{j-cath} \tag{B42}$$

$$P_L = \sum_j P_{j-anod} \quad .$$

The mass flowrates of the gas species are related to partial pressures in the cathode stream by

$$\dot{m}_{j-cath} = A_j \frac{P_{j-cath}}{P_L} \sum_k \frac{\dot{m}_{k-cath}}{A_k} \tag{B43}$$

and the anode stream by

$$\dot{m}_{j-anod} = A_j \frac{P_{j-anod}}{P_L} \sum_k \frac{\dot{m}_{k-anod}}{A_k} \quad . \tag{B44}$$

The anode and cathode streams are assumed to be in thermal equilibrium entering and exiting the condenser so an energy balance on the cold side gives

$$\begin{aligned} 0 = \dot{m}_{H_2O(l)-cath} \left(h_{H_2O(l)}(T_{c-i}) - h_{H_2O(l)}(T_{c-o})\right) + Q_{tp} - \\ \sum_j \dot{m}_{j-cath} \left[h_j(P_{j-cath}, T_{c-i}) - h_j(P_{j-cath}, T_{c-o})\right] + \\ \sum_j \dot{m}_{j-anod} \left[h_j(P_{j-anod}, T_{c-i}) - h_j(P_{j-anod}, T_{c-o})\right] \end{aligned} \tag{B45}$$

where

$T_{c\text{-}I}$ = temperature of the cold side streams entering the condenser, and
$T_{c\text{-}o}$ = temperature of the cold side streams exiting the condenser.

The cold side equations are examined for the existence and uniqueness of a solution. If the variables $\dot{m}_{H_2O}, \dot{m}_{H_2-cath}, \dot{m}_{O_2-anod}$, P_L, $T_{c\text{-}I}$, and Q_{tp} are taken as boundary conditions, then there remain seven variables that must be solved for P_{N_2-cath}, P_{N_2-anod}, P_{H_2-cath}, P_{O_2-anod}, $\dot{m}_{N_2-cath}$, $\dot{m}_{N_2-cath}$, and $T_{c\text{-}o}$, There are seven equations for the hot side so a solution exists for these boundary conditions. Not written are mass balances for species. For these the outlet mass flowrate equals the inlet.

D.3 Interface

The temperatures and the heat transferred are related by

$$Q_{tp} = (UA)_{cond} \frac{(T_{c-o} - T_{sat}) - (T_{c-i} - T_{sat})}{\ln((T_{c-o} - T_{sat})/(T_{c-i} - T_{sat}))} \tag{B46}$$

where *UA* is the product of the overall heat transfer coefficient and the heat transfer area. The superheat and two-phase regions have been lumped as a single region so the value for *UA* must reflect this.

Alternatively, working in terms of heat exchanger effectiveness

$$\varepsilon = \frac{T_{c-o} - T_{c-i}}{T_{sat} - T_{c-i}} . \tag{B47}$$

When a solution is sought with heat exchanger effectiveness specified in place of UA, then Eq. (B47) should be used in place of Eq. (B46).

E. Single-Phase Heat Exchanger

It is assumed that there is no phase change and each species is conserved.

E.1 Hot Side

The mass flowrate for species *l* in stream *j* in the heat exchanger is

$$\dot{m}_{l_j} = A_l \frac{P_{l_j}}{P_H} \sum_{l_j} \frac{\dot{m}_{l_j}}{A_l} \tag{B48}$$

or for the mole flowrates

$$P_{l_j} = \frac{\dot{n}_{l_j}}{\dot{n}_{tot}} P_H \tag{B49}$$

where l_j is an index over all species *l* in stream *j* .

The partial pressures of each of the species *l* in stream *j* in the heat exchanger satisfy

$$P_H = \sum_k P_{l_j} \quad . \tag{B50}$$

The streams are assumed to be in thermal equilibrium entering and exiting the heat exchanger so an energy balance on the hot side gives

$$0 = -Q + \sum_j \sum_{k_j} \dot{m}_{k_j} [h_{k_j}(P_{k_j}, T_{h-i}) - h_{k_j}(P_{k_j}, T_{h-o})] \tag{B51}$$

where *j* is the stream, *k* is an index over the species, and k_j represents species *k* in stream *j*

$T_{h\text{-}i}$ = temperature of the hot side streams at the inlet to the heat exchanger and
$T_{h\text{-}o}$ = temperature of the hot side streams at the outlet of the heat exchanger.

E.2 Cold Side

The first two equations for the hot side apply equally to the cold side. An energy balance gives

$$0 = Q + \sum_j \sum_{k_j} \dot{m}_{k_j} [h_{k_j}(P_{k_j}, T_{c-i}) - h_{k_j}(P_{k_j}, T_{c-o})] . \tag{B52}$$

E.3 Interface

The temperatures and the heat transferred are related by

$$Q_{sp} = AU \frac{(T_{ho} - T_{ci}) - (T_{hi} - T_{co})}{\ln((T_{ho} - T_{ci})/(T_{hi} - T_{co}))} \tag{B53}$$

where *AU* is the overall heat transfer coefficient and subscripts *h, c, hi, ho, ci, and co* represent hot side, cold side, hot inlet, hot outlet, cold inlet, and cold outlet, respectively. This equation assumes constant specific heat along the length of the heat exchanger. When the specific heat does not vary significantly over the temperature range a good approximation is

$$c_k = \frac{\sum_k \dot{m}_k \left[h_k(P_k, T_{c-i}) - h_k(P_k, T_{c-o})\right]}{(T_{c-i} - T_{c-o}) \sum_k \dot{m}_k}. \tag{B54}$$

where *k* has the values *h* and *c* for hot and cold, respectively .

The effectiveness is then

$$\varepsilon = \frac{c_h}{c_{\min}} \frac{T_{hi} - T_{ho}}{T_{hi} - T_{ci}} = \frac{c_c}{c_{\min}} \frac{T_{co} - T_{ci}}{T_{hi} - T_{ci}}. \tag{B55}$$

where *c* is the product of the specific heat and the mass flowrate and c_{min} is the smaller of c_h and c_c.

F. Fluid Properties

Fluid properties are needed for enthalpy and entropy as a function of pressure and temperature for water, hydrogen, oxygen, and nitrogen. The enthalpy of subcooled and superheated water and the saturation temperature as a function of pressure are taken from polynomials in [The SAS4A/SASSYS, 1996]. The enthalpy of hydrogen, oxygen, and nitrogen are taken from polynomials in [Zehe, 2002]. The entropy of water, hydrogen, oxygen, and nitrogen are also taken from [Zehe, 2002].

Presently the polynomials are evaluated directly. In the case where a needed property appears implicitly in a polynomial expression, Newton's method is used to find the root of the expression. The GAS-PASS/H code also has the capability for table lookup of properties. Tables of the above properties were generated. They will be used should property evaluation be a limiting factor in achieving fast run times. This will likely be the case in transient rather than steady-state simulation.

INTERCONNECTIONS AMONG COMPONENTS

The component models described in the previous section are linked together to obtain a representation of the HTE plant. The model descriptions however are in terms of generic input and output variables specific to the type of component and not specialized to the integration of the component in the HTE plant. This section describes the relationships that connect components in the plant.

A. Mass and Mole Flowrates of Individual Species in Reactant and Product Streams

The interconnection of components in the steady state is physically in terms of a reactant stream and a product stream. The reactant stream is defined to be the collection of all physical streams that enter the electrolyzer. The product stream is similarly those streams that exit the electrolyzer. The electrolyzer separates these streams and species balances between the input and output of the electrolyzer bridge these two streams. The species flowrates in any component in the reactant or product streams is linked to its neighbors in the code by continuity of species. Thus, in the steady state all components in the reactant (product) stream will have the same species flowrates.

The code provides for up to a possible four species in the reactant and in the product stream. Since the HTE process tends to be conceptualized in terms of mole fractions, the input deck is cast in terms individual specie mole fractions for water, hydrogen, and oxygen plus a total species mass flowrate. But the conservation equations for each component in these streams are in terms of individual species mass flowrates and not mole flowrates. The relationship between input deck variables (i.e. three species mole fractions and total stream mass flowrate) and a component's species mass flowrates is as follows.

The mole flowrate of species k at the outlet of a component is given by

$$\dot{n}_{k-tot-o} = \frac{\dot{m}_{tot-o}\, f_{k-tot-o}}{\sum_j A_j\, f_{j-tot-o}}, \qquad k = H_2O,\ H_2,\ O_2, \text{ and } N_2. \tag{B56}$$

where A_j is the atomic weight of species j in kg, subscript *tot-o* refers to all occurrences at the component output, and where the summation is over all species in the reactant (or product) stream. Here f_k appears in the input deck and is defined as the mole fraction of species k

$$f_{k-tot-o} = \frac{\dot{n}_{k-tot-o}}{\dot{n}_{tot-o}} \quad , \quad \dot{n}_{tot-o} = \sum_j \dot{n}_{j-tot-o}\ . \tag{B57}$$

where the summation is over all species in the reactant (or product) stream. The total mass flowrate appears in the input deck for each component and is related to mole quantities as follows

$$\dot{m}_{tot-o} = \sum_j A_j\, \dot{n}_{j-tot-ok} = \dot{n}_{tot-o} \sum_j A_j\, f_{j-tot-o} \tag{B58}$$

For individual species

$$\dot{m}_{k-tot-o} = A_k\ \dot{n}_{k-tot-o}\ , \qquad k = H_2O,\ H_2,\ O_2, \text{ and } N_2. \tag{B59}$$

B. Reactant Stream Into Electrolyzer

The code input assumes the electrolyzer communicates with the other components through a reactant stream at its input and a product stream at its output. But the model for the electrolyzer has been developed in terms of electrode stream mole fractions rather than component stream mole fractions. A means is needed then to convert from electrode mole fractions to component stream mole fractions.

The species mole flowrates into the electrolyzer model are related to the reactant stream species mass flowrates by

$$\dot{n}_{H_2O-cath-i} = \dot{m}_{H_2O-tot-R} / A_{H_2O} \tag{B60}$$

$$\dot{n}_{H_2-cath-i} = \dot{m}_{H_2-tot-R} / A_{H_2} \tag{B61}$$

$$\dot{n}_{O_2-anod-i} = \dot{m}_{O_2-tot-R} / A_{O_2} \tag{B62}$$

where the left-hand side is the mole flowrate in to the cathode by species while the right-hand side gives the total mass flowrate by species in the reactant stream. The subscripts *cath*, *i*, *tot*, and *R* represent cathode, input, total, and reactant stream, respectively. Note that water, hydrogen, and oxygen each appear at only one electrode. Nitrogen is a special case since it can appear at both the cathode and anode. A parameter $f_{N2\text{-}split}$ is defined as the fraction by mole of the total nitrogen in the reactant stream that enters the cathode. Thus, at the inlet to the cathode

$$\dot{n}_{N_2-cath-i} = \dot{n}_{N_2-tot-R}\ f_{N_2-split} = \dot{m}_{N_2-tot-R} f_{N_2-split} / A_{N_2} \tag{B63}$$

while at the inlet to the anode

$$\dot{n}_{N_2-anod-i} = \dot{n}_{N_2-tot-R}\ (1 - f_{N_2-split}) = \dot{m}_{N_2-tot-R}\ (1 - f_{N_2-split}) / A_{N_2} \quad . \tag{B64}$$

The species mass flowrates into the electrolyzer model are related to the reactant stream species mass flowrates by multiplying the above five equations through by atomic weight

$$\dot{m}_{H_2O-cath-i} = \dot{m}_{H_2O-tot-R} \tag{B65}$$

$$\dot{m}_{H_2-cath-i} = \dot{m}_{H_2-tot-R}$$

$$\dot{m}_{O_2-anod-i} = \dot{m}_{O_2-tot-R}$$

$$\dot{m}_{N_2-cath-i} = \dot{m}_{N_2-tot-R} f_{N_2-split}$$

$$\dot{m}_{N_2-anod-i} = \dot{m}_{N_2-tot-R} (1 - f_{N_2-split}) \quad .$$

C. Electrolyzer Output Into Product Stream

The species mole flowrates in the product stream are related to the species mole flowrates exiting the electrolyzer through

$$\dot{n}_{H_2O-tot-P} = \dot{n}_{H_2O-cath-o} \tag{B66}$$

$$\dot{n}_{H_2-tot-P} = \dot{n}_{H_2-cath-o}$$

$$\dot{n}_{O_2-tot-P} = \dot{n}_{O_2-anod-o}$$

$$\dot{n}_{N_2-tot-P} = \dot{n}_{N_2-cath-o} + \dot{n}_{N_2-anod-o}$$

The subscripts *o* and *P* represent output and product, respectively. Again note that water, hydrogen, and oxygen each appear at only one electrode and nitrogen is a special case since it can appear at both the cathode and anode

The mole fractions of species in the combined product stream that exits the electrolyzer are related to the individual electrode streams. The water mole fraction in the product stream is

$$f_{H_2O-tot-P} = \frac{\dot{n}_{H_2O-cath-o}}{\dot{n}_{elect-o}} \tag{B67}$$

where the numerator is the mole flowrate of water vapor exiting the electrolyzer and the denominator is the sum of mole flowrates over all species and is given by

$$\dot{n}_{elect-o} = \dot{n}_{H_2O-cath-o} + \dot{n}_{H_2-cath-o} + \dot{n}_{N_2-cath-o} + \dot{n}_{O_2-anod-o} + \dot{n}_{N_2-anod-o}\,. \tag{B68}$$

Similarly,

$$f_{H_2-tot-P} = \frac{\dot{n}_{H_2-cath-o}}{\dot{n}_{elect-o}} \tag{B69}$$

$$f_{O_2-tot-P} = \frac{\dot{n}_{O_2-cath-o}}{\dot{n}_{elect-o}}$$

$$f_{N_2-tot-P} = \frac{\dot{n}_{N_2-cath-o} + \dot{n}_{N_2-anod-o}}{\dot{n}_{elect-o}}\,.$$

GAS-PASS/H SIMULATION

The component models described above have been implemented in the GAS-PASS/H code as Fortran subroutines, an input deck has been assembled for a representative HTE plant, comparison of some models with work by others has been performed, and simulations have begun.

Results from the electrolyzer model have been compared against the 1-D model of Stoots (2005). The main difference between the model described in Appendix B and that of Stoots is the assumed distribution of temperature and species concentration in the electrolyzer. In Appendix B a perfectly mixed or uniform distribution is assumed whereas Stoots allows for some spatial dependence. The two models were compared to determine the relative error in operating voltage for different current densities. When the boundary conditions including current density are the same between the two models the error in electrical power consumption is equal to the error in operating voltage. Table B1 shows this error as a function of current density. The calculated electrical power for the two models differs by less than 5 percent.

A GAS-PASS/H input deck was prepared for the HTE plant configuration shown in Figure B5. The conditions simulated are a 50 MWt reactor heat load and an electrolyzer output of 95 percent hydrogen and 5 percent steam by mole fraction. The water feed by mole fraction is 95 percent water and 5 percent hydrogen at room temperature. The electrolyzer operates at 5 MPa and has an inlet temperature of 850 C. Estimates for the process conditions for initializing the simulation were obtained by solving four heat balances equations. This yielded a water feed flowrate of 21.5 kg/s and powers for heat exchangers SHX1 and SHX2 that supply reactor power of 45 and 5 MWt, respectively. The high temperature recuperator power is 30 MWt.

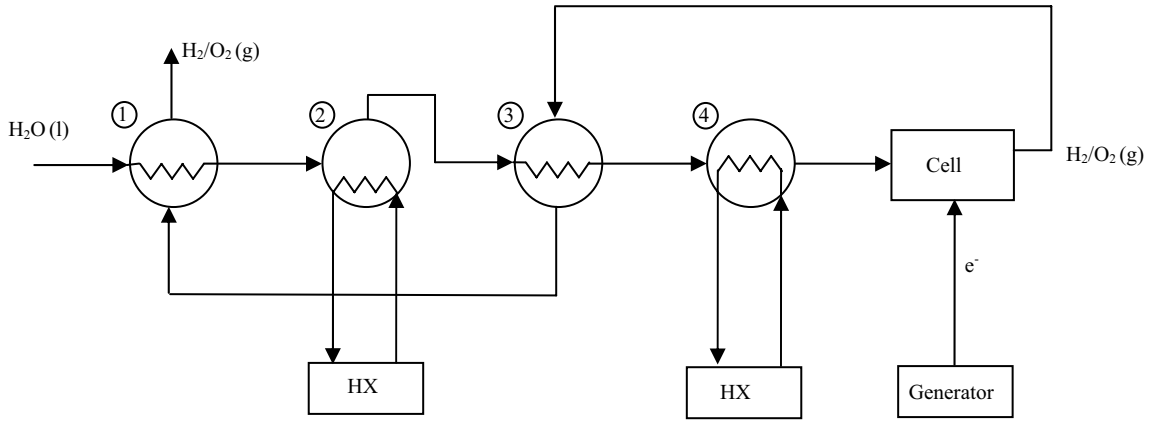

Figure B1 Simple Schematic of HTE Process Heat Equipment

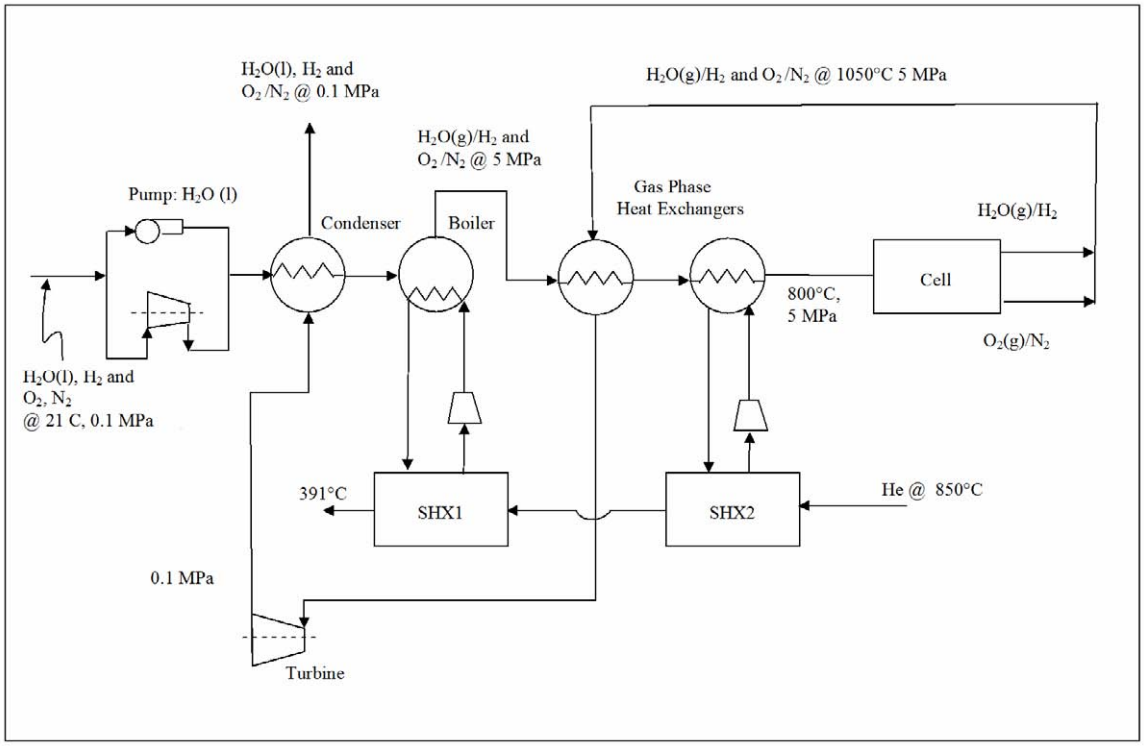

Figure B2 Lumped Representation of Multiple Material and Energy Streams.

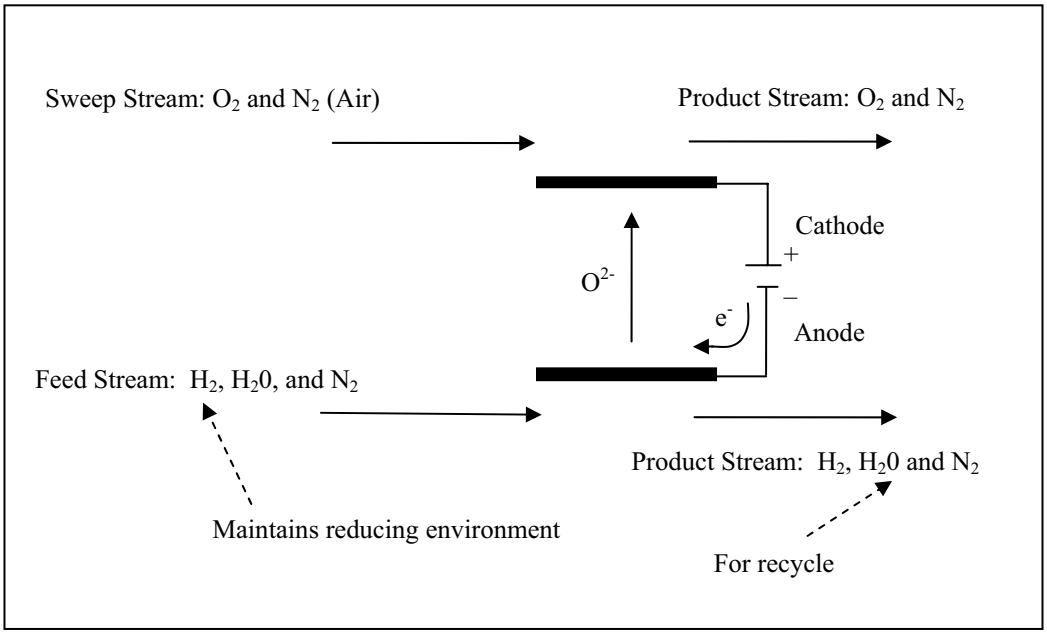

Figure B3 Schematic of Electrolyzer

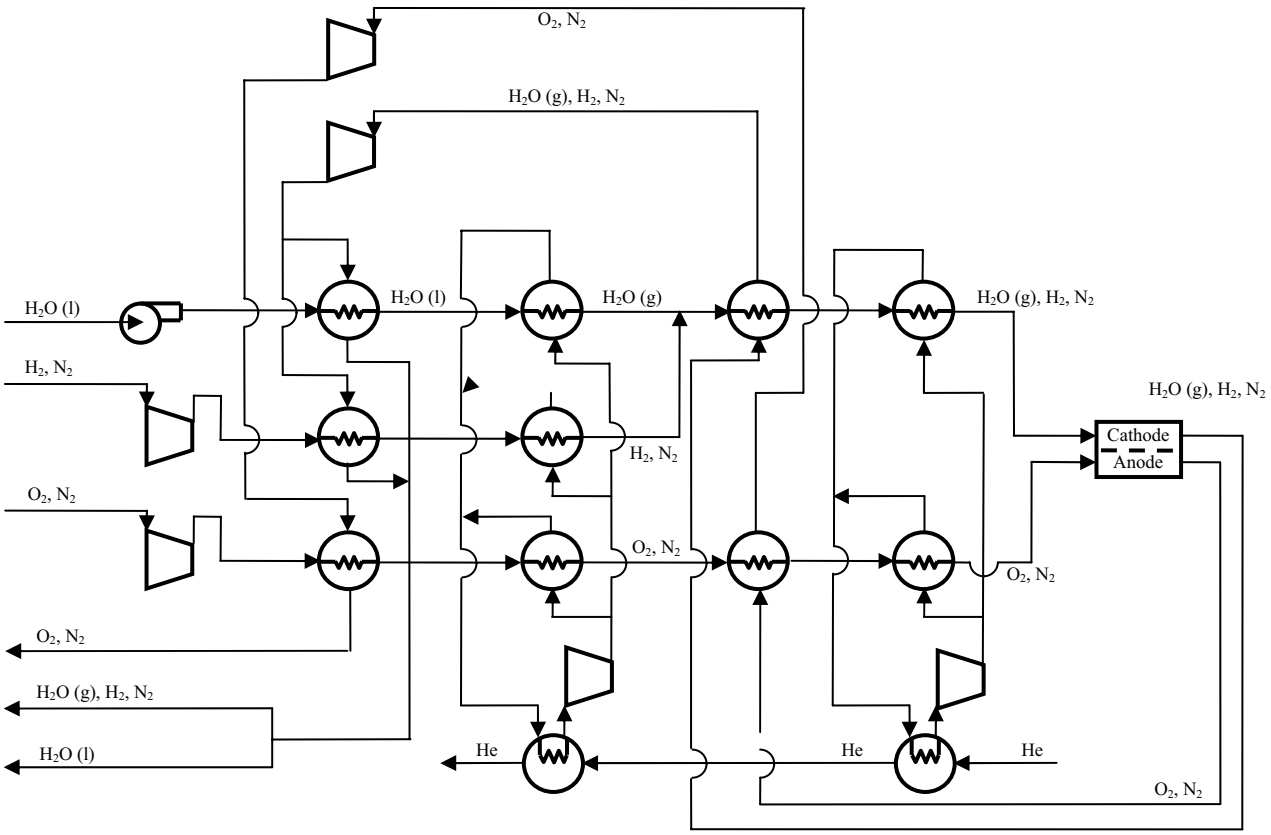

Figure B4 HTE Process Diagram Before Lumping of Components

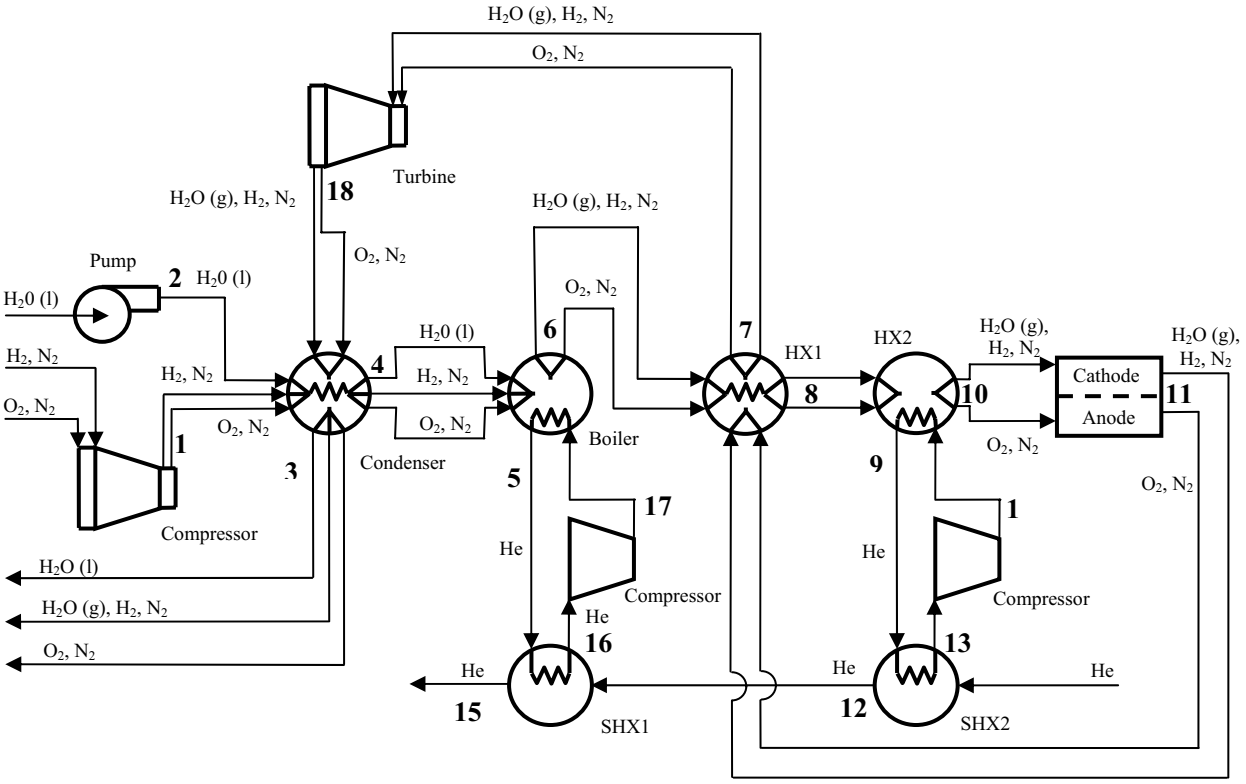

Figure B5 GAS-PASS/H HTE Process Network Diagram for Lumped Components

Table B1 Comparison of Results from 1-D Electrolyzer Models. Simplified model on right assumes a uniform distribution for temperature and species concentration between inlet and outlet. Error in calculated electrical power input to the cell is equal to the error in the operating voltage which is shown in the right-most column.

		Non-Uniform Temp/Concentration Profile [Stoots]						Uniform Temperature/Concentration [Vilim]					Vop Error
Case	ma/cm2	Eo	E_corr	V_ner	Vop	<T>	T_exit	Eo	E_corr	V_ner	Vop	<T>	(%)
1	0	0.982	0.138	0.8396	0.8396	1073	1073	0.977	-0.138	0.839	0.839	1073	0
2	15			0.85	0.861	1061	1051	0.983	-0.124	0.859	0.87	1051.5	1
3	78	0.991	0.108	0.88	0.937	1027.6	982	1.006	-0.085	0.915	0.97	992	3
4	156			0.909	1.018	1004	934	1.01	-0.055	0.954	1.064	958.4	4.5
5	234			0.925	1.089	997	921	1.009	-0.0033	0.976	1.14	960.6	4.7
6	313	0.997	0.0627	0.934	1.153	1005	937	1.0006	-0.014	0.986	1.205	990.9	4.5
7	391			0.939	1.212	1026	979	0.985	0.0068	0.9916	1.265	1046	4.4
8	469	0.982	0.042	0.939	1.268	1059	1044.5	0.962	0.033	0.995	1.323	1126	4.3

Appendix C

Gibbs Free Energy Change for a Reaction of Gases

The Gibbs free energy for a substance is defined on a single mole basis as

$$\begin{aligned} G &= H - T\,S \\ &= U + PV - T\,S \end{aligned} \tag{C1}$$

where H is enthalpy, S is entropy, U is internal energy and V is volume. The total differential is then

$$dG = dU + VdP + PdV - T\,dS - S\,dT\,. \tag{C2}$$

But for temperature constant, $dT = 0$, and for reversible heat flow to the substance, $dQ = S\,dT$ where Q is heat flow, we have

$$dG = dU + VdP + PdV - dQ\,. \tag{C3}$$

But the change in internal energy is $dU = -P\,dV + dQ$ so that

$$dG = VdP\,. \tag{C4}$$

If the substance is taken from pressure P_R to a pressure P while maintaining constant temperature T, then the change in Gibbs free energy is from Eq. (A.4) and the ideal gas law

$$\Delta G_R(T,P) = RT\,\ln P/P_R \tag{C5}$$

where the subscript R on the left hand side of the equation denotes pressure P_R.

The Gibbs free energy of reactant i at temperature T and pressure P_i is 1) the Gibbs free energy at temperature T and reference pressure P_R of the individual elements making up the reactant (taken as zero) plus the change in the Gibbs free energy in forming the reactant from these elements at this condition (the term inside the first summation on the right-hand side below) plus the change in the Gibbs free energy in taking the reactant from pressure P_R to P_i (the term inside the second summation on the right-hand side below). The Gibbs free energy for all the reactants is then

$$\sum_{REAC} G(T,P_i) = \sum_{REAC} r_i\,\Delta G_{f-i}(T,P_R) + \sum_{REAC} r_i\,\Delta G_{R-i}(T,P_i) \tag{C6}$$

where r_i is the number of moles of species i of the reactants and the Gibbs free energy on the right-hand side is on a per mole basis. A similar expression can be written for the products. The change in Gibbs free energy for the reaction conducted at pressure P is then the difference in these two expressions

$$\Delta G(T,P) = \sum_{PROD} p_i \left[\Delta G_{f-_i}(T,P_R) + \Delta G_{R-i}(T,P_i)\right] - \sum_{REAC} r_i \left[\Delta G_{f-_i}(T,P_R) + \Delta G_{R-i}(T,P_i)\right] \tag{C7}$$

where p_i is the number of moles of species i of the products.

Now define

$$\Delta G_f(T,P_R) = \sum_{PROD} p_i \, \Delta G_{f-i}(T,P_R) - \sum_{REAC} r_i \, \Delta G_{f-i}(T,P_R) \ . \tag{C8}$$

Upon substituting Eqs. (C5) and (C8) into Eq. (C7)

$$\Delta G(T,P) = \Delta G_f(T,P_R) + RT \ln \frac{\prod_{PROD} (P_i / P_R)^{p_i}}{\prod_{REAC} (P_i / P_R)^{r_i}} . \tag{C9}$$

A.1 Non-Standard Pressure

In Eq. (C9) set the reference pressure, P_R, to the pressure of the reaction, P. The resulting partial pressure ratio for species i is from Dalton's Law equal to the mole fraction, f_i. Substituting this into Eq. (C9) gives

$$\Delta G(T,P) = \Delta G_f(T,P) + RT \ln \frac{\prod_{PROD} f_i^{p_i}}{\prod_{REAC} f_i^{r_i}} . \tag{C10}$$

A.2 Standard Pressure

Consider the special case of Eq. (C9) where $P_R = P_{STD}$ (i.e. 1 atm.) so that $\Delta G_f(T,P_R) = \Delta G_f^{\,o}(T)$. In this case Eq. (C9) can be rewritten as either

$$\Delta G(T,P) = \Delta G_f^{\,o}(T) + RT \ln \left[\frac{\prod_{PROD} (P_i / P_{STD})^{p_i}}{\prod_{REAC} (P_i / P_{STD})^{r_i}} \right]$$

or

$$\Delta G(T,P) = \Delta G_f^{\,o}(T) + RT \ln \left[\frac{\prod_{PROD} f_i^{p_i}}{\prod_{REAC} f_i^{r_i}} \left(\frac{P}{P_{STD}} \right)^{p_i - r_i} \right] \tag{C11}$$

where P is the reaction pressure and this second equation follows from application of Dalton's Law.

A.3 Electrolysis of Water

For the reaction

$$H_2O\,(g) \rightarrow H_2\,(g) + \frac{1}{2}O_2\,(g) \tag{C12}$$

at temperature *T* and pressure *P*, the change in Gibbs free energy is from Eq. (C10)

$$\Delta G(T,P) = \Delta G_f(T,P) + RT\,\ln\left[\frac{f_{H_2}\,f_{O_2}{}^{\frac{1}{2}}}{f_{H_2O}}\right] \tag{C13}$$

where from Eq. (C8)

$$\Delta G_f(T,P) = \Delta G_{f-H_2}(T,P) + 1/2\,\Delta G_{f-O_2}(T,P) - \Delta G_{f-H_2O}(T,P)\,. \tag{C14}$$

If electrical work is performed by the species in the course of the reaction, then a voltage is developed. To find this voltage note that

$$\begin{aligned} dG &= dH - TdS - SdT \\ &= dU + VdP + PdV - TdS - SdT \end{aligned} \tag{C15}$$

But the change in internal energy equals the heat added to the system minus the work done by the system

$$dU = dQ - PdV - dW_e\,. \tag{C16}$$

where W_e is electrical work done by the system. If the heat is added reversibly so $dQ = T\,dS$ and temperature and pressure are maintained constant, then Eq. (C15) and (C16) yield

$$dG = -\,dW_e = -V_N\,dq \tag{C17}$$

where dq is the charge transferred and V_N is the voltage. Thus, for the reaction given by Eq. (C12) whose Gibbs free energy change is given by Eq. (C10), Eq. (C17) yields

$$V_N = \frac{-1}{2F}\left[\Delta G_f(T,P) + RT\,\ln\left(\frac{f_{H_2}\,f_{O_2}{}^{\frac{1}{2}}}{f_{H_2O}}\right)\right] \tag{C18}$$

where the charge transferred in the reaction of Eq. (C12) is $2F$ where F is Faraday's constant. Here P and T are the pressure and temperature of the reaction. Alternatively, from Eq. (C11)

$$V_N = \frac{-1}{2F}\left[\Delta G_f{}^0(T) + RT\,\ln\left[\left(\frac{f_{H_2}\,f_{O_2}{}^{\frac{1}{2}}}{f_{H_2O}}\right)\left(\frac{P}{P_{STD}}\right)^{\frac{1}{2}}\right]\right] \tag{C19}$$

where $P_{STD} = 0.101$ MPa

.

Appendix D

Coupling Results from HYSYS Simulations for Benchmarking with HyPEP

PLANT CONFIGURATION

The baseline plant configuration was based on configuration 6 from Davis et al. (2005). Figure X.0.1 illustrates the configuration of the plant. In this configuration the an indirect cycle was used with the reactor coupled to the secondary side by means of an intermediate heat exchanger (IHX) as recommended by the Independent Technology Review Group (2004). The reactor was assumed to produce 600 MW of thermal power with a 900 °C outlet temperature with a nominal pressure of 7MPa and use helium coolant on the primary side. The nominal rise in fluid temperature across the core was assumed to be 400 °C, based on the point design (MacDonald et al. 2003). The reactor pressure drop and the primary side pressure drop of the IHX are assumed to be 50kPa.

The power conversion unit (PCU) consists of a recuperated Brayton cycle. Referring to Figure D1, the fluid exits the IHX and the flow is split with most of the flow entering the PCU. The rest of the flow, approximately 10%, goes to the HTLHX. Upon entering the PCU the fluid enters the turbine for expansion. After leaving the turbine the fluid passes through the hot side of the recuperator and is further cooled by a precooler before entering the low pressure compressor. The fluid is the cooled aging by an intercooler before entering the high pressure compressor. The fluid leaves the high pressure compressor and enters the cold side of the recuperator before combining with the fluid from the HTLHX and returning to the IHX.

The reactor was coupled to the hydrogen processing facility by means of an intermediate heat transport loop (IHTL). The IHTL was placed in parallel with the PCU as seen in Figure D1. It was assumed that 50MW of thermal power are transported to the IHTL. A circulator is needed in the secondary side account for pressure losses in the heat transport loop heat exchanger (HTLHX). Estimations of the required separation distance between the nuclear and hydrogen process plant vary considerable. For example, Sochet et al. (2004) recommended 500 m for the High-Temperature Reactor while Smith et al. (2005) recommended a separation distance of from 60 to 120 m for the NGNP and the hydrogen production plant. For this analysis, a nominal value of 90 m was used. The working fluid in the loop is assumed to be helium.

The coupling of the IHTL to the hydrogen processing facility was accomplished by means of three process heat exchangers (PHX). Figure D2 details the configuration of the 3 PHX's in the IHTL. Two heat exchangers in parallel are followed by one heat exchanger in series. This configuration was chosen to deliver high inlet temperatures on the hot side of the first two heat exchangers where high cold side outlet temperatures are needed for the hydrogen production facility. The third heat exchanger however, does not require high cold side outlet temperatures and the hot side inlet temperature from the outlet of the prior heat exchangers is sufficient for heating the cold side fluid.

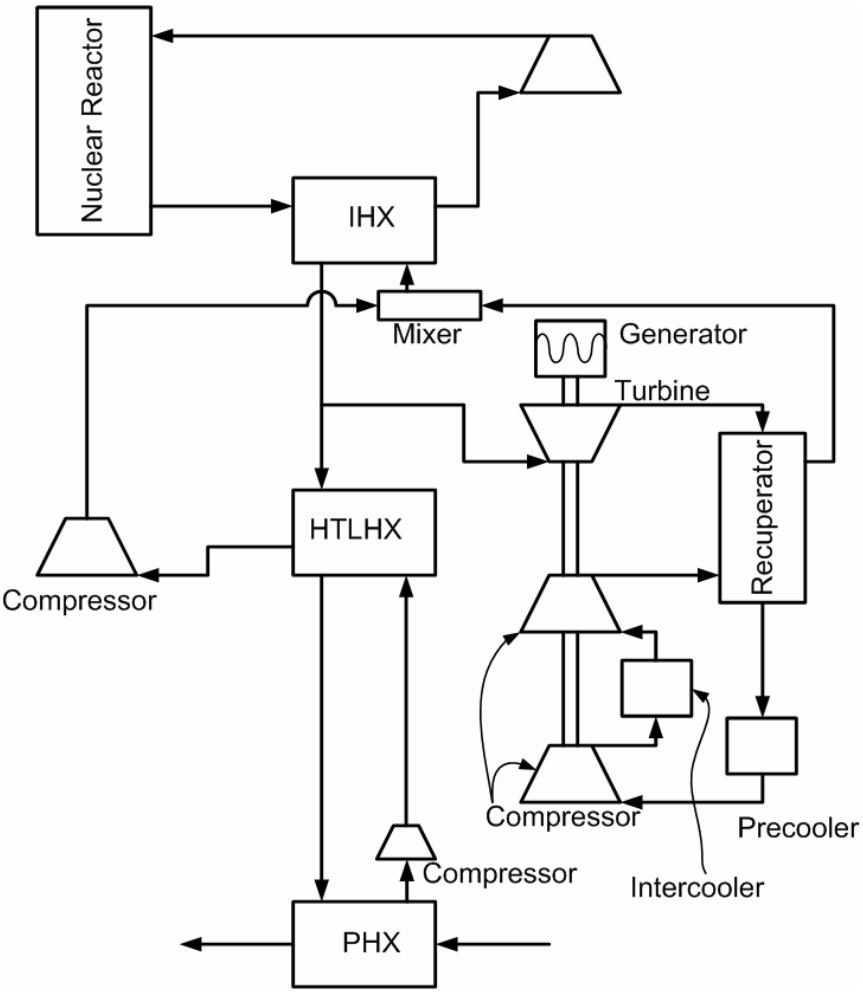

Figure D1: Baseline plant configuration for electrical and hydrogen production

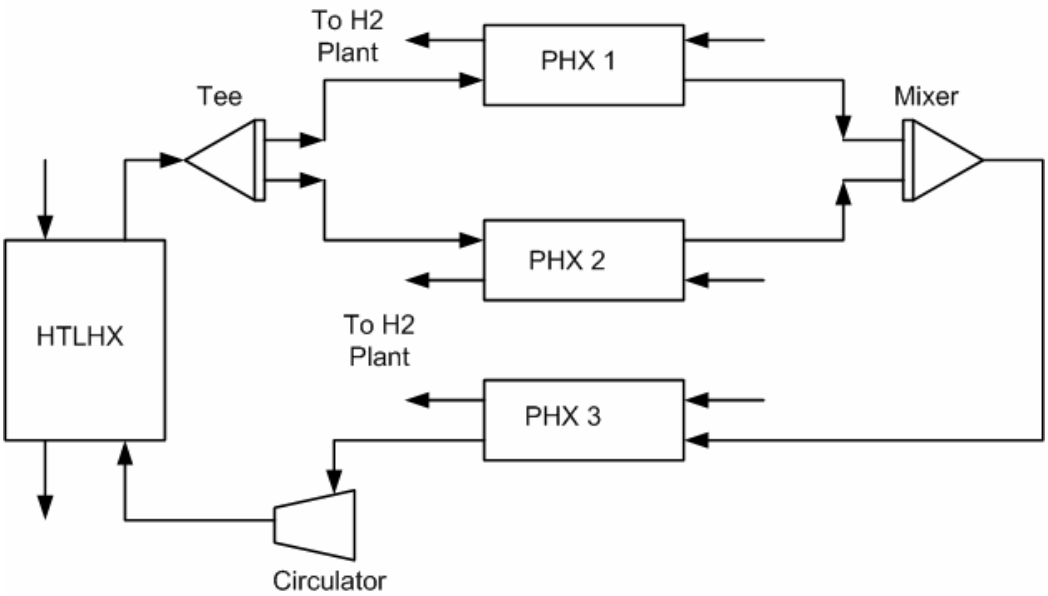

Figure D2: IHTL process heat exchanger configuration

HYSYS High Temperature Electrolysis

The hydrogen plant was modeled as a high temperature electrolysis plant was coupled to the reactor by means of the intermediate heat transport loop (IHTL). The baseline HTE model used here was adapted from the work done by Stoots et al. (2005). A model of the HTE operations was developed that includes all of the components that are actually present in a HTE plant including pumps, compressors, heat exchangers, expanders and the electrolyzer. A one dimensional electrolyzer model was developed for the HYSYS modeling code. A comparison of this model with a fully 3-D computational fluid dynamic model and experimental results was done by O'Brian et al. (2005).

On Figure D3, the process water enters on the left. The water is then pumped up to the operating pressure of 5 MPa. The efficiency of the pumps and circulators is assumed to be 75%. This water is then combined with water condensate returned from the hydrogen/water product stream. This stream then enters the low temperature recuperator (HX1). The pressure drop through the heat exchangers is assumed to be 20 kPa. From there the steam is further heated by PHX 3. Upon leaving PHX 3 the steam is mixed with hydrogen from the product stream by a recirculator which works to overcome the pressure drops in the system. A mole fraction of 90% water and 10% hydrogen is maintained in this model. This hydrogen helps to maintain reducing conditions at the electrolysis stack to prevent oxidation. The mixed stream then enters the high temperature recuperator (HX2) which takes advantage of the high temperature outlet from the electrolysis stack. The hydrogen/water stream is then heated to the operating temperature for the electrolysis stack, in this case 827 °C, in PHX 1.

The electrolyzer has another inlet stream which contains the sweep gas. This is used to sweep away the oxygen from the electrolysis process. A steam sweep gas is used in this model and enters the plant in the middle-bottom of Figure D3. It is first pumped up to operating pressure and then heated in the sweep recuperator using the hot sweep outlet from the electrolyzer. Before it enters the electrolysis stack it is heated to the operating temperature of 827 °C in PHX 2.

Upon leaving the electrolyzer, the product stream is 90% (mole fraction) hydrogen and 10% (mole fraction) water. This then passes through the high and low temperature recuperators. The steam condensate is then separated from the hydrogen and recycled back into the system. After leaving the electrolyzer, the sweep gas enters the sweep recuperator (HX3) to preheat the sweep inlet. The sweep outlet contains approximately 55% water (mole fraction) and 45% oxygen. It is then partially separated before entering an expander to recuperate some of the power. The expander has an efficiency of 80%. Finally the sweep stream is further separated and high purity oxygen and water are produced at the top and the bottom of the separator, respectively.

The model developed by Stoots et al. (2005) was originally envisioned for a 300 MW HTE plant. However, under the assumption of ~50 MW process heat, a 300 MW plant was not possible. Therefore the plant was scaled down to meet the needs of that assumption. To do this the balance of plant must still work and key working condition such as stream compositions, and electrolyzer inlet temperature must remain constant. This was accomplished by reducing the mass flow of the inlet process stream and the sweep stream while keeping the compositions and temperatures constant. The electrical power to the electrolyzer was reduced from 292 MW to 234.4 MW and 198.8 MW for the helium and molten salt IHTL working fluids, respectively. This was done to account for the smaller mass flow rate and to keep an outlet composition of 90% hydrogen and 10% water.

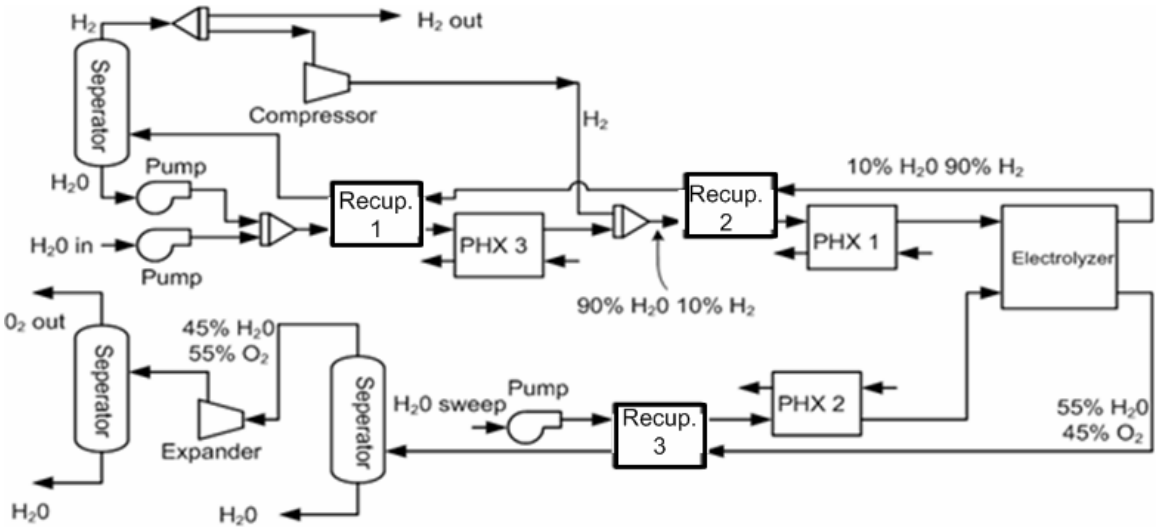

Figure D3: Schematic of HTE process

Simplified HTE Model

The dynamic behavior of the HTE facility must be modeled to study certain issues when it is coupled to the VHTR. To do this a simplified version of the model developed earlier was created. In this model only the phenomena important for predicting efficiency have been included, such as heat exchangers, pumping equipment and the electrolysis cell. Unnecessary components such as the separator columns have been removed. Since only the energy and mass balances need to be determined it is possible to combine the streams when modeling shaft work and heat exchanger energy balances. Figure D4 depicts the simplified block model where the mass and energy balance of the sweep gas and main feedwater streams have been combined. The streams are pumped up to operating pressures before entering the first set of heat exchangers. They are then heated by PHX 2 & 3 before the H_2 is introduced into the stream from the hydrogen product stream. The main and H_2 stream are then further heated in recuperator 2 and PHX 1 before entering the electrolyzer. The sweep stream is not heated in this step to be consistent with the HYSYS model and enters the electrolyzer. The streams then exit the electrolysis cell and pass through the hot side of the recuperators. The product streams then exit the final recuperator. The simplified model does not include further separation processes of the sweep and H_2 product streams.

A comparison of the two models shows excellent agreement of the energy and mass balances. Using the inlet conditions, obtained either from the entire balance of plant model or conditions set in the HTE facility for the, simplified model supplied in Table D1, the energy and mass balance for each component was compared with value obtained from the more complex model. Table D2 AND D3 summarize the energy balance for the heat exchangers, shaft work for the pumping and circulation equipment, and the energy and mass balance for the electrolyzer, respectively.

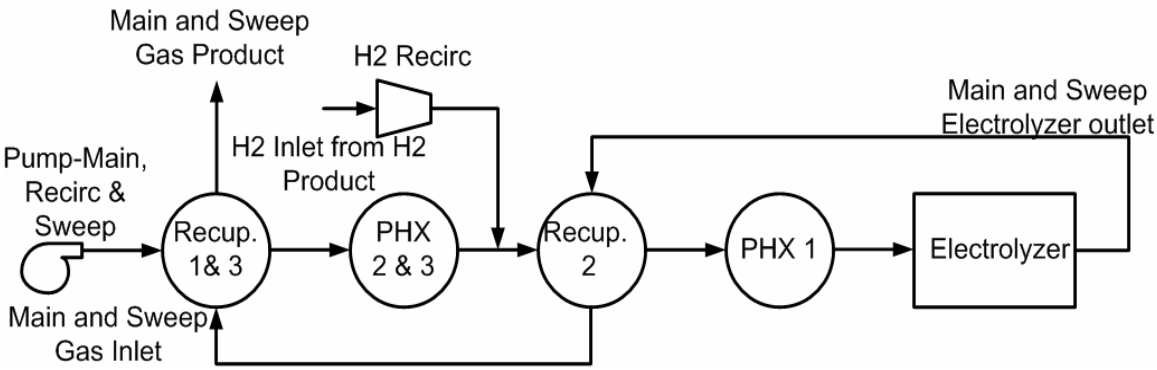

Figure D4: Simplified block model of HTE facility

Table D1: Energy balance for heat exchangers.

Heat Exchanger Energy	Full Model (kW)	Simplified Model (kW)
Recup. 1 & 3	5.167×10^4	5.167×10^4
Recup. 2	1.527×10^4	1.525×10^4
PHX 1	4.471×10^4	4.471×10^4
PHX 2 & 3	1.031×10^4	1.038×10^4

Table D2: Shaft work for pumping and circulation equipment.

Pumping and Circ Equip.	Full Model (kW)	Simplified Model (kW)
Main, Sweep and H_20 Recirc Pumps	176.1	175.7
H_2 Recirc	6.34	6.35

Table D3: Electrolysis cell energy and mass balance.

Electrolysis Cell	Full Model	Simplified Model
Total Energy (Electrical Work + Heat addition)	2.344×10^5 (kW)	2.344×10^5 (kW)
H_20 inlet/out mass flow	28.9 (kg/s)	28.9 (kg/s)
H_2 inlet/out mass flow	0.235 (kg/s)	0.235 (kg/s)
0_2 inlet/out mass flow	14.9 (kg/s)	14.9 (kg/s)

Plant Efficiency

The overall plant efficiency including the PCU and HTE was calculated using HYSYS.

The efficiency of the overall cycle was calculated as follows

$$\eta_{overall} = \frac{\Sigma W_T - \Sigma W_C - \Sigma W_{CIR} + \Sigma W_{H2} - Q_{EL} + Q_{H2}}{Q_{th}} \quad \text{(D1)}$$

where ΣW_T is the total turbine workload, ΣW_C is the total compressor workload, W_{CIR} is the circulator workload in the primary and secondary side, W_{H2} is the workload in the HTSE plant, Q_{EL} is the power supplied to the electrolyzer, Q_{H2} is the lower heating value of the produced hydrogen and Q_{th} is the reactor thermal power.

The polytropic efficiency of the turbomachinery was used for efficiency calculation rather than the isentropic efficiency. The polytropic efficiencies for the turbines and the compressors were assumed to be 92% and 90%, respectively. These values are representative of expected efficiency that will be available for the NGNP project. The efficiency of the pumps and circulator components in the HTE facility are assumed to be 75%, and 80% efficiency is assumed for the expander. For expansion the efficiency is calculated from

$$\frac{T_{0,ex}}{T_{0,in}} = \left(\frac{P_{0,ex}}{P_{0,in}} \right)^{\left(\frac{R}{C_p} \eta_{p,e} \right)}, \tag{D2}$$

where T_0 is the stagnation temperature, P_0 is the stagnation pressure, R is the gas constant, C_p is the specific heat, $\eta_{p,e}$ is the polytropic efficiency and the subscripts *in* and *ex* refer to the inlet and outlet conditions. For compression, the efficiency is calculated as

$$\frac{T_{0,ex}}{T_{0,in}} = \left(\frac{P_{0,ex}}{P_{0,in}} \right)^{\left(\frac{R}{C_p} \frac{1}{\eta_{p,c}} \right)}. \tag{D3}$$

A model to solve for the effectiveness ε of a heat exchanger is not defined in HYSYS and had to be developed. The effectiveness of a heat exchanger is defined as the ratio of the actual heat transfer rate to the maximum heat transfer rate. The spreadsheet function was used and the following equations were input:

$$\varepsilon = \frac{q}{q_{\max}} \tag{D4}$$

$$q_{\max} = C_{mim}(T_{h,i} - T_{c,i}) \tag{D5}$$

Where C_{min} refers to the smaller of C_{hot} or C_{cold}.

$$C_{hot} = c_{p,hot} \dot{m}_{hot} \tag{D6}$$

$$C_{cold} = c_{p,cold} \dot{m}_{cold} \tag{D7}$$

Figure D5 shows the HYSYS simulation model of the overall plant using the baseline PCU an HTE configurations. The excess electrical power generated by the PCU that was not used in the electrolysis process was 32.2 MW. In previous calculations pressure drop values were assumed to be 50kPa in the hot and cold side of the recuperator Davis et. al, 2005). A detailed calculation of the pressure drop values determined the hot side pressure drop in the recuperator to be 100kPa and the cold side to be 30kPa. This decreased the overall cycle efficiency by approximately 0.8% for the original value of 49.61% report by Davis et. al (2005) to a more accurate 48.84%. Further, a full scale model of the HTE facility was included into the model. Previously, 50% efficiency was assumed for the process heat from the PHX for the HTE plant, and the electrical power need to power the electrolysis cell was ignored. In this study a more accurate model takes into account the use of the electrical energy produced by the PCU to run the

electrolysis cell and a detailed plant model and efficiency calculation are included. This further reduced the final overall plant efficiency to 44.06% using Eq. X.3.1. The plant was also modeled with CO_2 and an 80% nitrogen, 20% helium mixture (by weight) working fluids in the PCU. CO_2 gave an overall efficiency of 40.02%, while the nitrogen helium mixture gave an efficiency of 43.61%. The excess electrical power generated by the PCU that was not used to power the electrolysis cell was 38.68MW, 16.37MW and 35.96MW for the helium, CO_2 and nitrogen-helium mixture working fluids, respectively.

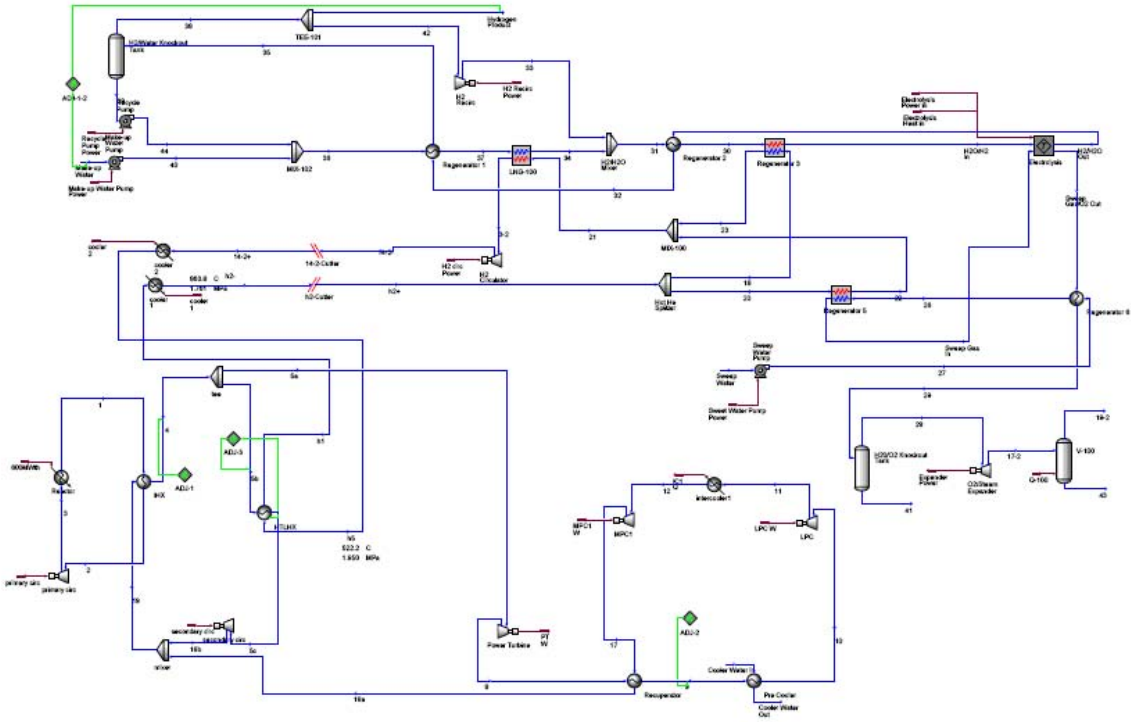

Figure D5: HYSYS simulation of overall plant including PCU and HTE

Heat Exchanger Sizing

Once the cycle efficiencies had been calculated, sizing data of the heat exchangers was estimated. For single phase heat exchangers the method given by Davis et al. (2005) was used. For heat exchangers containing two-phase heat transfer the UA value of the heat exchanger was calculated. The UA value elucidates to the overall size of the heat exchanger.

To determine the relative sizes of the single-phase heat exchangers, the UA values (overall heat transfer coefficient times the heat transfer area) of the heat exchangers were calculated by HYSYS. The U values were calculated, the heat transfer areas were determined, and the heat exchanger volume was calculated.

The IHX, HTLHX, and recuperator were assumed to be printed circuit heat exchangers (PCHE) as designed by Heatric (www.heatric.com). PCHE are composed of channels chemically etched into plates. The plates are then stacked and diffusion bonded together and headers are attached to form the heat exchanger. For this study Alloy 617 was used as the construction material for the heat exchangers. The thermal conductivity was assumed to be constant over the length of the heat exchangers and was obtained from www.specialmetals.com. The heat exchangers are assumed to be in counter flow to reduce the required surface area. The width and height of the heat exchangers were assumed to be equal. The flow

channels are assumed to be semicircular with a diameter of 1.5 mm, which is a representative value. From the stress analysis by Davis et al. the pitch to diameter ratio was taken as 1.2 and the plate thickness to diameter ratio was taken as .57 for the IHX, assuming a maximum hot side pressure of 7 MPa and a minimum cold side pressure of 5 MPa. For the HTLHX and the recuperator the pitch to diameter ratio assumed as 1.7 and the plate thickness to diameter ratio was assumed as 1.19, assuming a maximum pressure of 7 MPa on one side and a minimum of 2 MPa on the other.

The PHX's are assumed to be tube-in-shell heat exchangers. First, the tube inner diameter is assumed. The tube thickness is then calculated from the tube thickness to diameter ratio of .15 according to the stress analysis in Davis et al. (2005). The pitch-to-outer-diameter ratio of the tubes was set to 1.3, a typical value for tube bundles.

The sizing data of the heat exchangers in the plant is summarized in Table D4. The volume of the single-phase heat exchanger was calculated along with the UA value. For the more complex two-phase heat exchangers only the UA was calculated. However comparing the UA values and volumes of the single-phase heat exchangers in Table D4 shows the correlation between the two values. For example the IHX volume and UA values were found to be approximately one order of magnitude higher than those for the HTLHX. The PHX and HTE recuperator sizes do not change for the varying working fluids modeled in the PCU.

Fluid	Heat Exchanger	UA (kW/K)	U(W/m^2-K)	Volume (m^3)
He	IHX	5.38×10^4	812.8	52.9
	HTLHX	1.52×10^3	1058.0	2.53
	Recuperator	2.55×10^4	956.6	62.9
CO_2	IHX	5.18×10^4	609.1	67.9
	HTLHX	1.48×10^3	329.9	2.34
	Recuperator	1.21×10^4	850.8	86.2
N_2-He	IHX	5.18×10^4	896.3	46.17
	HTLHX	1.52×10^3	1089.0	1.91
	Recuperator	2.38×10^4	909.1	61.84
	PHX 1	2.62×10^2	--	N/A
	PHX 2	1.06×10^2	48.6	3.64
	PHX 3	6.03	179.0	.056
	HTE recup. 1	5.85×10^2	--	N/A
	HTE recup. 2	4.01×10^2	--	N/A
	HTE recup. 3	2.70×10^2	--	N/A

Table D4: Sizing data for plant heat exchangers